UNIVERSITY OF BIRMINGHAM

Evaluation of Mild Thermal Processes for Food Pasteurisation

by

SUWIJAK HANSRIWIJIT

A thesis submitted to
The University of Birmingham
for the degree of
DOCTOR OF PHILOSOPHY

Department of Chemical Engineering
School of Engineering
The University of Birmingham
February 2019

.

Abstract

The objectives of this research were to evaluate the heat transfer behaviour of in-container pasteurisation using heated water, which was chosen as a first approach to the study of the heating dynamics of spray pasteurisation systems.

A series of experiments were designed to test the response of vessels using a variety of experimental setups. Thermocouples were placed in specified positions inside glass jars, filled with one of a variety of fluids, ranging from water to highly viscous CMC. Enzymic Time-Temperature Indicators were also tested. Two types of heating medium were used; a heated water bath and one of a series of spray heads. It is important that the spray is correctly designed to avoid wasting time and cost by using the correct flow rate. Otherwise poorly optimised processing will have excessive pumping and heating costs. The results demonstrated that heat transfer was primarily controlled by the internal behaviour of the system. Heat transfer is slowest within the packs, i.e. either convection (in low-viscosity systems) or conduction (for high viscosity products) is the controlling thermal process. The greatest effect on the overall heating rate was given by the viscosity of the system. However, external flow or temperature had some effect; heating in the water bath was in all cases faster than heating from the range of sprays used. The type and distribution of spray used had an effect, both in the rate of heating and the final temperature. Pasteurisation values ('P-values') for processes were calculated from the thermal data and used to identify the best process conditions. Suggestions for process operation and further work are made.

The results of this study will help in the understanding of pasteurisation processes exhibiting internally controlled heating dynamics, and they will be also valuable in the process of characterisation of the shower spray pasteurisation operations.

Acknowledgements

I would like to express my gratitude to my supervisors, Prof. Peter J Fryer and Prof. Serafim Bakalis, for their invaluable guidance and advice throughout my project. I would like to thank them for their patience and kindness which helped me to achieve this work. A special thank you goes to Dr Estefania Lopez-Quiroga, whose help and guidance helped me to achieve so much in my research project.

I am also grateful to the workshop of the Chemical Engineering Department for their kindness and help to built the spray pasteuriser equipment.

A massive thanks must be expressed to Mrs. Lynn Draper and Mrs Emily Owen for their helps, support, kindness and patience throughout my project.

I would also like to express my big thank the Campden BRI company, and Prof. Martin George and Dr. James Luo for their valuable industrial input.

My thanks also go to all my friends for their support and help throughout my project to Patcharin Kangkha, Konsun Nuntasoontorn, Parichart Dudley, Flora Challou, Ju Zhu, Ourania Gouseti, Marie Lunel, and my housemates whoes were always there for me.

Most of all I would like to express my sincere thanks to my parents and my beloved family for their unconditional support, care throughout and encouragement.

Table of Contents

List of Figures

List of Tables

Nomenclature

Bi	Biot number		q	Heat transfer flux (W/m^2)
Cp	Specific heat capacity of water (J/kgK)		R	Outer radius of jar (m)
g	Acceleration due to gravity (m/s^2)		T	Temperature (^{o}C)
h	Heat transfer coefficient (W/m^{2}K)		u	Velocity of falling film (m/s)
H	Jar height (m)		W	Width of Jar Walls (m)
k	Thermal conductivity (W/m.K)		δ	Thickness of falling film (m)
L_c	Characteristic length (m)		ρ	Density of water (kg/m^3)
$\dot{m}_w$	Mass flow of water (kg s^{-1} jar^{-1})		μ_w	Dynamic viscosity of water (Pa s)
t	Time (seconds)			

Note: all the symbols employed are properly described and noted in the text as they are used for the first time.

Chapter 1

Introduction

Pasteurisation is a common thermal process that is used for food preservation since its effectiveness has been proved for a wide range and variety of products, guaranteeing both nutritional quality and food safety. Effort have been devoted to investigate the correspondence between food quality and quantity, and to minimise the cost of each pasteurisation operation. The main aim of pasteurisation is to eliminate all spoilage microorganisms in food using a processing temperature not higher than 100°C. Most commercial pasteurised food products are milk and dairy products, fruit-in-jar products, pickled vegetables, jams and chilled ready meals in pouch. (Lewicki, et al, 1983; Lewicki, 1984; Xie, and Sheard, 1996; Singh, et al, 2015;)

Although pasteurisation is widely employed in the food industry, there are other thermal processes that can extend food shelf life and make it safe for human consumption. Van der Plancken et al., (2008) reported that a combination of temperature and high hydrostatic pressure processing - or other process - lead to products of high quality too. Unfortunately, the operation costs of these combined methodologies are much higher than pasteurisation.

Pasteurisation, generally is good for acid food (pH value in the range 0 – 4.6, as oranges, lemon, apple juice, jam and vinegar) rather than acidified or low acid food (pH > 4.6) (Leadley et al., 2008). However, there are several factors (such as the pH, water activity, or the chemical composition) that will effect on the heat resistance of the pasteurised food (Miri et al., 2008).

The spoiling pathogen microorganisms mostly targeted by thermal processes are bacteria, yeast and mold and their spores. Most of the pasteurisation studies focus on microbiological analysis, usually for *Escherichia coli*, *Enterobacteriaceae*, *Bacillus cereus, Clostridium perfringens* and aerobic plate count (APC). In general, pasteurisation using hot water (as surface pasteurisation) eliminates 99.5% *E. coli, Enterobacteriaceae, B. cereus* and APC (all P < 0.001). This significantly decreasesthe risk of food product spoilage and diseases for consumers (Hauge, et al, 2011).

Usually pasteurisation is divided in two categories: Low Temperature Long Time (LTLT) and High Temperature Short Time processes (Lewis and Heppell, 2000). However, Fryer and Robbins (2005) showed that with these conventional procedures food are significantly over-processed to ensure safety. This over-processing can lead to bad quality - both physical and chemical- as a nutrition values as vitamins are lost. What is more, there are also important wastes of food, time and labour. They suggested dynamic optimization as a tool to be obtained optimal operation conditions

that guarantee the maximum product quality while enssuring food safety (Fryer and Robbins, 2005; Miri et al, 2008).

Spray pasteurisers or tunnel pasteurisers are suitable for sealed food in packages, as glass bottles of beer (Lewicki, et al, 1983), cans (Singh, et al, 2015), and pouches (Xie, and Sheard, 1996; Simpson, et al, 2004). This work focuses on the evaluation of mild thermal processes for food pasteurisation and it will investigate heat transfer during a spray pasteurising process.

1.1. Aims and Objectives

The aims and objectives of this research study can be summarised as follows:

•   Evaluation of heat transfer phenomena of pasteurisation using a water bath system, and the effect on the process, such as temperature, container geometries, percentages of headspace and filling product viscosities, have been performed at lab scale.

•   Evaluation of mild thermal processes for food decontamination using a new design of spray pasteurisation unit on variation factors as different types of nozzle, process heating conditions and the intergrated P values.

•   Evaluation of the thermal transfer phenomena occurred during surface pasteurisation of a mixture phase of food studied.

1.2. Thesis Plan

Chapter 2 gives a review of published literature. The first part begins with an overview of the theory for thermal treatment. The second part of this Chapter focuses on the theory of pasteurisation and heat transfer. Moreover, the use of TTIs background to validate thermal process efficiency is also shown.

Chapter 3 explains and details the materials and experimental methods employed to perform both water bath and spray pasteurisation experiments at laborlatory and pilot scale. The effect of different process conditions on thermal treatment efficiency was studied.

Chapter 4 describes the lab scale study on the heating dynamics of the water bath system. The aim of this work is to analyse the thermal response - described as temperature-time profiles - of the system under different heating conditions and different solution viscosities. The effect of the container size and headspace on the dynamics of the water bath system were also investigated. The process values (P values) for all these experimental conditions were calculated form the temperature profiles recorded too, and presented alongside the performance evaluation of TTIs. The last part of this chapter studies the heating dynamics of a two-phase (solid-liquid) system.

Chapter 5 describes the experiments performed to assess the effect of different spray pasteuring conditions on heat transfer phenomena. Effect of parameters such as types of nozzle, viscosity, geometry of package and flow rate were investigated. A

study of a two-phase solid-liquid mixture pasteurised within the spray rig is also presented.

Finally Chapter 6 presents conclusions and discuss the results of this work. Recommendations for future work are also summarised.

1.3. Publications

(Papers and Posters are given in the CD included with this work at the back of the thesis).

Journal (Peer-Reviewed)

P. J. Fryer, M.J.H. Simmons, P. W. Cox, K. Mehauden, **S. Hansriwijit**, F. Challou, S. Bakalis (2011). Temperature Integrators as tools to validate thermal processes in food manufacturing. Procedia Food Science. 1, 2011, 1272 - 1277, doi:10.1016/j.profoo.2011.09.188.

Conferences

S. Hansriwijit, E. Lopez-Quiroga, S. Bakalis, P.J. Fryer (2015). Spray pasteurisation of food packages: a study on the heating dynamics. 12th International Congress on Engineering and Food - ICEF12. June 2015, Quebec (Canada).

Chapter 2

Literature review

2.1   Introduction

Today people are careful about foods and expect to consume safe and healthy food products. Most research is concerned about food safety because food can be contaminated and spoil easily due to the action of pathogen microorganisms, such as bacteria, yeast and mold, and their spores. The major target of food processing is to avoid pathogenic microorganisms and deliver safe food for the consumers (Miri *et al*., 2008). Thermal treatment, such as commercial pasteurization, has been developed to make food safe. There is a balance between food safety and food quality; for example, methods such as a combination of temperature and high hydrostatic pressure processing are claimed to give a high quality products, but they are more expensive. (Van der Plancken *et al*., 2008).

Hurdle technology is a concept of food preservation which combines several preservation factors, either 'process' or 'additive' hurdles including high temperature, low temperature, low water activity, acidity, redox potential, competitive microorganisms (e.g. Lactic acid Bacteria), preservatives (e.g. Nitrite, sorbet, sulphite) (Lee, 2004), modified packaging atmospheres and high sugar content (Tucker *et al*., 2002). This approach is more effective for eliminating microorganisms and maintaining the quality of food than using only one method alone.

In commercial pasteurisation, the main purpose is to destroy spoilage microorganisms using a processing of temperature not higher than 100 °C. Food production, which commonly uses pasteurisation, include milk, fruit products, pickled vegetables, jams and chilled ready meals. This mild heat treatment level only eliminates moderately heat stable microorganisms (Tucker *et al.*, 2009). Recently, food manufactures have used a combination of chilled distribution and storage systems or hurdles to make longer shelf-life and higher quality of food products. The effect of thermal damage on food quality using pasteurisation is less than sterilisation (Tucker *et al.*, 2002)

Foods have been classified by The United States Food and Drug Administration (FDA), in the federal registers (21 CFR Part 114), into three types depending on the pH (Awuah *et al.*, 2007 and, Leadley *et al.*, 2008):

(i) *Acid foods*: with the pH value in the range 0 – 4.6, for example oranges, lemon, apple juice and vinegar*.*

(ii) *Acidified food* where the water activity is greater than 0.85 and the finished food product have the 4.6 pH values or lower. For example cucumbers, cabbage, artichokes, cauliflower, puddings, peppers, tropical fruits and fish*.*

(iii) *Low acid foods* are foods which have pH values higher than 4.6 and a water activity higher than 0.85, for example rice, bread, milk and alcoholic beverages.

Food safety usually focuses on the low acid foods because this is the optimal condition (food and pH) for the dangerous pathogen to surviveing and grow. The

importance pathogen microbial is *Clostidium   botulinum* which it can produce

botulinum toxin, which is fatal even in a small dose.

Recently, it has been researched and reported that spores of *C. botulinum* will not

develop and grow below a pH of 4.8. *C. botulinum* is rod-shaped and produces

spores. This microorganism can survive under anaerobic conditions, produce the

botulism poison, and is an extremely heat resistant microorganism (Awuah *et al*.,

2007). The heat resistant will change depending on the environment , such as the

pH, water activity, or the chemical composition; and the change in resistance will

affect the thermal process length required (Miri *et al*., 2008). Awuaha *et al*., (2007)

added that length at 4.6 pH or lower has been accepted as the pH below which *C.*

botulinum cannot grow and they cannot produce any poison. Therefore, the 4.6 pH

stands for a unique food processing condition between low and high acid foods.

2.2.   Heat transfer in food processing

To ensure food safety in food processing, especially in thermal food processing such

as in canning food, food in jars, cartons juice or pouches food, food processing has

been studied by a number of authors.(such as Singh and Ramaswamy, 2015; Singh

et al., 2015: Chen et al., 2015; Kannan and Sandaka, 2008; Xie and Sheard, 1996;

Simpson et al.,2004; Abdul Ghani et al.,, 2001), and optimal heating conditions were

investigated in terms both of its effect and heat transfer efficiency (Lewicki et al.,

1983; Lewicki, 1984; Dilay et al.,2006). However, nutritional properties after the end

of processing, in the finished products is always a concern. Heat transfer while food

is processed is important because it is necessary to reduce the bacterial, fungal, and viral load on the product – it must, however, not excessively reduce the nutritional and organoleptic qualities of the food. Heat transfer information is used to optimize the processing time and temperature profiles of thermal process to save both energy and cost and also maximize the quality of food products.

2.2.1 Mechanisms of heat transfer

There are three basic mechanisms of heat transfer: conduction, convection, and radiation (Incropera et. al., 2006).

Conduction

Energy transfer between two objects that are in physical contact occur by conduction. The conduction of heat is mostly evaluated in terms of Fourier's Law for heat conduction. Fourier determined that Q/A, the heat transfer per unit area (W/m^2), is proportional to the temperature gradient dT/dx. The constant of proportionality is called the material thermal conductivity, k.

$$\frac{Q}{A} = -k\frac{dT}{dx}$$ **Eq. (2.1)**

The mechanism of conduction heat transfer is energy transport due to molecular motion and interaction. In this work conduction occurs within solids such as (i) the food container, and (ii) solid food particles or highly viscous fluids.

Convection

Convection heat transfer is energy transfer caused by bulk fluid movement. Convective heat transfer through fluid, both gases and liquids from a solid boundary results from the fluid movement alongside the surface.

Convection can be expressed in terms of the heat flux, Q/A, which is proportional to the fluid solid temperature difference (T_s-T_f). The temperature difference normally occurs across a thin layer (boundary layer) of fluid nearby to the solid surface. The constant of proportionality is called the heat transfer coefficient, h, so that:

$$Q = Ah(T_s - T_f)$$

Eq. (2.2)

The heat transfer coefficient depends on the type of fluid and the fluid velocity. The heat flux, depending on the area of interest, can be local or area averaged. In this work convective heat transfer occurs (i) between the outside of a food pack and the heating or cooling fluid, and (ii) within the pack.

Radiation

The thermal radiation transfer is energy transport caused by photon (or emission of electromagnetic waves) from an objects surface or volume. Radiation can pass though a vacuum, it does not need a heat transfer medium. The radiation heat transfer is proportional to the fourth power of the absolute material temperature. The heat transfer by radiation depends on the properties of material, which is represented

by the emissivity of the material. In this work the temperature differences are such that radiation can be neglected

2.2.2 Heat transfer coefficient and thermal conductivities.

Factors that affect the rate of heat transfer are (i) the driving force or difference in temperature, (ii) heat transfer coefficient, and/or (iii) thermal conductivities of material; and its environment.

2.2.2.1 The driving force or difference in temperature

In this work heating temperatures is the range 90-70 ^{O}C, provided by hot water flow. The fluid being heated is in the range 20-70 ^{O}C; in practice; jars might be hot or cold filled before spray pasteurization.

2.2.2.2 Heat transfer coefficient

There are different correlations for heat transfer coefficient in different systems; correlations are generally expressed in terms of the Reynolds and Prandtl numbers for the flow. In this case, heat transfer is via impact and from hot water in a falling film over the vessel. Heat transfer coefficient (h_f) has the units of W /m^2 K. In some cases the resistance to heat transfer is very small, for example in condensing steam, when the heat transfer coefficient can be ignored (Holdsworth and Simpson. 2007).

2.2.2.3 Thermal conductivities

The thermal conductivity relates the heat flow to the temperature driving force. Thermal conductivity values can be determined experimentally. Thermal conductivities of fluids and solids vary as in Table 2.1 (Lewis *et al*, 2000).

Table 2. 1: Thermal conductivities of different materials.

Material	Temperature (^{0}C)	Thermal Conductivity (W m^{-1} K^{-1})
Silver	0	428
Copper	0	403
Copper	100	395
Aluminum	20	218
Stainless steel	0	8-16
Glass	0	0.1-1.0
Ice	0	2.3
Water	0	0.573
Corn oil	0	0.17
Glycerol	30	0.135
Ethyl alcohol	20	0.24
Air	0	2.42x10^{-2}
Cellular polystyrene	0	3.5x10^{-2}
Freeze-dried peach(1 atm)	0	4.18x10^{-2}
Freeze-dried peach (10^{-2} Torr)	0	1.35x10^{-2}
Whole soya beans	0	0.097-0.133
Starch (compact powders)	0	0.15
Beef, parallel to fibers	0	0.491
Frozen beef	-10	1.37
Fish		0.0324+0.3294m$_w$
Sorghum		0.564+0.0858m$_w$

m_w is the mass fraction of moisture. 1 Btu h^1 ft^{-1} degF^{-1} = 1.731 *W m^{-1} K^{-1}*.
 Source: Reprinted with permission from MJ. Lewis, *Physical Properties of Foods and Food ProcessingSystems,p. 249, © 1990, Woodhead Publishing, Ltd.*

Thermal conductivity of container materials (W /m.K) are; ferrous metal containers, 40–400 W /m.K; aluminum, 220 W /m.K, glass, 1–2 W /m.K, polyvinylchloride, 0.29 W /m, polyethylene, 0.55 W /m.K (Holdsworth and Simpson. 2007)

The balance between external and internal heat transfer in a solid is described by the Biot number, hD/k, where h is the surface heat transfer coefficient, k the internal thermal conductivity and D some characteristic dimension of the pack. High Bi (> 10) implies external heat transfer is much faster than the internal processes, and thus that the slower conduction process controls. Low Bi (<0.1) implies the reverse, that it is the external heat transfer coefficient that is the slowest process. Here, for food products, Bi is generally high; but if the food product is replaced by a high-conductivity material such as a metal, the heat transfer coefficient can be measured from the thermal response of the solid – this is sometimes used to estimate heat transfer coefficients in food processes (Holdsworth and Simpson, 2007).

2.3   Pasteurisation

Pasteurisation describes a mild heat thermal process used to to extend a shelf life of food product longer than fresh food. The process also keeps the product to be more like natural food as the high heat treatment required for full sterilization results in a large loss of nutritional value and quality. Pasteurisation is a method of microbial reduction that does not expose the food to very high temperature (up to 100°C). For example, pasteurized milk can be pasteurised at 62.8 °C for 30 minutes, to destroy harmful pathogenic bacteria and the enzymes that cause food spoilage. However, the resulting pasteurised food needs to have its subsequent microbial load controlled by storing it at low temperatures such as in a refrigerator. This will help to prevent the growth of microorganisms. The food needs to be consumed once it was opened, within three days to a week. Many researches show that the pasteurisation process

can maintain the quality of food including its fresh taste because the heat load is not very high (ref). For this reason most foods such as milk or juice commonly use this pasteurisation process to extend their shelf life.

There are two concepts of pasteurisation, at low temperature long time (LTLT) and a high temperature short time (HTST).

Low temperature long time (LTLT)

Low temperature long time describes the thermal processes using low heat and long time to kill all pathogenic bacteria. For example, milk can be pasteurized at 62.5ºC/144.5ºF and for 30 minutes.

High temperature short time (HTST)

High temperature short time is the thermal processes using a higher temperature than LTLT and thus which needs less time to kill all - pathogenic bacteria. For example, milk can be pasteurized at 72ºC/161.5ºF for 15 seconds. The layout of an HTST pasteuriser can be shown in figure 2.1(Lewis and Heppell, 2000)
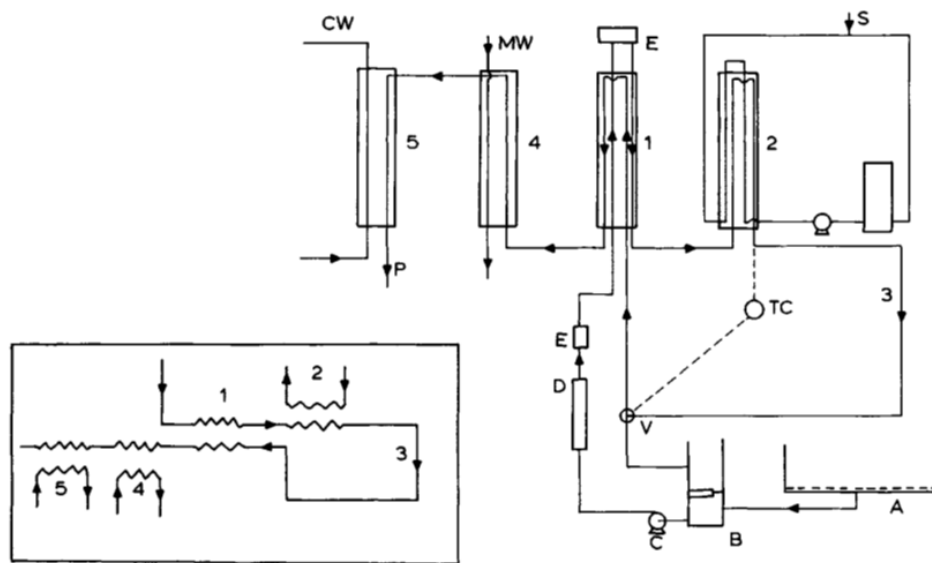
Layout of HTST pasteurizer (the insert shows a schematic diagram of the heat exchange sections). (A: feed tank; B: balance tank; C: feed pump; D: flow controller; E: filter; P: product; S: steam injection (hot water section); V: flow diversion valve; MW: mains water coolings; CW: chilled water; TC: temperature controller; 1: regeneration; 2: hot water section; 3: holding tube; 4: mains cooling water; 5: chilled water cooling). *Source:* Reprinted from M.J. Lewis, Physical Properties of Dairy Products, in *Modern Dairy Technology*, Vol. 2, 2nd ed., R.K. Robinson, ed., © 1994, Aspen Publishers, Inc.

Figure 2. 1: HTST pasteuriser schematic (Lewis and Heppell, 2000)

2.3.1 Pasteurisation/ pasteuriser

2.3.1.1 Pasteurisation steps

There are several kinds of food that are commercially pasteurized, for example:

(i) Milk and milk products – both low temperature and UHT (Ultra-High-Temperature (UHT) Pasteurization).

(ii) Juices such as orange, grape, pineapple, apple or mango juice.

(iii) Seafood

(iv) Poultry product (Silva and Gibbs, 2012)

(v) Beef and other meat products

(vi) Bakery product

(vii)   Drinking beverages; beer and other alcohol

A process for pasteurization has several steps from a raw food to a processed product. Zeki Berk (2016) described the steps of pasteurisation as follows:

(i)   *Filling* - food can be filled in to containers by hand filling or much more commonly by machine filling.

(ii)   *Expelling air* from the head-space above the food, either in a can head-space or between lid and product. If the space above the hot food can be filled with steam or hot air the resulting cooling will create a partial vacuum above the food. Such a vacuum head space can be made by hot filling, steam injection or by applying a mechanical vacuum.

(iii)   *Sealing:* this can be done either by attaching a fixed lid to the pack, which could be metal (as in canning) or plastic, by heat-sealing a plastic pouch, or attaching a screw-top to a jar.

(iv)   *Heat processing:* the food can either be pasteurized before packaging or processed in-pack (see below);

(v)   *Cooling:* after thermal process the food product needs to be cooled down immediately to shock all remaining microorganisms and lower the product temperature.

2.3.1.2 Pasteuriser

(i)   *Batch pasteuriser.*

Lewis and Heppell (2000) discuss early batch processes; that were highly labour intensive and involve filling, heating, holding, cooling, emptying, and cleaning in the same vessel.

This type of process is still widely used, particularly by small-scale producers and in the manufacture of products such as ready meals (James and James, 2014) They are relatively slow because heating and cooling times are considerable; the total time for one batch may be up to 2 hours; product is then packaged and either (i) passed into a refrigerated chill chain, for example with ready meals, or (ii) filled into vessels such as jars that can be stored at ambient for a limited time. The batch pasteuriser lay out is shown in Figure 2.2
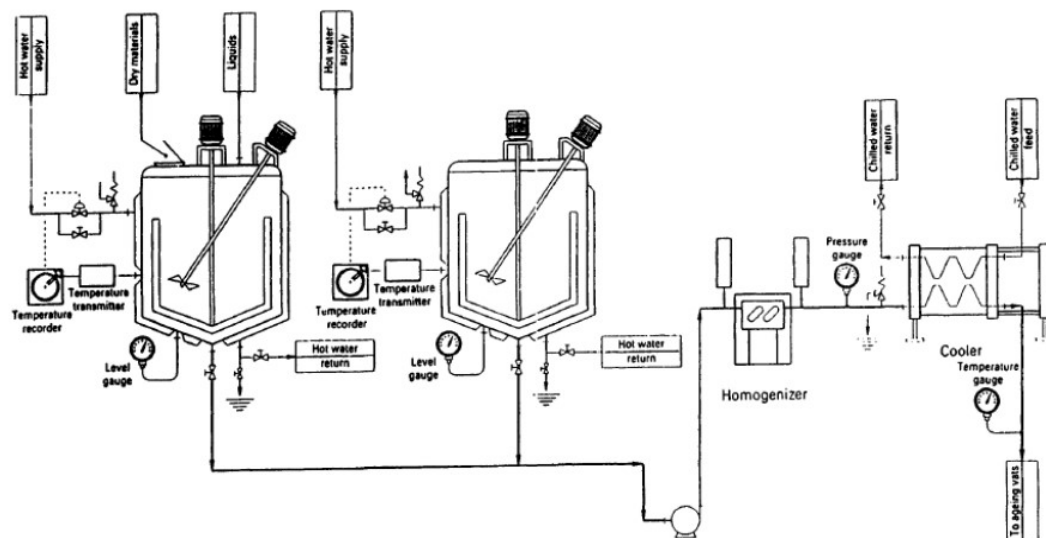
Figure 2. 2: Batch pasteuriser, from Lewis and Heppell (2000)

(ii) *Continuous pasteuriser*

In continuous pasteurizing operations, the process is carried out in a system consisting of heat exchangers and piping. The product leaves the system after continuous sterilization or pasteurization (depending on the time temperature profile), holding, and continuous cooling. If filling and sealing occurs in an open space, recontamination of the cold product may occur. This may not be objectionable if the product is to be refrigerated and its planned shelf life is sufficiently short, as for pasteurized milk and dairy products (Walstra et al., 2005).

A typical process for the continuous pasteurization of liquid milk is shown schematically in Figure 2.3.

- The pasteurizer, in this case, is a plate heat-exchanger consisting of three sections. Raw milk is admitted to Section 1 (preheating, regeneration), where it is heated to about 55°C by hot pasteurized milk flowing on the other side of the plates

- It then passes to Section 2 (heating), where it is heated to the specified process temperature, with hot water on the other side. The hot water for this purpose is heated by steam and circulated in closed circuit by appropriate pumps (not shown).

- The milk, thus pasteurized, passes through a holding tube of appropriate dimensions (according to the specified holding time). (Berk, 2013)

The system is efficient, and as heat is recycled by using hot product to preheat the feed, thermally efficient. The systems are widespread but limited to single-phase and relatively low viscosity fluids.
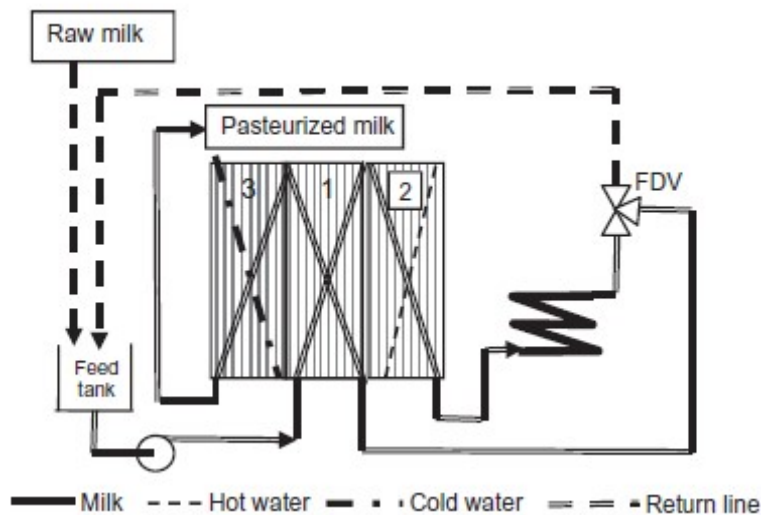
Figure 2. 3: Schematic of the continuous pasteurization of milk. Berk (2013)

(iii)   *Tunnel Pasteurization*

Tunnel pasteurisation is mostly used in the food industry as can deliver a safe finished food product at high throughput. This process is suitable for pasteurising food in a sealed container such as s, glass jars , polyvinyl chloride packages, and a flexible packaging such as pouches, plastics, or paper cups. Food pasteurised products, examples include soft and carbonated drinks, juices, beers, and sauces (Lewis and Heppell, 2000; Horn et al; 1997)

The tunnel pasteurizer (Horn et al; 1997) as shown in Figure 2.4 is divided into two main parts as heating and cooling section, however in each main part they are

separated into several zones with a different water temperatures in each section. The heat can be recovered between heating and cooling zones as they are connected a pump. After filling food in their packages, automatically, these food containers are passed through both heating and cooling zones continuously by a conveyor belt. After that they are sent to labeling and storage .
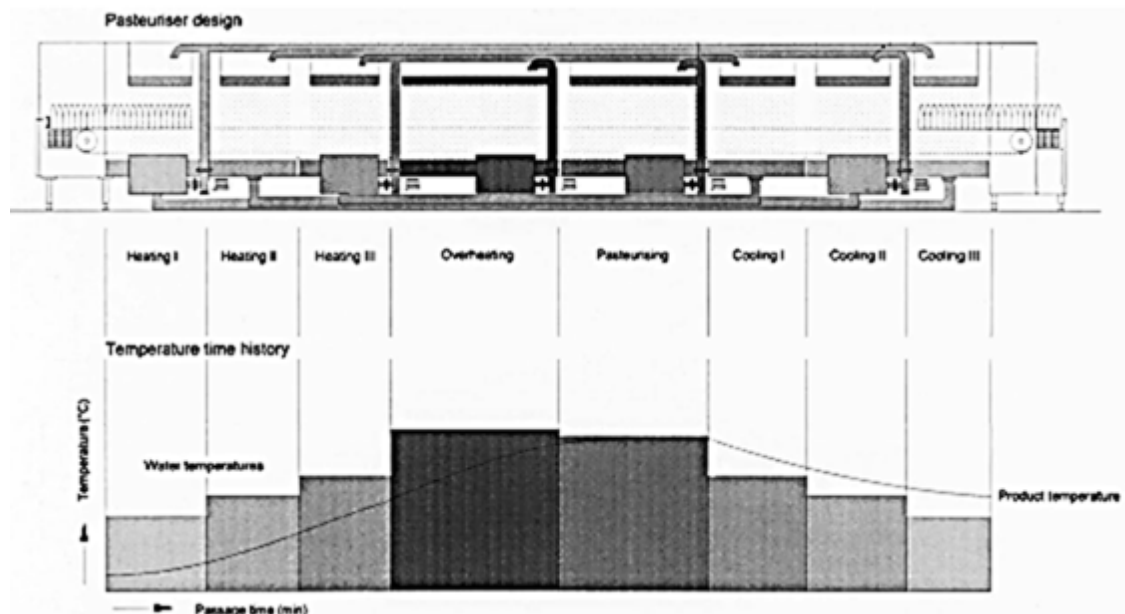
Figure 2. 4: Tunnel pasteurization, Horn *et al*; (1997)

Lewis and Heppell (2000) note that tunnel (spray) pasteurizers are widely for continuous heating and cooling of products in sealed containers, ideally for a very high-volume throughput of food product. They reported that the tunnel pasteurisation can be divided into three main stages: heating, holding, and cooling. Spray water at the different temperature was spray over the food container in the different stages. These processes use longer time/lower temperature processes than plate or tubular

heat exchangers. Because their heating rates are not higher as previous two processes, plate or tubular heat exchangers. The overall processing time is about 1 hour, including a holding stage at temperatures between 60°C and 70°C for about 20 minutes.

2.3.2 Pasteurisation of liquid foods

2.3.2.1 In-pack pasteurisation.

Some pasteurised liquids, such as beer and some juices, are pasteurised after they are filled into the containers. In this case, care has to be taken to ensure that when the glass is filled with liquid that there is no thermal shock, which can cause cracks in the packaging. The maximum temperature difference which the glass container can be resistant to is 20 °C for heating and 10 °C for cooling .

The end of the process involves cooling to <40 °C, to stop further reactions taking place in the product, and to remove water that can cause of matal packaging or labels attached to the lid. This process can be both batch and continuous pasteurisation process. A simple water bath or retort, that heats the packaged food through some temperature and time process, followed by cooling.

However, the system may include other pasteurisation tunnels that is divided into multiple of heating and cooling units. A hot spray of water rains over the food

package on the belt through the unit. The food temperature then rises to the environment temperature and after pasteurisation is cooled with water in the end of the tunnel.

The advantage of using tunnel pasteurization is that heating is faster than some other pasteurisation methods, such as batch heating in vessels. Berk (2013) notes that the pasteurised temperature for food products with a pH of lower than 4.5 such as tomato products, vegetable pickles, fruit in syrup and artificially acidified products, is lower than 100 ^{0}C. However the processing time interval for heating and cooling stage along the tunnel that depends on the kind of food products and the container size.

2.4 Heat transfer in packs

There have been a number of studies of heat transfer in pasteurization such as:

- In bottled beer (Lewicki, et al, 1983; Lewicki, 1984; Dilay, et al, 2006))

- In cans (Kannan and Sandaka, 2008; Singh, et al, 2015; Chen, et al, 2015),

- In pouches (Xie, and Sheard, 1996; Ghani, et al, 2001; Simpson, et al, 2004)

Heat transfer in a spray pasteuriser has been less well studied. Heat transfer of beer in a pasteurisation tunnel was studied by Lewicki, et al, (1983), and Lewicki, (1984). In the first paper a model of a pasteuriser was built and a number of parameters investigated; bottle shape, hot water spray intensity, location of bottle in relation to

the spray nozzle axis, and the spray nozzle pattern and the deflection angle of nozzles with respect to the vertical. All variables for this experiment affect the heating rate of fluid in bottles. The important factors for this pasteurizing are spray intensity and location of the bottle in relation to the nozzle axis. While, the bottle shape has small effect in the heating processes. However, the angle of the nozzle effect to the horizontal was unclear, due to its resulting to improve heating rate at just some locations along the tunnel.

Lewicki, (1984) continued his study on heat transfer in a tunnel pasteuriser, and focused on heat transfer coefficients. Resulting, there were effect of variation factors; hot water spray intensity, location of bottle in relation to the spray nozzle axis and the shape of the bottle; on the overall heat transfer coefficient of process. The heated fluids viscosity had more effect on the overall heat transfer coefficient. The glass of the jar was the largest heat transfer resistance when the liquid to be heated is water. With more viscous fluids, which had viscosity higher than $1{\cdot}1 \times 10^{-3}$ Pa s, this viscosity causes conduction into the fluid to be the main resistance in the heating liquid processes. However, heat transfer resistance for the stage of heat transfer from the hot spray of water to the container wall is smaller than the glass wall resistance by around eight times. In shortly, the fluid physical properties that being pasteurised heating were an extremely affect heat transfer rate under tunnel pasteuriser conditions.

Horn, et al (1997) researched the modelling and simulation of pasteurization and staling effects during tunnel by investigated and simulated a model for the varies of unsteady convective heat transfer inside a bottle of beer. The simulation results show that the model gives a good correlation between model and experiment for both laboratory and process data. The traditional procedure, can be simulated for determining pasteurization units (PU), shows that it was overestimate the actual effect significantly if it is not chosen the accurate reference point with reference to the bottle size and shape.

Dilay, et al (2006) studied modeling, simulation and optimization of a beer pasteurization tunnel. A basic physical model was combined with a fundamental and empirical correlations, principles of classical thermodynamics, and heat transfer concept developed and the outcome result of three-dimensional differential equations are re-simulating in space using a three-dimensional cell centered finite volume scheme.

2.5   Modelling of heat transfer in spray pasteurisation

A model of a conduction/convection process was built by Kitt (2015) and Kitt et al., (2015). The geometry of the container used in the experiments (glass jar) can be approximated by a cylinder. Figure 2.5(a) shows the three-dimensional geometry considered. It represents the cylindrical package, with radius $r = R$ and height of

filling *z* = *H*. Given the axial symmetry of the cylinder, this geometry can be further simplified to the two-dimensional domain depicted in Figure 2.5(b).

The model assumes that hot water flows down over the package, and that:

- Conduction is the governing heat transfer mechanism through the filling.

- The falling film has a uniform temperature (isothermal) in the radial direction.

- Laminar flow in the falling film.

- No heat was lost to the surroundings from the film.

(a)   (b)
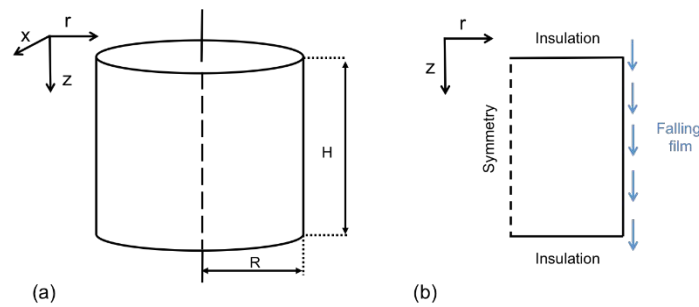
Figure 2. 5: (a) Three dimensional geometry representing the package (jar) considered. (b) Axial symmetric two-dimensional domain employed for numerical simulation, together with the imposed boundary conditions.

The model developed is based on first principles, and it describes heat transfer from the falling film and through the package and product Since the filling considered here is characterised by a high viscosity, conduction is the main mechanism involved in the product heating up (Bird et al., 2007):

$$\frac{\partial T_{prod}}{\partial t} = \nabla\left(\alpha_{prod}\nabla T_{prod}\right)$$ **Eq (2.3)**

where T_{prod} is the temperature of the filling product (°C), t represents the time (seconds) and α_{prod} (m²/s) is the thermal diffusivity of the filling. On the other hand, the temperature of the falling film T_{film} (°C) will be given by the following diffusion-convection equation:

$$\frac{\partial T_{film}}{\partial t} = -\alpha_w \frac{\partial T_{film}}{\partial r} - u_z \frac{\partial T_{film}}{\partial z}$$ **Eq (2.4)**

where α_w (m²/s) is the thermal diffusivity of the film water and u_z (m/s) is the film velocity; i.e. the film cools down as it moves down the pack.. The thickness of the falling film, δ (m), is a function of the mass flow $\dot{m}_w$, and it can be computed using the next correlation (Sinkunas et al., 2005):

$$\delta = \left(\frac{3\dot{m}_w\,\mu_w}{2\pi R g \rho_w^2}\right)^{\frac{1}{3}}$$ **Eq (2.5)**

Insulation has been imposed on the top boundary of the domain to take into account the effect of the headspace:

$$\frac{\partial T_{prod}}{\partial z}\left(0,z,t\right) = 0$$ **Eq (2.6)**

The bottom boundary is also defined as an insulated surface:

$$\frac{\partial T_{prod}}{\partial z}\left(r,0,t\right)=0 \qquad\qquad \textbf{Eq. (2.7)}$$

Axial symmetry is considered at *r = 0*:

$$\frac{\partial T_{prod}}{\partial z}\left(0,z,t\right)=0 \qquad\qquad \textbf{Eq. (2.8)}$$

while the temperature of the falling film is defining the condition over the exterior wall boundary at *r = R*:

$$T_{prod}\left(R,z,t\right)=T_{film} \qquad\qquad \textbf{Eq. (2.9)}$$

Initially, the temperature of the product is considered to be constant:

$$T_{prod}\left(r,z,0\right)=T_{ini} \qquad\qquad \textbf{Eq. (2.10)}$$

The conductive model describing heat transfer in the jar filling (system formed by Eq. (2.3) and Eqs. (2.5)-(2.10)) was solved employing the Finite Difference method in a uniform spatial 2D grid as the one depicted in Figure 2.6.
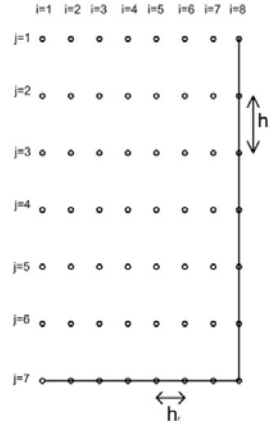
Figure 2. 6: Schematic of a uniform 2D spatial grid employed I the numerical simulations.

The mass flow rate of the water falling film, $\dot{m}_w$, varied from 1x10^{-2} kg/s to 1 x 10^{-4} kg/s, and the initial conditions were set such that every point was at T_{ini} = 20 °C. The film was given a temperature T_{film} = 90 °C. With these parameters the model was validated making use of the analytical solution existing for Eq. 2.3 (Incropera et al., 2006):

$$\theta = C_1 \exp(-\lambda_1^2 * F_o) * J_0\left(\lambda_1 * \frac{r}{r_0}\right) \qquad \textbf{Eq (2.11)}$$

where F_o is the Fourier number of the system, defined as:

$$F_o = \frac{t\alpha_{prod}}{R^2} \qquad \textbf{Eq (2.12)}$$

and θ is the dimensionless temperature calculated as follows:

$$\theta = \frac{T_{prod} - T_{ini}}{T_\infty - T_{ini}} \qquad \textbf{Eq (2.13)}$$

The constants C_1 and λ_1 in Eq. (2.11) were found to be 1.6021 and 2.4048,

respectively, and were considered for an infinite Biot number (Incropera et al. , 2006).

The *Biot* number is usually employed used to determine whether a system is lumped

or not, and it is defined as follows (Incropera *et. al.*, 2006):

$$Bi = \frac{hL_c}{k}$$ **Eq (2.14)**

where, L_c (m) is the characteristic length of the solid under study. High *Biot* numbers

imply that the heat transfer to the system is faster than thermal conduction within it;

on the other hand, a low *Bi* implies the opposite. If *Bi* < 0.1, then the system is

considered to be a lumped heat capacity system and equation (3.5) can be used to

calculate the solid temperature.

 The Bessel function J_o was computed using MATLAB's inbuilt function *Bessel j(nu,z)*

with argument nu being zero and z being $\lambda_1 * \frac{r}{r_o}$.

Analytical results were gathered over the following range of t and r values:

2000<t<4000 seconds and $0 < r \leq 0.0365$ meters. The validation results are

presented in Figure 2.7 for two different spatial grids, showing in both cases a very

good agreement between the analytical solution and the results obtained through the

numerical solution of the proposed conductive model.

(a)   **(b)**
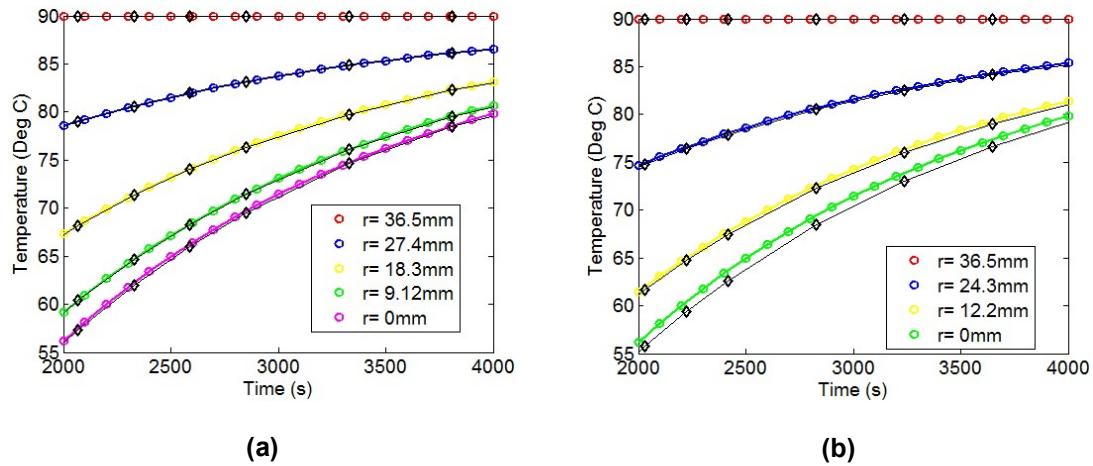
Figure 2. 7: Comparison between analytical solution and simulated results for a 2D spatial grid of (a) 21 x 21 nodes (b) 10 x 10 nodes.

A number of cases were modelled; critical is the effect of different flow rates: the system operates:

- At very low flow rate there is insufficient heat supplied to the vessel; in the limit, the 'heating' fluid will reach the same temperature as the vessel by the time it has reached the bottom of the vessel;

- Whilst at high flow rate, beyond a certain point increasing the flow rate has no further effect on the heat transfer response of the vessel; this arises because the system is controlled by internal heat transfer (high Bi). Increasing the flow rate beyond this point has no effect on the temperature of the vessel and simply wastes water and pumping costs.

2.6 Lumped system analysis

In general, the basic mechanisms of heat transfer have three mechanisms namely; conduction, convection, and radiation as shown in part 2.2.1 Mechanisms of heat transfer in Chapter 2 (Incropera et. al., 2006). However, there are only 2 main mechanisms of heat transfer; conduction and convection that are the focus on this research.

Heat transfer conduction can be defined as a heat transfer mechanism from a region of high temperature to aregion of low temperature within a solidmedium. The conduction heat transfer is mostly referred to the terms of Fourier's Law for heating conduction as presented in Eq (2.1) [$\frac{Q}{A} = -k\frac{dT}{dx}$]. In this research conduction of heat can be occurred within solids such as the container of food and solid food particles or highly viscous fluids.

Convection can be termed as a process of a heat transfer between a solid surface and a fluid; liquid or gas; medium, but they are at different temperatures. Convection occurs through flow in the fluid medium. Convection of heat can be expressed in terms of the heat flux and the heat transfer coefficient as shown in Eq. (2.2)[$Q = Ah(T_s - T_f)$]. In this research convective of heat transfer can be occurred between the outside of a food container and the heating or cooling fluid, and within the container. The heat transfer coefficient factors depend on the fluid type and the velocity of fluid. The heat flux also based on the area of interest which can be local or area averaged.

Heat transfer in packs has been studied in beer bottles (Lewicki, et al, 1983; Lewicki, 1984; Dilay, et al, 2006)), in cans (Kannan and Sandaka, 2008; Singh, et al, 2015; Chen, et al, 2015; in pouches (Xie, and Sheard, 1996; Ghani, et al, 2001; Simpson, et al, 2004). Modelling of heat transfer in spray pasteurization was investigated in this research and details and equation as in Chapter 2 section 2.5. Kitt (2015) and Kitt et al., (2015) built a model of a conduction/convection process. The geometry of the container as presented in Figure 2.5(a) shows the three-dimensional geometry that used in thiswork experiments (glass jar). It can be approximated by a cylinder.

The model assumed that hot water flows down over the package as falling film, and that:

•   Conduction is the governing heat transfer mechanism through the filling.

•   The falling film has a uniform temperature (isothermal) in the radial direction.

•   Laminar flow in the falling film.

•   No heat was lost to the surroundings from the film.

The equation for this model as in eq. 2.1 to 2.13

The constants C_1 and λ_1 in Eq. (2.11) were found and were considered for an infinite

Biot number (Incroperaet al., 2006). The Biot number is the ratio of the internal resistance (conduction) to the external resistance to heat convection. The Biot

number is used to determine whether a system is lumped or not, and so it can be

defined as in   Eq. (2.14) $[Bi = \frac{hL_c}{k}]$

2.7 Monitoring Thermal Processes

The main kinetic process to ensure the safety of thermal processes is the kinetic of

the death of microorganisms. Heat efficiency or process value can be calculated in

term of F-values (for sterilisation) or P-values (for pasteurisation) as:

$$P \, (or \, F) = \int_0^t 10^{\frac{T(t)-Tref}{z}} . dt, = D_{T(ref)}.\log\left(\frac{N_{initial}}{N_{final}}\right), \qquad \textbf{Eq (2.15)}$$

where, $T(t)$ = the product temperature (ºC)

   T_{ref} = the reference temperature for the D_T value (ºC)

   t   = the process time (min)

   z   = the number of degrees centigrade needed to bring about 10 times

change in the rate of reduction of microbial load

   N   = number of micro organisms (-)

   D   = Decimal reduction time: the time necessary to reduce the number of

      microorganisms by 90% (s)

Commonly, a z value of 10 °C is used to monitor sterilization safety and target

microorganisms, and z values range from 5 °C to 12 °C for pasteurization (Van Loey

et al., 1996).

The behaviour of a system can thus be understood if the temperatures are accurately measured, in which case equation (2.15) can be used to calculate P-values. In much of this thesis, thermocouples will be used as they have advantages in static situations – however in moving systems the length of wires needed is a major problem. One solution has been put data recorders through thermal processes, but this is difficult because of their bulk. Much work has therefore been done on time-temperature integrators, enzyme markers that can be passed through a process and assayed afterwards to see what activity they retain. The ratio of the initial to the final activity is a measure of the thermal treatment that the system has received.

Van Loey *et at* (1996) and Van Loey *et al* (1997) defined TTI as 'a small measuring device that shows a time-temperature dependent, easily, accurately and precisely measurable irreversible change that mimics the changes of a target attribute undergoing the same variable temperature exposure'.   As an alternative to thermocouples, TTIs have been developed over the last two decades for use in food industries for monitoring the heat treatment impact on microorganisms and food quality as enzymes, color and texture (Van Loey *et al*., 1996; Hendrickx *et al*., 1995). TTI replaced the conventional method or thermocouples, which have the serious limitation in that they must be connected to a logging system. (Hendrickx *et al*., 1995). TTIs are a very small measuring tool whose behaviours depend on time and temperature.   In the same variation of temperature condition, they can be easy, accurate and specific determination for irreversible change (Van Loey *et al*., 1996; Van Loey *et al*., 1997; Mehauden *et al*., 2007).

In terms of working principle, TTIs can be classified in five ways according to their working principle, response type, origin, application in the food materials and position in foods (Van Loey *et al*., 1996) . On the other hand, in terms of the substances contained in the TTIs can be classified into four types; microbiological, enzymatic, chemical or physical (Van Loey *et al*., 1996; Mehauden *et al*., 2007). Each method (microbiological, chemical and physical TTIs) has limitation and disadvantages of application in the food process (Van Loey *et al*., 1997; Mehauden *et al*., 2007), this study focus on enzymatic TTIs.

Several enzymes have been used in researches for pasteurisation such as α-amylase from *Bacillus* species (Van Loey *et al*., 1997; Mehauden *et al*., 2007; Mehauden *et al*., 2008; Tucker *et al.,* 2002; Tucker, 2009), and pectinmethylesterases (PMEs) from cucumber and tomato fruits (Guiavarc'h *et al*., 2003). However, high thermal resistance enzymes have been used to develop TTIs for extremely heat treatment as sterilisation process. These enzymes are α-amylase from *B. lichenniformis* (Guiavarc'h *et al*., 2002a; Guiavarc'h *et al*., 2004), *Pyrococcus furiosus* (Tucker *et al*., 2007) and β-xylanases from *Thermomyces lanuginosus* (Gogou *et al.,* 2010). Several different types of enzyme have been used in TTI research as in Table 2.2.

Table 2. 2: The application of the Enzymatic TTIs.

Enzyme	Application description	z (°C)	Reference
α-amylase (*B. amyloliquefaciens*)	Yoghurt batches (Temp. 70-90 °C)	z-value of 9.7(±0.3)°C	Tucker (1999)
α-amylase (*B. amyloliquefaciens*) (*B. lichenniformis*)	The tubular process, batches of fruit (Temp. 76-85 °C) (Temp. 85-95 °C)	$D_{85°C}$ -value of 6.8 min and z-value of 9.4(±0.3)°C $D_{93°C}$ -value of 8.8 min and z-value of 9.1(±0.3)°C	Tucker *et al.* (2002)
α-amylase (*B. amyloliquefaciens*)	Peltier Stage, nonisothermal (Temp. 80-90 °C)	$D_{85°C}$ -value of 6.1(±0.4) min and z-value of 12(±1.3)°C	Mehauden *et al.* (2007)
α-amylase (*B. lichenniformis*)	Peltier Stage, nonisothermal (Temp. 85-95 °C)	$D_{85°C}$ -value of 29.15(±4.7) min and z-value of 10 (±0.8)°C	Mehauden *et al.* (2008)
α-amylase (*B. amyloliquefaciens*)	Mild heat pasteurisation, in water bath and silicone bath (Temp. 64-73 °C)	$D_{70°C}$ -value of 8.4 min and z-value of 8.9 °C	Tucker *et al.* (2009)

According to previous researchers, enzymatic TTIs have more potential for evaluation and are easier to handle than protein-based system. This has led to more

applications for enzymatic TTIs than other types as microbiological TTIs and these most wildly used in several researches (Van Loey *et al*., 1996; Mehauden *et al*., 2007; Tucker, 2009). This is because of the special specification of these TTIs; small in size, relatively low-priced and easy to prepare (both enzyme activity and reaction enthalpy). It is also possible rapidly and accurately to measure their properties thermostability properties and their heat inactivation kinetics can be handled in various ways. (Van Loey *et al*., 1997)

New enzymatic TTIs have been developed with applications in pasteurisation. Mehauden *et al.,* (2007a) evaluated the potential of α-amylase (*B. amyloliquefaciens*) time temperature integrators (TTIs) using a peltier device to get controlled heating and cooling profiles. The study found that the kinetic parameters of the enzyme were measured as $D_{85\ °C}$ of 6.1 (±0.4) minutes and z of 12 (±1.3) °C. These TTIs can be consistently used over the range for thermal pasteurisation such as the new enzymatic TTI made from the α-amylase (from *B. licheniformis*) which can be used from 5 to 30 minutes at 85°C. However, the thermal resistance of the enzyme is the main factor for determined the range of time temperature profiles using enzymatic TTIs (Mehauden, 2008). The limitation of enzymatic TTIs efficiency depends on the changing of enzyme condition (such as enzyme immobilization) and environment (such as pH, water activity and moisture content) (Van Loey, el al, 1996 and Mehauden, 2008).

Tucker *et al*., (2009) developed a new enzymatic time–temperature integrator (TTI) for measurement of the heat profile in mild pasteurisation process at 70°C, for few minutes. After these treatments, food products sold either under refrigerated conditions (<10 days storage), or are high acid food products that can be stored in a ambient condition for many months. This new TTI was referred to as BAA70 and consisted of 0.5mg/mL α-amylase from *B. amyloliquefaciens* in 10 mM acetate buffer. The study of BAA70 in a water bath shows the Decimal reduction time ($D_{70 ^{o}C}$-value) of 8.4 minutes and z-value of 8.9 °C. The maximum P-values of BAA70 were calculated at up to 25.2 minutes at 70 °C. The new BAA70 TTIs were applied for surface pasteurisation in hot-filled mini jam jars and for continuous oven cooking of quiches in industrial practice. The result shows that using TTIs in both these operations could be give results for measurement of P- values, which compared well with conventional temperature sensors.

Gogou *et al*. (2010) reported that the D-value at 80 °C of xylanases TTI made from *Thermomyces lanuginosus* , was found to be 61.2, 46.0 and 50.6 minutes for the three enzyme solutions (Unpublished data). After study to improving the thermostability of xylanases by reduction of water activity then used the new developed TTIs to be study sterilisation process in the temperature range of 100–130 ^{0}C. The result of this show the high impact of the water activity on the observed D and z-values reducing from 0.63 to 0.13, which were given the D120 C and z-values of the three xylanases ranged from 20.4 to 37.6 minutes and from 23.3 to 28.9 C, respectively.

Recently research on TTI validation study in both lab scale and pilot plant scale has been considered (Guiavarc'h *et al*., 2002b; Mehauden *et al*., 2007; Mehauden *et al*., 2008; Tucker *et al*., 2009). However, these researches show mostly D, z and P value correlation between thermocouple and amylase TTI made from *B. amyloliquefaciens* for pasteurisation at 85 °C (Mehauden *et al*., 2007, 2008) and 70 °C (Tucker *et al*., 2009). This research aims to evaluate heat treatment using the alternative amylase TTI from *B. lichenniformis* for pasteurisation process at 80°C.

2.7. Comparison between different monitoring methods

There are several way to validate for the efficiency of the thermal processes to ensure that the finish food product is safe enough for commercial and consumption as thermometer, thermocouple and data logger (Hendrickx et al., 1995; Mehauden, 2008; Marra and Romano, 2003) and time temperature integrators (TTI) (Guiavarc'h *et al*., 2002b; Mehauden *et al*., 2007; Mehauden *et al*., 2008; Tucker *et al*., 2009). However, in this work we focus on two common techniques that used to validate thermal treatment efficiency; (i) thermocouple and data logger and (ii) enzymatic time temperature integrators. The comparison of both of them as follow:

2.7.1 Advantages of Thermocouples and data loggers

1) They can be placed inside the food container to record the thermal treatment undergone by the food.

2) It is easy and fast to analyse the data as we can download all the data record directly.

2.7.2 Disadvantages of Thermocouples and data loggers

1) Not convenient for some type of thermal processes such as batch processes.

2) Not optimal for moving processes, for example a wire data logger is not suitable for validation in jar while the jar was pasteurised in a tunnel pasteurisation.

3) Not suitable for some narrow locations, such as the corner of a jar, which was too small to fit the wireless data logger (Hendrickx *et al.*, 1995; Marra and Romano, 2003).

2.7.3 Advantages of enzymatic time temperature integrators.

The advantages of enzymatic TTIs are (Taoukis, 2012; Mehauden *et al.*, 2007; Tucker *et al.*, 2009, Van Loey *et al.*, 1996a; Van Loey *et al.*, 1996b, Mai et al (2007))

1) As 1-2 cm long tubes it is very easy to attach and place them in in any conditions of individual food processing and product.

2) Not necessary to know the product time temperature history to determine the thermal treatment effect on the food product.

3) They are wireless and shock resistant.

4) They can validate in points that the thermocouples and the data logger cannot measure.

2.7.4 Disdvantages of enzymatic time temperature integrators.

1) Not convenient for some type of thermal processes such as on-line monitoring for the efficiency of thermal treatment because their need time to analysis an enzyme activity, not immediately analysis.

2) They need extensive preliminary experiments to calibrate each batch of before use.

3) They tend to be inaccurate for short temperature-time processes, owing both to thermal lag between the outside and inside of the TTI and to errors in measurement and calibration.

2.8 Conclusions

This chapter has introduced the subject of this thesis, the monitoring of temperature profiles inside vessels undergoing pasteurization. The critical factors in heat transfer are: (i) supply of heat to the system by fluids flow, (ii) conduction and convective processes within the outside fluid, the glass wall of the jar and the food product.

Models for heat transfer have been developed in which conduction is assumed within the pack, and these models have been used to identify different heating regimes. In most commercial processes, the Biot number of the material is so large that internal processes are controlling the heat transfer response. Thermal processes can be validated by using thermocouples in static situations, or in process by using systems such as TTIs.

Chapter 3

Materials and Methods

3.1   Introduction

This chapter discusses the materials and methods utilised throughout this research. The first three sections contain information regarding the general approaches on materials and how to calculate heat transfer efficiency, the heat transfer coefficient in a pasteurised process, the preparation of Temperature Time Integrators (TTIs), an enzyme amylase activity analysis and a pasteurisation process value calculation (Mehauden, 2007). The fourth part of this work describes applications in a study of the thermocouples and TTI validation, using both a water bath and a spray pasteuriser rig as isothermal heating system. Several aspects were investigated including the heat transfer between a food container and its environment, its effect on temperature, fluid viscosity and driving force. The heat transfer in a two-phase liquid and solid system was studied both in a water bath and a spray pasteurisation experiment.

The potential enzymatic activity of the time temperature integrators (TTIs) made from BAA (as described in Chapter 2) was evaluated using a Peltier stage, which can deliver defined non-isothermal temperature profiles. The aims of the work conditions are to deliver variable temperature profiles, using controlled temperature-time programme that can be used to derive to test and apply TTIs for the mild thermal processes at the surface of pasteurised products. As discussed, the aim of the work

is to identify TTIs for the mild thermal processes on the surface of pasteurized products whether it is possible to determine heat transfer and within model equipment to mimic industrial surface pasteurisation.

3.2 Materials

3.2.1 Tris buffer preparation

A 0.05 M Tris buffer, pH 8.6 was prepared. A mass 6.057 g of Trizma base ($C_4H_{11}NO_3$) was dissolved in distilled water and adjusted to the targeted pH value of 8.6 using hydrochloric acid. After that, the required amount of distilled water was added to reach a total volume of 1000 ml and the solution was then stored at room temperature.

3.2.2 Amylase solutions preparation

A concentration 10 mg/ml of α-amylase solution was prepared. This was done by dissolving 200 mg of α- amylase powder (isolated from *Bacillus amyloliuefaciens* (BAA: A6380, Sigma, UK) into 20 ml of 0.05 M Tris buffer solution. The prepared amylase solution was stored at -18°C. The pH activity range for BAA was between 5.5 and 6.5, with the optimum activity rate being reported for a pH value of 5.9 and at a temperature of 65°C.

3.2.3 Temperature Time Integrators (TTIs) preparation

Temperature Time Integrators (TTIs) were prepared according to the method provided by Tucker (2002) and Mehauden *et al.* (2007). BAA TTIs were prepared by

adding the amylase solution (20 μl) into high strength, small sized silicone tubes. Two different sized tubes were used (Altec, Cornwall, UK): 2.0 mm and 2.5mm bore respectively with a 0.5 mm thick wall. Firstly, the tubes were cut into 1.5 cm segments as shown in Figure 3.1. Then, one end of each tube piece was dipped into a silicone elastomer (Sylgard 170, Dow Corning, USA) to produce a seal that was approximately 2-3 mm thick. After that, the tubes were treated in a hot air oven at 70°C for 30 minutes. A volume of 20 μl of the BAA solution was injected into the tubes using a syringe and the tubes were then sealed off using the Sylgard silicone elastomer (at a cold temperature). The enclosed TTI tubes were then re-heated in hot air oven at 40°C for another 30 minutes. Given that the activity of amylase can easily be destroyed by heat, it is important to maintain heating temperatures below 40°C at a duration no longer than 30 minutes per sample (Tucker, 2008). The readily prepared TTIs were then stored in Tris buffer solution in a freezer for up to 6 months.
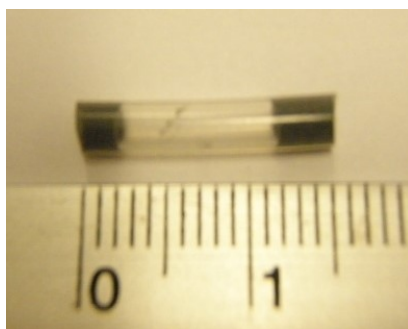
Figure 3. 1: Picture showing real size TTI tube.

3.2.4 Fluids preparation

Fluids with similar viscosities to those of real foods, corn starch and guar gum, were studied to find the effect of viscosity on thermal process efficiency. The fluids used for the experiments were:

(i)   water,

(ii)   a solution of 4% (w/v) of modified corn starch (Colflo 67, National Starch & Chemicals, Manchester UK),

(iii)   a solution of 4% (w/v) of pre-gelatinised modified corn starch,

(iv)   a solution of 1% (w/v) of guar gum (G4129, Sigma Aldrich, UK) and

(v)   a solution of 3% agar (w/v)

Colflo 67 and guar gum are used as thickening and stabilising agents in the food industry and therefore are directly relevant to this section of study. Colflo 67 normally starts to gelatinise at 69°C and its maximum viscosity is reached at 80-85°C. Guar gum solutions are non-Newtonian fluids with a good stability between pH 1 and 11.

The solutions of interest (the 4% (w/v) corn starch solution, the solution of 4% (w/v) of pre-gelatinised corn starch and the solution of 1% (w/v) of guar gum) were prepared as it will be described in Section 3.7.1.

For experiments with solids, potatoes were purchased from the *Aldi* convenient store located near the Birmingham University. The potatoes were peeled and cut into 1 cm^3 pieces, and were then blanched for 5 minutes at 80°C. For each solution, two solids fractions of potato cubes were considered, which were 10% (w/w) and 50% (w/w).

3.3 Convective heat transfer coefficient calculation

According to Incropera *et. al.* (2006), there are three fundamental forms of heat transfer: convection, conduction and radiation. We can calculated these three values as equation as eq 2.1 and eq.2.2 in section 2.2.1.

Generally, heating in a solid results in temperature changes that usually lead to internal thermal gradients. If the solid has a high thermal conductivity, however, the lumped approximation can be used (Incropera *et. al.*, 2006). A lumped heat capacity system model is a simple system in which the temperature changes the uniformly throughout a piece of solid (Incropera *et. al.*, 2006). The lumped capacitance method can be used to study heat transfer to a solid, in an experiment where the solid is affected only by its thermal environment. Given that the solid will exhibit and uniform temperature throughout in, it can be considered a lumped system. From the energy balance on the solid at a time *t,* the rate of thermal energy given to the fluid must equal the rate of change of the the internal energy. This can be expressed in the following form:

$$-hA_s(T_s - T_\infty) = \rho C_p V_c \frac{dT}{dt}$$
Eq (3.1)

where ρ is the density (kg/m³) of the solid, C_p is the specific heat of the object (J/kgK) V_c is the solid volume (m³) and T is temperature. Consecutive manipulation of equation (3.1) will lead to the following two expressions:

$$\frac{(T-T_\infty)}{(T_i-T_\infty)} = exp\left[-\left(\frac{hA_s}{\rho V_c c_p}\right)t\right]$$

Eq (3.2)

$$\ln\left(\frac{(T-T_\infty)}{(T_i-T_\infty)}\right) = -\left(\frac{hA_s}{\rho V_c c_p}\right)t$$

Eq (3.3)

where T_i is the initial temperature of the object.

3.4   Time Temperature Integrators (TTIs)

3.4.1 Amylase activity measurement

The Randox Amylase Test method (AY 1582 Amylase; Ethylidene PNPG7 method) (Randox, 2010) was used to measure amylase activity. Ethylidene-blocked p-nitrophenyl-maltoheptaoside was used as the substrate, and was reduced by amylase. The resulting solution was then hydrolysed by α-glucosidase to yield glucose and a yellowish solution of p-nitrophenol. The concentration of p-nitrophenol (yellow colour) was determined by measuring the absorbance using a spectrophotometer. The following procedures were undertaken:

1) A sample of 10 µl was taken from the TTIs using a syringe; it was placed into a 1 ml cuvette and diluted with 290 µl of the Tris buffer. A volume of 1ml of the enzyme assay reagent from the Randox (UK) was then added. After that, the cuvette was immediately placed into a spectrophotometer cell and the absorbance at a

wavelength of 405 nm was measured. The absorbance values were recorded at 0, 1, 2, 3 and 4 minute. The different absorbance value (ΔA) can be calculated from the difference of the final absorbance values (A at t=4 min) and the initial absorbance values (A at t=0 min)

2) The amylase activity (Randox, 2010) can be calculated as:

$$\text{Amylase activity(U/l)} = 4712 \times (\Delta A) \qquad \qquad \textbf{Eq (3.4)}$$

where ΔA is the difference between the final and initial absorbance values at 405 nm.

According to Mehauden *et al*., (2007) and Mehauden (2008), the reaction rate can be calculated using these data. At a constant concentration of amylase, the initial reaction rate is given by:

$$r_A = k_f \, C_{BAA} \qquad \qquad \textbf{Eq (3.5)}$$

where r_A is the reaction rate, k_f is the first order rate constant, and C_{BAA} is the concentration of BLA (Cornish-Bowden and Wharton, 1988). The absorbance slope and time data were collected from the spectrophotometer. Then the reaction rate was estimated using this information. Hence, the initial concentration of the sample ($C_{BAA}(0)$) and the initial rate can be compared.

Therefore, the initial and the final enzyme activity ratio can be calculated using equation (3.6):

$$\frac{A_{initial}}{A_{final}} = \frac{C_{BAA}(0)}{C_{BAA}} = \frac{r_{A0}}{r_A} \qquad\qquad \textbf{Eq (3.6)}$$

3.4.2 Time Temperature Integrators (TTIs) calibration procedure

To calibrate the TTIs is necessary to study their behaviour under known conditions (Mehauden et al., 2007; Mehauden et al., 2008; Tucker, 2009), the influence of time and temperature on enzyme activity was thus investigated. The BAA TTIs were placed into a water bath at five different temperatures (65°C, 70°C, 75°C, 80°C, and 85°C). The TTI samples were removed from the water bath at different time intervals starting at 0, 1, 2, 3, 4, 5, 6, 8, 10, 12, 15, 20, 25, 30, 35, 40 and 50 minutes, respectively. They were then cooled down immediately in an ice-cold water bath to fix the amylase activity until such samples could be analysed. Subsequently, a syringe was used to taken the enzyme solution from the tube so that the amylase activity was determined as described above in Section 3.4.1.

3.4.3 TTIs calibration curve

TTI calibration curves were plotted in the way defined in previous studies (Mehauden et al., 2007; Mehauden et al., 2008; Tucker, 2009). Using the data of all experiments the calibration curve of TTI from BAA was plotted so that the D and Z values could be calculated. The initial enzyme activity (X_0) is the average of three unheated TTI samples. The TTI calibration curve shows the relationship between $log(X/X_0)$ versus time. The slope of each temperature was used to determine the D value. The curves were fitted using Microsoft Excel 2010 software.

Figure 3.2 shows the relationship between the heating times and logarithm of the final rate of enzyme activity divided by the initial rate of enzyme activity of TTIs made from BAA at five different temperatures. The D values were calculated from $-1/slope$.
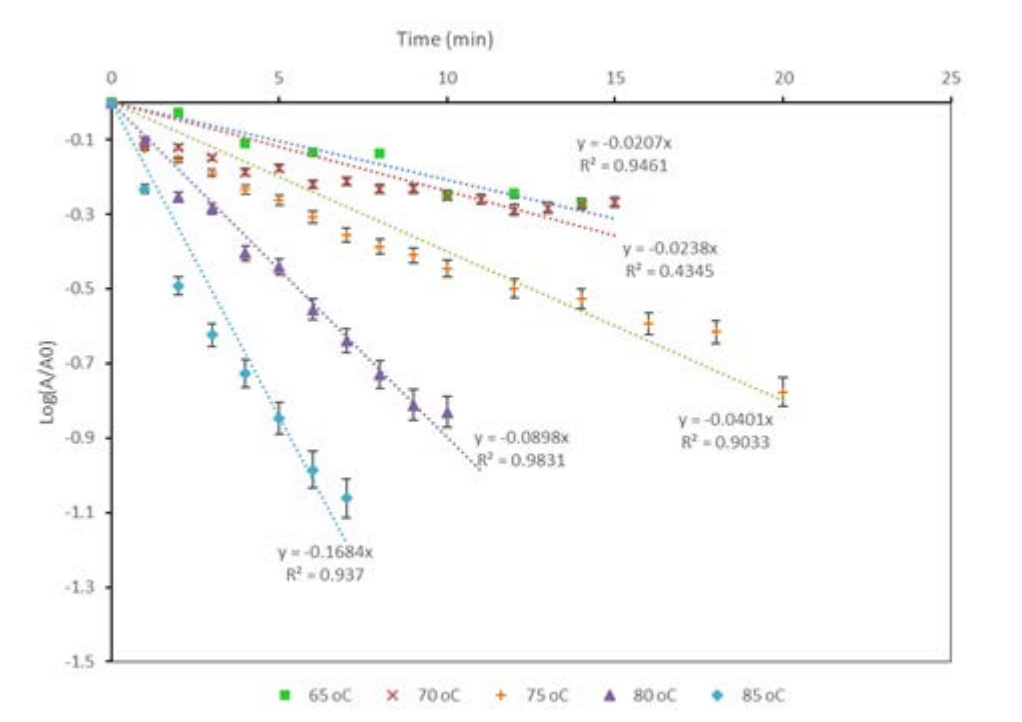
Figure 3. 2: BAA TTIs calibration curve.

3.4.4 Calculating the D-values and z values

According to Mehauden (2008), the z value represents the relationship between the D_T values and temperature. It can be calculated using equation (3.7) shown below. D_T values were determined at three different temperatures (75, 80, and 85°C) and the z values were obtained from the variation of the D_T value. Hence, the z value can be calculated from the D_T values using:

$$z = \frac{\log[{}^{D_{T_2}}\!\big/\!{}_{D_{T_1}}]}{T_1 - T_2}$$ **Eq (3.7)**

where D_{T_2} and D_{T_1} are the decimal reduction times at T_2 and T_1.

From Section 3.4.3, D values for all temperature and enzyme were calculated from – 1/slope of each line in Figure 3.2. D values of BAA calculated at 65°C, 70°C, 75°C, 80°C, and 85°C are 48, 42, 25, 11, and 6 minutes, repectively. A graph showing log D_T against the heating temperature for TTI made from BAA is shown below in Figure 3.3. The slopes of these graphs were used to determine the z value using equation (3.7) (Mehauden *et al.*, 2007; Mehauden *et al.*, 2008; Tucker, 2009). The variations of D values were used to calculate the Z values, resulting in 16.0 °C at 80°C for this research.
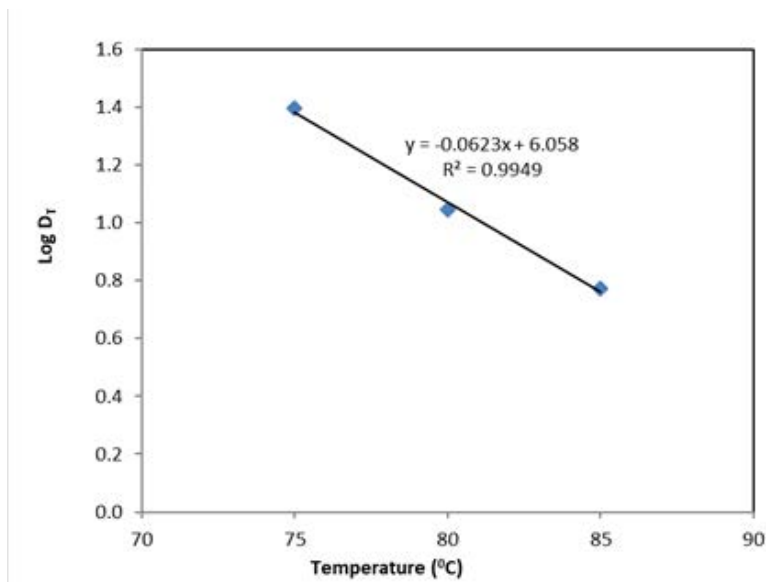
Figure 3. 3: Logarithm of the D_T values against temperature for Z value calculation.

3.4.5 P- value calculation

The main kinetic parameter used to ensure safety is that of the kinetics of thermal death of microorganisms. TTIs should have temperature-induced denaturation kinetics that are close to the death kinetics of the targeted microorganisms; ideally the temperature sensitivity of the rate constant (z or E_a value) of the TTI and the microorganisms should be equal (Mehauden *et al*., 2007; Mehauden *et al*., 2008; Tucker, 2009). Heat efficiency or process values can be calculated in terms of F-values (for sterilisation) or P-values (for pasteurisation) as follows:

$$P \ (or \ F) = \int_o^t 10^{\frac{T(t)-Tref}{z}} . dt \ = D_{T(ref)}.log\left(\frac{N_{initial}}{N_{final}}\right) \qquad \textbf{Eq (3.8)}$$

where, *T(t)* is the product temperature (°C), T_{ref} is the reference temperature for the D_T value (°C), t is the process time (minutes), *z* is the z values the number of degrees centigrade needed to bring about 10 times change in decimal reduction time. The P values of a process have the dimension of time;, as it is the time that the process would take if carried out at the reference temperature. As well as from the integral form presented above, the P values can be calculated from the relative concentration of organisms too, as shown in the second part of the equation (3.8). There, *N* is number of microorganisms, D_T(s) is (decimal reduction time) time necessary to reduce the number of microorganisms by 90%.

3.5 Experimental apparatus

3.5.1 Instrumentation of vessel

This research was set up to instrument with both thermocouples into a vessel and its environment (both a water bath and a muti jet). A 330 ml glass jam jar (76 mm in diameter x 95 mm in length x 3 mm thickness) was used as container. The bottom of jar have a concave bottom. A small hole was made in the container lid to allow a transparent polyvinylchloride tube to pass through to fit the K-type thermocouples. The jar was siiting on the bottom of the water bath. The heating and cooling temperatures were measured in eight locations shown in Figure 3.4 and also listed next:

1) location 1 is at the centre (R) and the bottom (1/4H),

2) location 2 is at the centre (R) and the half height (1/2H),

3) location 3 is at centre (R) and the top of jar (3/4H),

4) location 4 is at the ½ of radius(1/2R) and the half height (1/2H),

5) location 5 is at the ¼ of radius(1/4R) and the half height (1/2H),

6) location 6 is at the inside jar wall ,

7) location 7 is at the outside jar wall and,

8) location 8 is at water in water bath
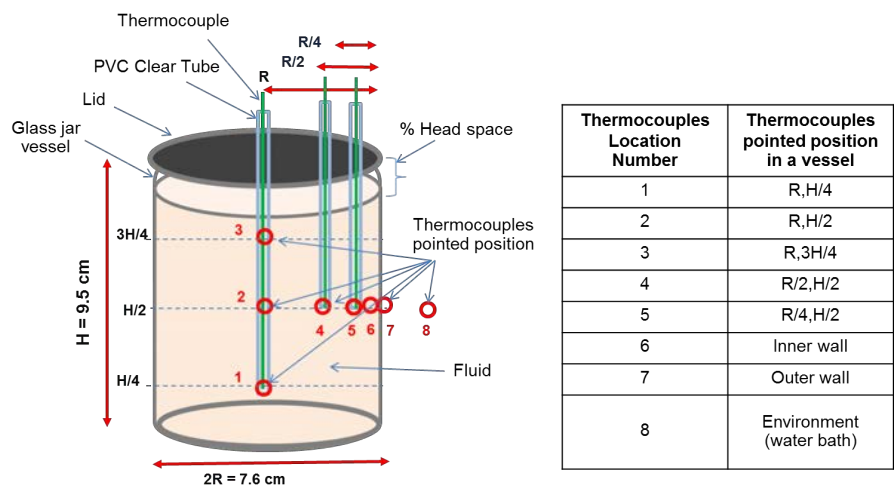
Figure 3. 4: Thermocouples set up for the jar vessel employed in the pasteurisation experiments.

Eight calibrated thermocouples (type K) and data loggers (model: USB TC-08 Thermocouple Data Logger, Pico Technology, UK, having a temperature accuracy of ±1˚C) were used. Sample solutions were added into the containers at ambient temperature, with 5% headspaces. Heating was provided either by immersion into a water spray or by placing the vessel under a water bath at 60°C, 70°C, and 80°C. Each experiment involved heating for 30 minutes and subsequently cooling down for 10 minutes.

3.5.2 Water bath

Generally, thermocouples are used to measure the effects of thermal processes. Before utilising the TTIs, the first step in the study used only thermocouples to characterise heat transfer in a glass container during pasteurisation. The aim of this

first part of the study was to evaluate the temperature profiles and heat transfer behaviour between the hot water bath, the glass jar container, the fluid inside the jar and the P values. The water bath experimental set up is shown in Figure 3.5. Parameters investigated in subsequent Chapters include (i) temperature of the water bath, (ii) water bath condition or convection mode effect (forced and natural convection, i.e. with or without water bath stirring), (iii) viscosity of the fluid inside the jar container, (iv) container size and (v) percentage of headspace (space between surface of solution and lid of container). Following, TTIs were applied also to the conditions analysed in the first step, and the accuracy between TTIs and thermocouples was compared.
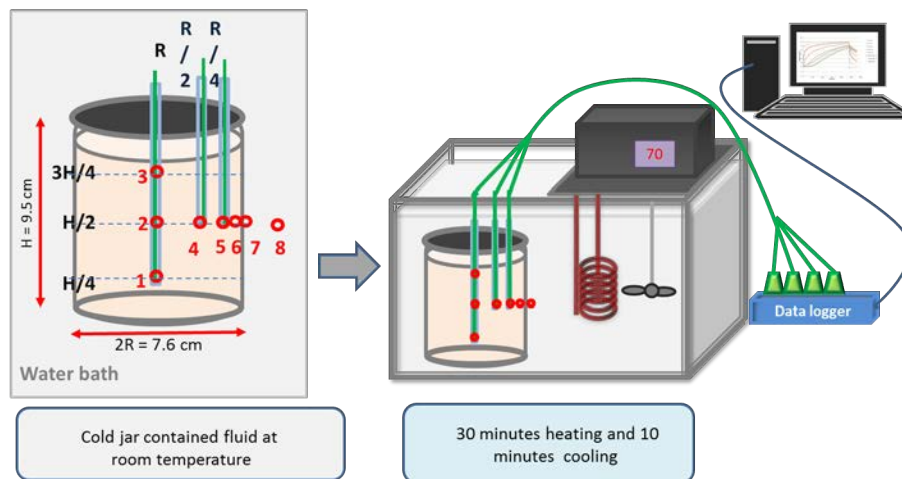
Figure 3. 5: Water bath experimental set up employed in this study.

3.5.2.1 Effect of temperature, solution viscosity, convection mode, and container size on heat transfer in a water bath

Thermocouples were used to measure the thermal response of the system during pasteurisation. Water and a 3% agar solution, which represent the single phase for liquid (convection) and solid (gel; conduction), were used to investigate the temperature changes before and after the thermal processes. A 330 ml jam jar (76mm in diameter x 95mm in length) was used as a glass container. The experiments were set up as detailed in Sections 3.5.1 and 3.5.2. Each experiment involved a heating stage for 30 minutes followed by a cooling step of 10 minutes.

3.5.2.2 Effect of the container's headspace percentage on heat transfer in a water bath

The investigation also included the effect of different percentages of the container's headspace on the systems heating rate. For this piece of the study, experiments were conducted in a stirring water bath at 70°C. Figure 3.6 shows the four locations where thermocouples were pointed:

1) location A: at head space and inner wall of vessel,

2) location B: at a container lid,

3) location C: at fluid surface, centre of jar, and

4) location D: water bath

As done previously, the temperature profiles, P values and heat transfer coefficients were obtained for various thermal treatments following the procedure detailed in Section 3.5.2.
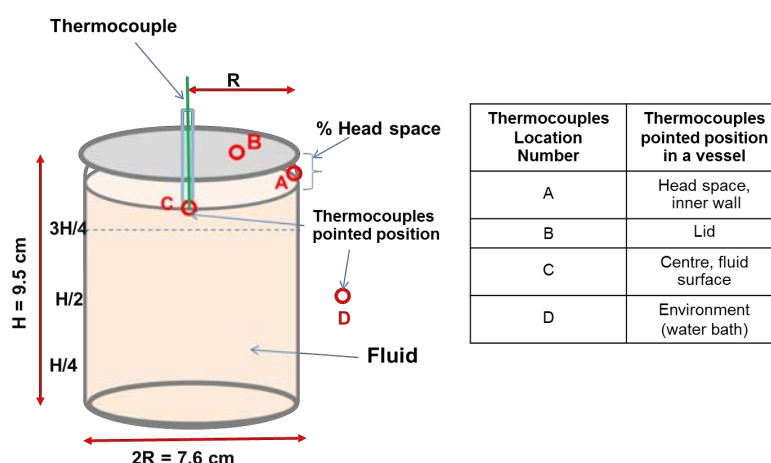
Figure 3. 6: locations of thermocouples for an effect of percentage of headspace study.

3.5.2.3 Repeatability

To make sure that the results obtained truthfully describe the behaviour of the system an experimental errors and sample variability effect on the measurements are minimised, every experiment was conducted in triplicate. Figure 3.7 shows a typical example of the triplicate temperature profiles obtained during the experiments. As can be seen, all them represent the same thermal behaviour without significant variations.
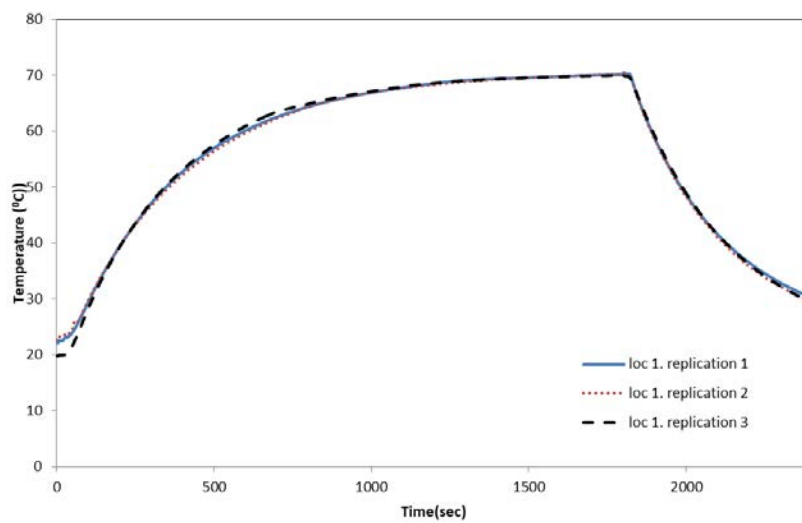
(a)
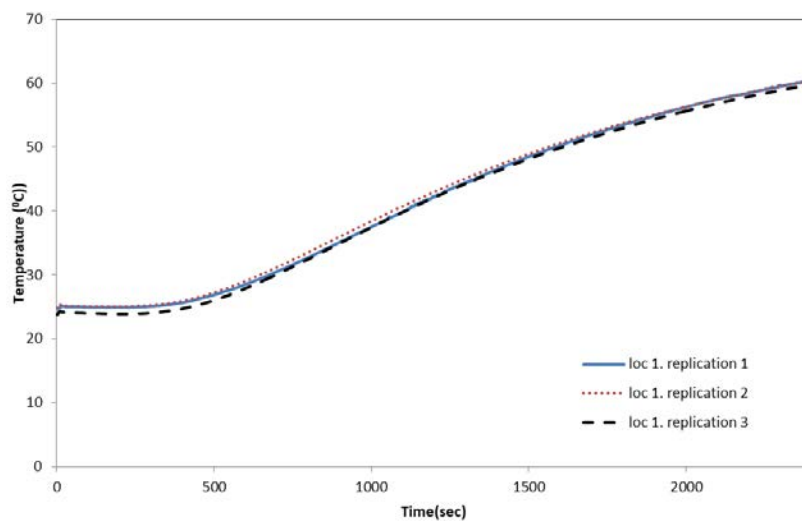
(b)

Figure 3. 7: Temperature profiles in triplicates: replication 1 (solid), replication 2 (dotted) and replication 3 (dashed) obtained during the pasteurisation experiments conducted in the water bath for jars containing (a) water and (b) 3% (w/v) agar solution. The temperature of the water bath was 70ºC in all cases. All the temperature profiles shown correspond to the center of the jar (location 1).

3.5.2.4 Heat transfer coefficient in the water bath

To calculate the convective heat transfer coefficient characteristic of the water bath operation the energy balance around the jar wall has been employed. The inward heat flux rising the temperature of the jar is a convective flux – heat transferred from the heating medium (water bath) to the jar wall:

$$q_{conv} = h(T_{bath} - T_{wall}^{out})$$ **Eq (3.9)**

while the heat transferred through the glass wall to the jar filling product is a conductive term:

$$q_{cond} = \frac{k_{glass}}{\delta_{glass}}(T_{wall}^{out} - T_{wall}^{in})$$ **Eq (3.10)**

As inward and outward fluxes must be equal, the following relationship is obtained:

$$h(T_{bath} - T_{wall}^{out}) = \frac{k_{glass}}{\delta_{glass}}(T_{wall}^{out} - T_{wall}^{in})$$ **Eq (3.11)**

from where the heat transfer coefficient h can be obtained once the external an internal wall temperature together with the temperature of the water bath are known. In this study, the reading of the thermocouples will provide the required T_{wall}^{in} , T_{wall}^{out} and T_{bath} data.
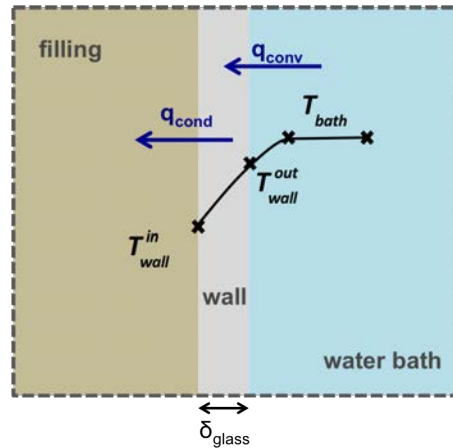
Figure 3. 8: Equivalent thermal circuit considered in the calculations for convective heat transfer coefficient in the water bath.

3.5.3 Shower spray vessel

Figure 3.9 shows the spray pasteuriser rig built to mimic at lab scale the operation of a real pasteurisation tunnel. The spray shower unit consist of a metallic box of dimensions 50cm x 50 cm x 100 cm (length x width x height). Temperature of the system was controlled by a thermostat at the feed tank. The hot water was pumped to a multijet head. The temperature at the nozzle was measured and controlled. Hot water after the pasteurisation process was then recirculated to feed tank. Water flowrate was controlled by pump speed. Multijet specifics are as follows; spray nozzle was a 120 degree spray angle

-*single jet* is a free end nozzle with 1.5 mm diameter

-*multijet* : all water flow was controlled flow directly to the top of jar. The water flow area was limited to 7.6 mm diameter.

The water temperature after the process dropped by around 2-4 ^0C
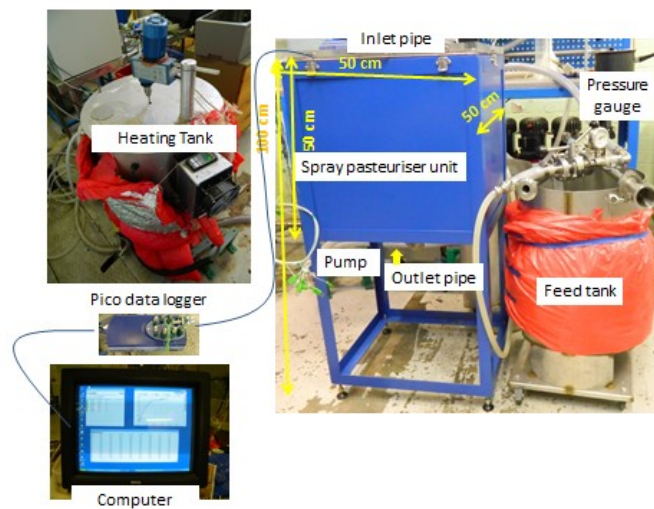
Figure 3. 9: Spray pasteurisation rig built for this study.
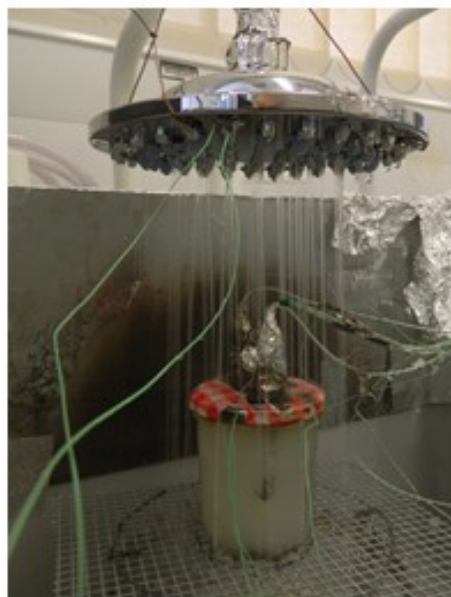
Figure 3. 10: Picture of one of the spray pasteurisation experiments performed in the spray rig showing the placement of the jar and the operation of the system.

3.5.3.1 Effect of temperature, solution viscosity, and container arrangement on the spray pasteurisation heat transfer dynamics

To study and better understand the fundamental aspects of heat transfer in a spray pasteurisation process, a simple shower was applied to simulate a pasteurisation tunnel.

In this part of research, temperature profiles and heat transfer behaviour of the shower, the jar container and the fluid inside the jar were investigated, as done with the water bath experiment in Section 3.5.2. Results obtained were then compared to the heat transfer profile acquired during the spray-pasteurised process.

Jars were equipped with thermocouples and were filled with (i) water (ii) 3% (w/v) agar solution and (iii) 3% (w/v) corn starch solution. Experimental variables potentially affecting the heat transfer dynamics during the spray pasteurisation problem include viscosity (water, 3% (w/v) agar and 3% corn-starch solution), temperature (60, 70 and 80°C) and shower flow rate (from 0.5 l/min to 1 l/min) were all investigated. The P values were calculated as explained in Section 4.3.5.

3.5.3.2 Heat transfer coefficient of a falling film

A lumped parameter experiment was set up for the determination of the convective heat transfer coefficient between spray film and vessel. An aluminum block was used in this lumped study. The heating tank temperature was set up to approximately 45°C. Spray water from the heating tank was sprayed onto the aluminium block at a

set flow rate, whilst temperature readings and time were simultaneously by the software monitoring the thermocouples. The aluminium block was placed into the vessel after the flow rate and recordings had begun. A note of the time at which the aluminium block was entered was made and data before this time was later disregarded. Once a steady temperature of 45°C was reached, the plate was removed from the spray and left to cool to room temperature. Temperature was measured on the surface and in the centre of the aluminium block throughout the heating and cooling processes.

The heat transfer coefficient was calculated using the lumped capacitance method as shown in equation (3.12) below (Incropera *et. al.*, 2006):

$$h = \frac{\rho C_p L_c}{t} \ln\left(\frac{T - T_{inf}}{T_0 - T_{inf}}\right)$$ **Eq (3.12)**

where ρ and C_p are the density (kg/m^3) and heat capacity (J/kgK) of aluminium, respectively, and T_{inf} is the temperature of the water in the heating tank in this particular case.

From section 2.5 chapter 2, **Eq (2.14)** The *Biot* number is usually employed used to determine whether a system is lumped or not, and it is defined as follows (Incropera *et. al.*, 2006):

$$Bi = \frac{h L_c}{k}$$ **Eq (2.14)**

3.6 Heat transfer in a two-phase (solid-liquid) system

As discussed in Chapters 1 and 2, many food materials are two-phase. In this part of the experiment, a two-phase solid-liquid system was used as a substitution to mimic the properties of real food that have similar solid and liquid proportions like that as soup, salsa, and sauces. The aim of this research was also to evaluate the use of TTIs as a potential industrial tool that can be applied during mild pasteurisation and can be used to optimise thermal processes in food industrial fluid studies. The variation in temperature for fluids of different viscosities and different amounts of solids will be investigated as in Section 3.5. The investigated parameters include fluid viscosity and proportion of solid and liquid.

3.6.1 Solid-liquid experimental set up

For this section, the aim was to investigate heat transfer in solid- liquid mixtures during mild thermal processing conducted in a water bath. Figure 3.11 show the container which was prepared and fitted with nine calibrated thermocouples (type K) of which five of those were used to measure the temperature of the container and the fluid. The remaining four thermocouples were used to measure the temperature of the potato at varying locations (centre bottom, half height and top of the container and ½ of radius) as shown in Figure 3.11. Pasteurisation experiments were carried out in which: (i) the container was placed in a mixing water bath at 70°C, as described in Section 3.5.2 (ii) the container was placed under the spray heads as described in Section 5.3.5.

Thermocouples Location Number	Thermocouples and cubed potato pointed position in a vessel
1, Fluid	R,H/4
2, Fluid	R,H/2
3, Fluid	R,3H/4
4, Fluid	R/2,H/2
1, Potato	R,H/4
2, Potato	R,H/2
3, Potato	R,3H/4
4, Potato	R/2,H/2
5	Environment (water bath/ spray head)
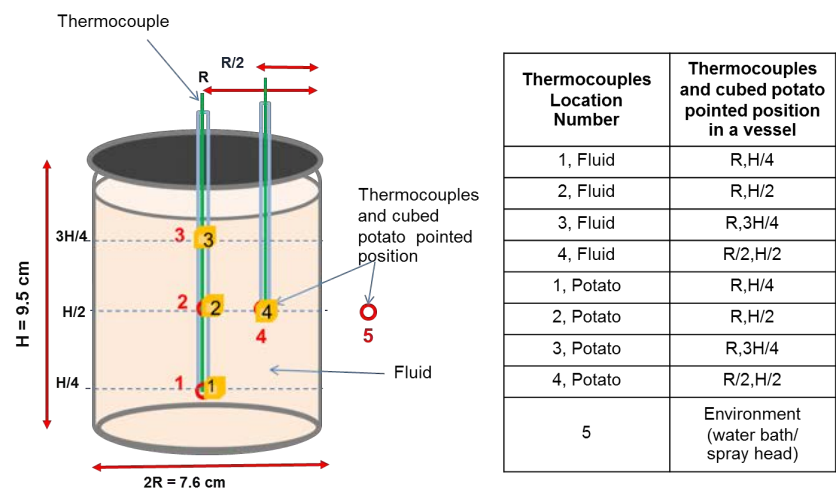
Figure 3. 11: Schematics of the vessel employed during the two-phase pasteurisation experiments showing the locations where the temperature has been measured for both solid and liquid phases.

Chapter 4

Evaluation of mild thermal processes for food decontamination: water bath study

4.1 Introduction

Pasteurisation is a mild heat treatment carried out at temperatures lower than 100°C with the aim of minimising concentrations of microorganisms within the food product and thus increasing its shelf life (Fellows, 2000). Industrially, this operation takes place in long tunnels where the already packaged food products go through a series of water jets/sprays, which are separated into a number of heating and cooling zones (Lewicki, 1983a, Horn et. al., 1997). This is a widely employed technology, which finds applications in areas such as brewing (Horn et. Al., 1997, Dilay et. al., 2006, Bhuvaneswari and Anandharamakrishnan, 2014), juices (Aganovic et. al., 2014, Saikia et. al., 2015, Escudero-López, et, al., 2016) or sauces (Fellows, 2000).

Although spray pasteurisation is considered to be a safe and reliable method of food and package decontamination (Briggs et al., 2004), it is also an expensive operation. According to Briggs et al. (2004), in the brewing industry, it is the most expensive method of pasteurisation in terms of both capital and operating costs. the water and energy required to heat the spray water define the operating cost, and they are closely related to the efficiency of the system: too low a water flow per pack would give slow heating to the process, which could lead to biological risks, whilst too high a water flow would result in heat efficiencies that would be excessive for a profitable

operation. In this processing scenario, the optimisation of the standard operation – by increasing the operation efficiency - could lead to significant savings in energy and water.

However, to control the heat transfer rates and obtain the desired – optimal – heating rates and safe processing values, a deeper understanding of the system heating dynamics is required. To help with this, a first approach of pasteurisation using a water bath as heating medium is presented in this chapter. The water bath can be seen as the very upper limit of the spray pasteurization tunnel operation, where the heat transfer rate is independent of the spray flow (i.e. infinite mass flow heating up the product and high Biot numbers), so heat transfer is internally controlled.

To analyse the heating dynamics of the water bath system, a series of experiments covering different process conditions, container geometries and filling product viscosities have been performed at lab scale, and the results are presented next.

The chapter is organized as follows: Section 4.2 presents the thermal response (experimental temperature-time profiles) of the system under different heating conditions for a range of filling products exhibiting different viscosities. The effect of both container size and headspace on the heating dynamics of the water bath system is also assessed in this subsection. The process values (P values) resulting of integrating those experimentally obtained temperature profiles are shown in Section 4.3. In Section 4.4 the TTI's performance is evaluated and finally in Section 4.5 the heating dynamics of a two-phase (solid-liquid) system are discussed.

4.2 Characterization of the thermal response of the water bath system

The thermal response of the system time-temperature profiles - has been characterized through a series of experiments conducted in a water bath for a range of different heating conditions. The experimental set up follows the design showed in Section 3.5. and Figure 3.4

The heating and cooling temperatures were measured in eight locations, as shown in Figure 3.4, using calibrated thermocouples (type K) and data loggers (model: USB TC-08 Thermocouple Data Logger, Pico Technology, UK, having a temperature accuracy of ±0.5°C). The temperature profiles were recorded every second for 30 minutes during heating and 10 minutes cooling.

Table 4. 1: Systems and experimental conditions employed in the water bath study

Solution	Container sizes (ml)	Convection mode	T (°C)
Water	330 and 660	Forced and natural convection	60, 70, 80
3%(w/v) Agar	330 and 660	Forced and natural convection	60, 70, 80
10%(w/v) Sugar	330 and 660	Forced and natural convection	60, 70, 80

Table 4.1 shows the different systems and conditions employed during the pasteurisation experiments carried out in the water bath. Temperature profiles, process values (P values) and heat transfer coefficients were obtained for all these thermal treatments.

The effect of five factors - listed next- on the thermal response of the system was evaluated:

(i)   Water bath temperature: 60°C, 70°C and 80°C.

(ii)   Viscosity: using water, a 10% (w/v) sugar solution and a 3% (w/v) agar solution as fillings.

(iii)   Convection mode: natural convection and forced convection (i.e. stirring water bath).

(iv)   Container size: 330 ml (7.6 cm diameter x 9.5 cm height) and 660 ml (8.7 cm diameter x 15.7 cm height).

(v)   Headspace: 5% and 10% of the container volume.

4.2.1 Effect of the heating temperature and fill liquid viscosity

Figure 4.1 shows the measured temperature profiles for three heating temperatures in the water bath for (a) water, (b) the 10 (w/v) % sugar solution and (c) the 3 % (w/v) agar solution with 5% headspace. The initial temperature in the three systems was approx. 20°C (room temperature). These temperature profiles show:

A rapid heating for the water filling between the beginning of the experiment up to approx. 800s, with the system reaching the water bath temperature before 1500s; a

rapid cooling can be also observed once the jar was removed from the bath (after 1800 s).

For the 10% sugar solution, slightly slower heating rate, with a slower approach to the water bath temperature (after 1700s).

For the 3% (w/v) agar filling, the graph shows (i) the slowest thermal response, characteristic of system with high viscosity or solids (and closer to conduction-driven dynamics), with the system temperature still approaching the water bath set point by the end of experiments (ii) no cooling stage.

Figure 4.2 shows temperature profiles for (a) the water system (with 5% headspace), (b) the 10 (w/v)% sugar solution and (c) 3% (w/v) agar solution. Table 4.2 lists the viscosity values of each filling product. The starting temperature of each experiment was approx. 20°C in all cases. The water bath was heating up the system for 30 min at 70°C, while the cooling stage was set up for 10 minutes.

Table 4. 2: Fillings employed in two-phase experiments and their viscosity values (at 20°C.)

Jar filling	Viscosity (Pa s)	Reference
Water	1.002×10^{-3}	Deen (2016)
10%(w/v) sugar	1.96×10^{-3}	Telis et al (2007)
3%(w/v) Agar	1450	Kasapis (2009)

Note: the 3% (w/v) agar had a hard gel texture.
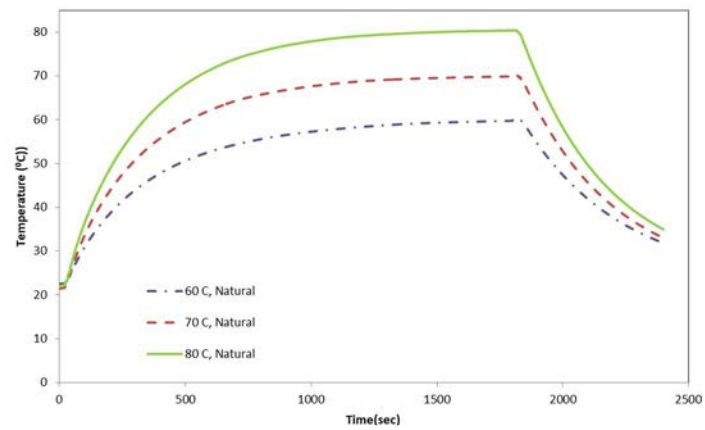
(a)
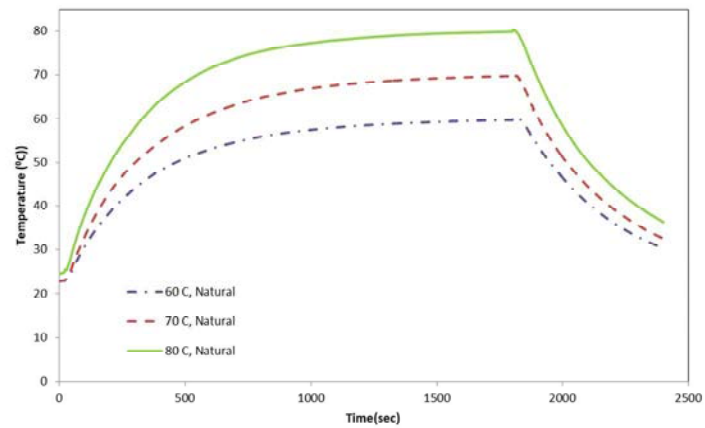
(b)
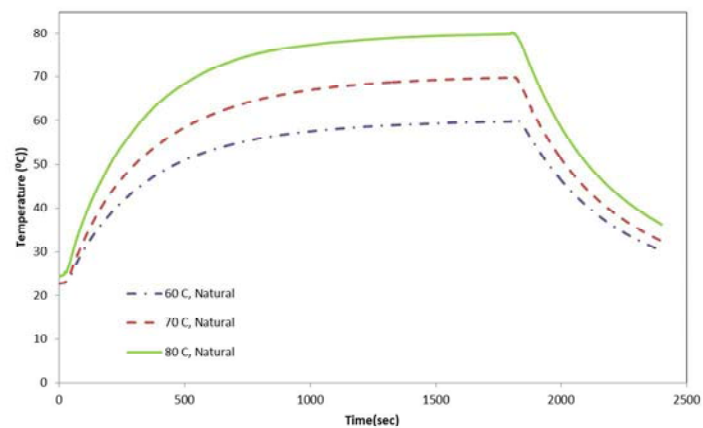
(c)

Figure 4. 1 Temperature profiles obtained for heating temperatures of 60 ºC (dashed-dot), 70ºC (dashed) and 80ºC (solid) in three different systems: (a) water, (b) 10% sugar and (c) 3% agar.

In both water and sucrose systems the coldest point was found at the bottom of the jar (location 1). Temperature values increase with height (hot spot at location 3, top of the jar), while there are no significant temperature gradients on the radial direction (similar temperature profiles at locations 2, 3, 4, and 5). The observed heating dynamics correspond to a system where convection drives heat transfer in the product: the filling water is heated, then expands and rises being replaced by cooler water, from the side of wall to the centre of jar.

On the other hand, the 3% (w/v) agar solution presents temperature values higher at the jar wall - i.e. closer to the heat source - that decrease on the radial direction, with the coldest point located at the centre of the container (location 2). Such heating dynamics are characteristic of conduction driven heating scenarios, as could be expected for a viscous filling as the 3% agar solution studied. As can be seen in Figure 4.2(c) the thermal response is the slowest of the three systems presented in this section, with the product temperature still increasing (and the interior points 20°C below the water bath temperature) by the final time of the experiment.

Figure 4.3 illustrates the differences between the heating dynamics of the product filling exhibiting a higher viscosity, i.e. the agar solution, and the behaviour of the 3% water and sugar solution. In this graph the temperature profiles corresponding to the centre of the jar (location 2) for the three product fillings are compared. A faster thermal response was observed also for both water and a 10% sugar systems – the ones with lower viscosities - during the cooling stage, while the 3% agar was still reaching its highest temperature at the same processing times.
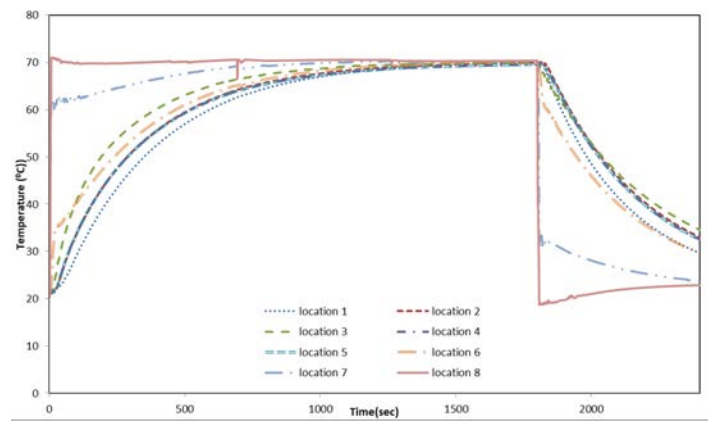
(a)
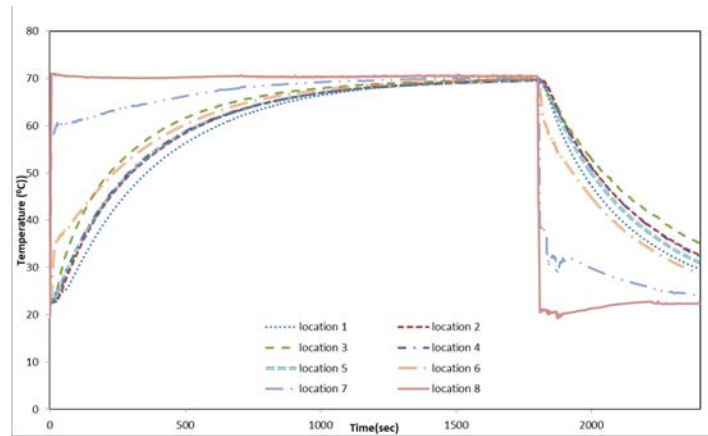
(b)
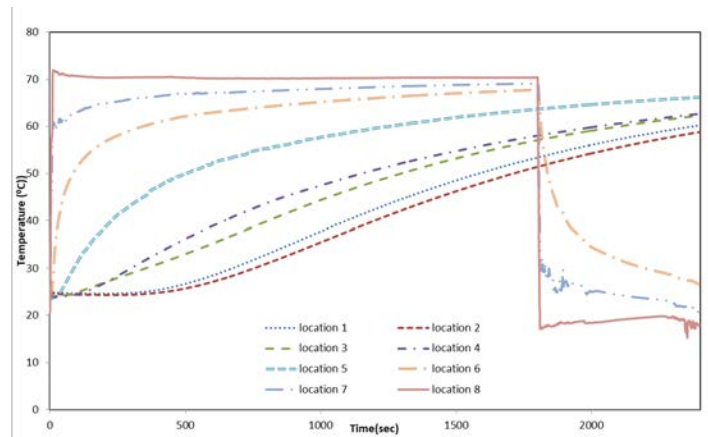
(c)

Figure 4. 2: Temperature profiles for three different solution systems: (a) water, (b) 10% (w/v) sugar and (c) 3% (w/v) agar. The water bath heating temperature was 70°C.
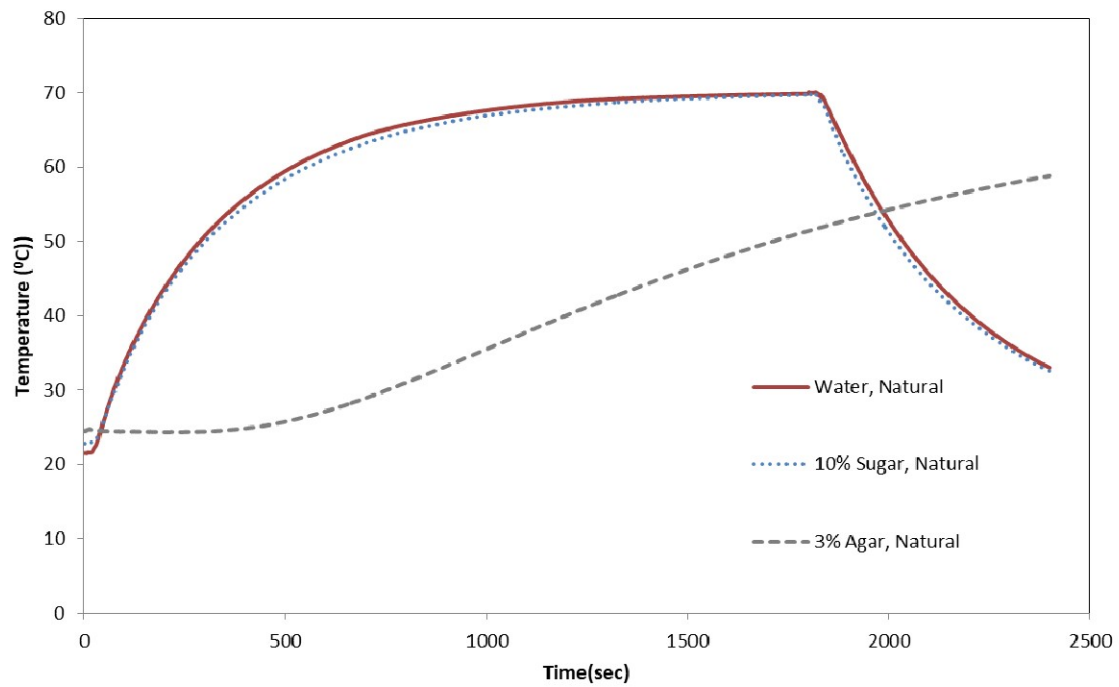
Figure 4. 3: Temperature profiles for systems exhibiting different viscosity values: water (solid), 10% sugar (dotted) and 3% agar (dashed). The heating temperature was 70ºC in all cases. The temperature profiles shown correspond to the centre of the jar (location 2).
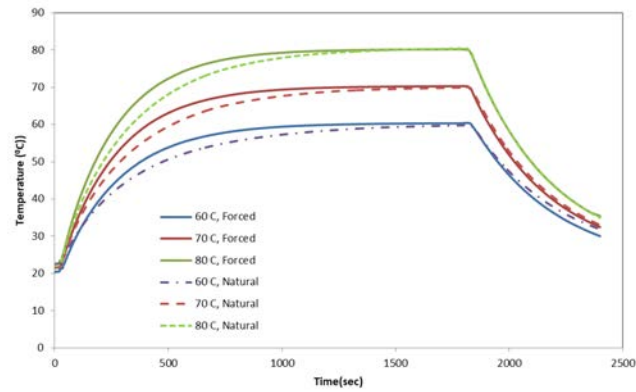
(a)
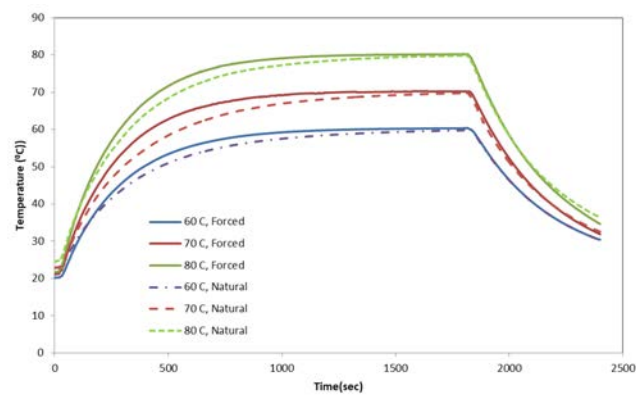
(b)
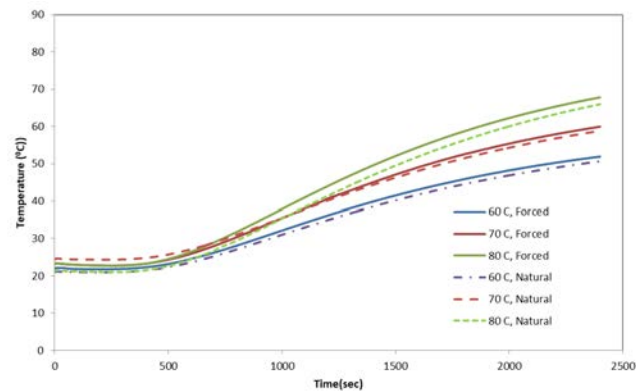
(c)

Figure 4. 4:Temperature profiles at location 2 for forced (solid) and natural (dashed) convection in jars containing: (a) water, (b) 10% sugar solution and (d) 3% agar solution for heating temperatures of 60°C (blue), 70°C (red) and 80°C (green).

4.2.3 Effect of convection

Figure 4.4 shows the time-temperature profiles obtained for forced (solid) and natural (dashed) convection mechanisms in jars containing: (a) water, (b) 10% sugar solution and (d) 3% agar solution. The experiments were performed for heating temperatures in the water bath of 60°C (blue), 70°C (red) and 80°C (green) in the three systems. In all cases, the profiles shown correspond to the centre of the jar (location 2).

The data of Figure 4.4 show the same behaviour in all experiments, for all heating temperature and system viscosities, with faster thermal responses for forced convection conditions. As example, system in Figure 4.4(a) – water – where the product temperature reaches the water bath value after 1200s; for natural convection the water bath temperature was reached around 1500s.

4.2.3.1 Convective heat transfer coefficient in the water bath

As mentioned previously (see Section 3.3, heat from the water bath medium – water – to the product container is transferred by convection. To properly characterise the thermal response of the system, it is necessary to measure the convective heat transfer coefficient, as this parameter is controlling the incoming heat flux (Eq. 3.3).

In this study, the convective heat transfer coefficient for the water bath, h_{bath} (W/m^{2}K) is estimated for both free and forced mechanisms, i.e. no stirred and stirred water bath, respectively, using a thermal resistance approach (Incropera and Dewitt, 2002). Using the recorded temperature profiles for the water bath and, the outer and inner

container walls, the heat transfer coefficient h_{bath} can be calculated from the energy balance across the container wall:

$$k_{glass} \frac{\left(T_{wall}^{out} - T_{wall}^{in}\right)}{\delta_{glass}} = h_{bath}\left(T_{bath} - T_{wall}^{out}\right)$$

Eq. (4.1)

Temperature profiles recorded for jars with (i) water and (ii) agar fillings were employed for the heat transfer coefficient calculations and results are presented below in Table 4.3. As expected, mixing conditions in the water bath - forced convection - led to a higher heat transfer coefficient h_{bath} in all cases.

The order of magnitude found for h_{bath} lies within the bounds expected for the operation of a water bath. Significant errors in the estimations are due to the sensibility of the calculation method with respect to temperature oscillations, and to the fast equilibration of the system temperatures, as can be deduced by the lower errors committed when the data of the agar solution was considered.

Table 4. 3: Convective heat transfer coefficient in the water bath

	h_{bath} (W/m²K)			
	Water		**Agar**	
T$_{bath}$(°C)	**Free**	**Forced**	**Free**	**Forced**
60	750 ± 250	1600 ± 730	430 ± 200	1250 ± 60
70	1000 ± 400	1880 ± 730	440 ± 200	1700 ± 500
80	700 ± 280	1700 ± 800	550 ± 90	1550 ± 570

4.2.4 Effect of Container size

Figure 4.5 shows temperature profiles corresponding to the systems with the lowest and the highest viscosity values in this study – i.e. water and agar, respectively - for two different jar sizes: 330 ml (solid) and 660 ml (dashed) and for the two different convection modes in the water bath (a) natural convection and (b) forced convection. The heating temperature of the water bath was 70°C in all the experiments shown, and the data corresponds to the thermocouple placed at the centre of the jar (location 2).

The data corresponding to these systems thermal response show that jars of 330 ml volume were heated faster than the larger ones (600 ml) for both water and a 3% agar cases. No significant differences in the heating dynamics of the water system can be observed. For agar, the thermal response of the large container was much slower, with a temperature 15°C lower than the small jar value by the end of the experiment, showing the effect of viscosity on heating dynamics.
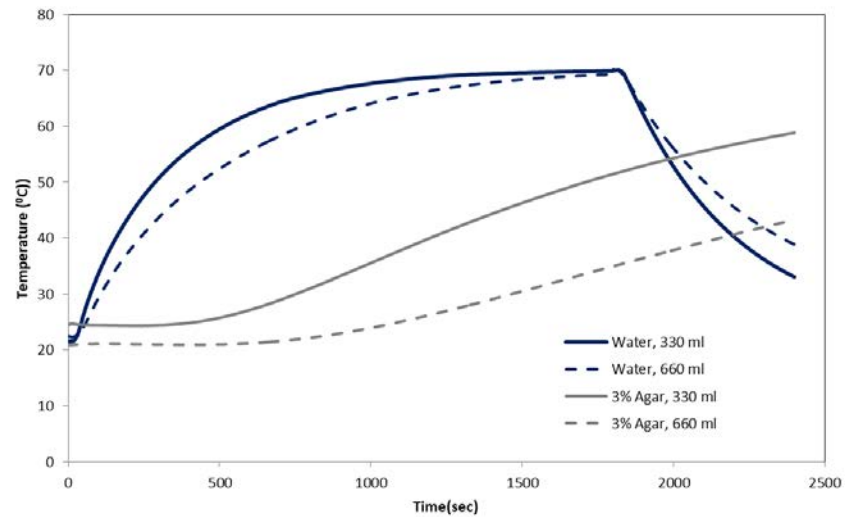
(a)
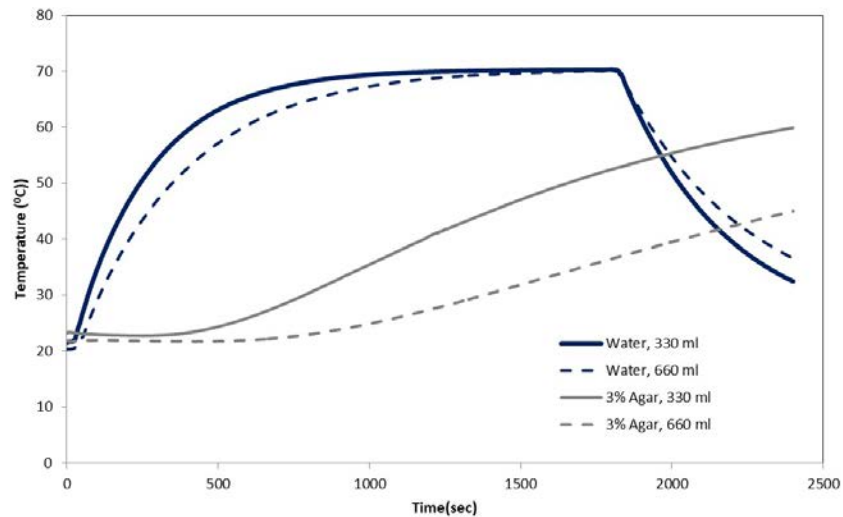
(b)

Figure 4. 5: Temperature profiles for two different jar sizes: 330 ml (solid) and 660 ml (dashed) and for (a) natural convection and (b) forced convection in the water bath. The heating temperature of the water bath was 70ºC in all the experiments shown, and the data corresponds to the thermocouple placed at the centre of the jar (location 2).

4.2.5 Effect of percentages of headspace

In this subsection, the effect on different percentages of headspace in the jar has been investigated for the case of a stirring water bath with a heating temperature of 70°C; the heating and cooling times were 30 min and 10 min, respectively.
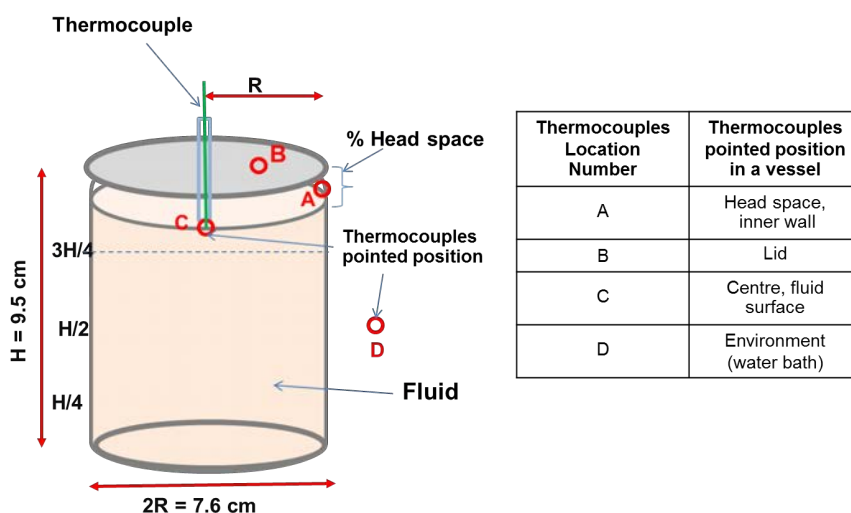
Figure 4. 6: Location of thermocouples for an effect of percentage of headspace study.

Figure 4.6 shows the four locations where the temperature has been measured: mid-head space in contact with the inner wall of vessel (location A), lid (location B), at fluid surface (location C) and water in water bath (location D). Temperature readings were recorded every second, and the temperature profiles obtained are presented next in Figure 4.7. A slightly slower heating can be seen for the jar with 5% headspace, although the differences in the headspace percentage do not seem to have any effect on the long time thermal response of the system (stationary state reached around 1100s independently of the headspace percentage).
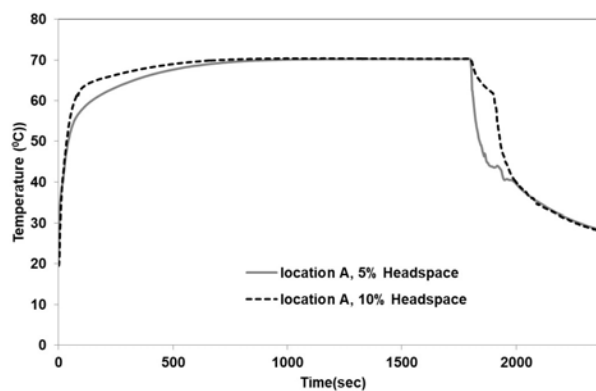
(a)
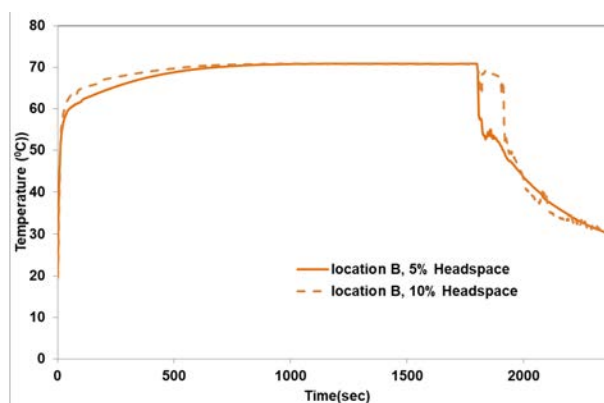
(b)
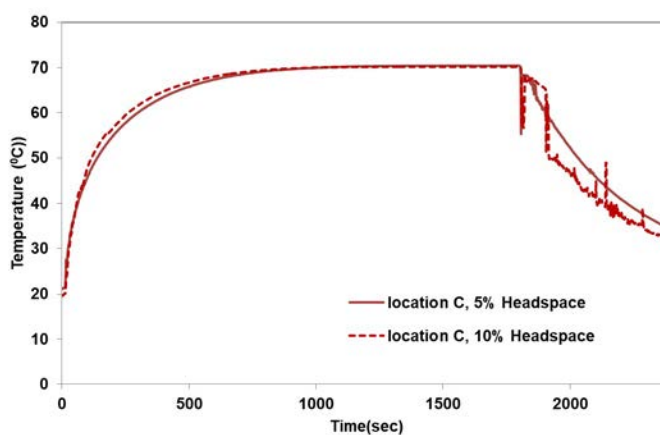
(c)

Figure 4. 7: Time-Temperature profiles for two different percentages of headspace: 5% (solid) and 10% (dashed) and for all heating conditions in the natural convection water bath convection: a) location A, b) location B, and c) location C; the inner wall of vessel (location A), lid (location B), at fluid surface (location C).

4.3 Pasteurisation values (P values) in the water bath

The time-temperature data corresponding to all the heating conditions shown in previous sections - (i) effect of temperature, (ii) solution viscosity, (iii) convection mode, (iv) container size and (v) percentages of headspace – have been converted into process values (P-values), following the procedure explained in Section 3.4.5, and then rescaled as P/P_{max} using the maximum P-value possible in the system (i.e. the corresponding to the water bath). The difference between the maximum P value for the three heating temperature reflects the temperature dependence of the rate processes.

4.3.1 Effect of the heating temperature and fill liquid viscosity

Figure 4.8 shows the normalised processing values for three heating temperatures: 60°C (lines), 70°C (solid) and 80°C (dots) for jars containing (a) water, (b) a solution of 10% sugar and (c) a solution of 3% agar. The starting temperature was 20°C in all cases, and the Z-value considered in the calculations was z = 10°C. The data shown corresponds to natural convection conditions in the water bath.

Overall, higher s were obtained when temperature increased from 60°C to 70°C and 80°C, respectively in the three system studied, as shown in Appendix I. Note that the process values presented in Figure 4.8 are the normalised ones, which would not necessarily follow the same trends.

(i) For water: P/P_{max} at location 1 (bottom of jar) is the smallest one. Very similar P/P_{max} obtained along the radial direction (see locations 2, 4 and 5).

(ii) For the 10% sugar solution, the calculated P/P_{max} values are about 10% smaller that those obtained for the water system, since the thermal response of the system was slightly slower.

(iii) In the 3% agar system, P/P_{max} at location 2 (centre of jar) is the smallest, as it corresponds to the coldest point of this conduction-driven system. Accordingly, P/P_{max} values increased along the radial direction (see locations 2, 3, 4, 5 and 6).

Figure 4.9 summarises the effect of the three fluids, showing normalised processing values calculated under natural convection conditions in the water bath for three systems with different viscosity values: water, 10% sugar and 3% agar. The heating temperature was 70°C in all the cases. Data represented in this figure shows that the system with the highest viscosity – the 3% agar solution - presents lower associated normalised P-values (P/P_{max}) than the systems with lower viscosity - water and 10% sugar solution.

In the water and sucrose systems, heat is transferred from environment (water bath) by conduction through the jar walls and by convection through the filling fluid. Convective heat transfer in both system leads to higher temperatures – as seen in Figure 4.3 – and therefore higher normalised P- values, and it rises the hot fluids to the top of the jar, resulting in the highest P/P_{max} values there (location 3).
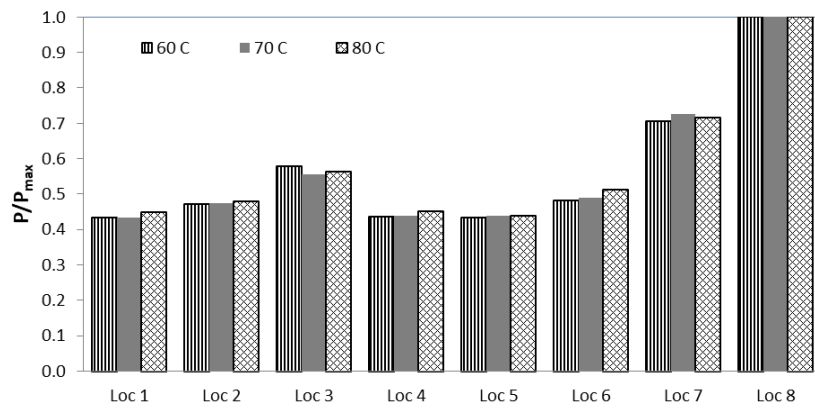
(a)
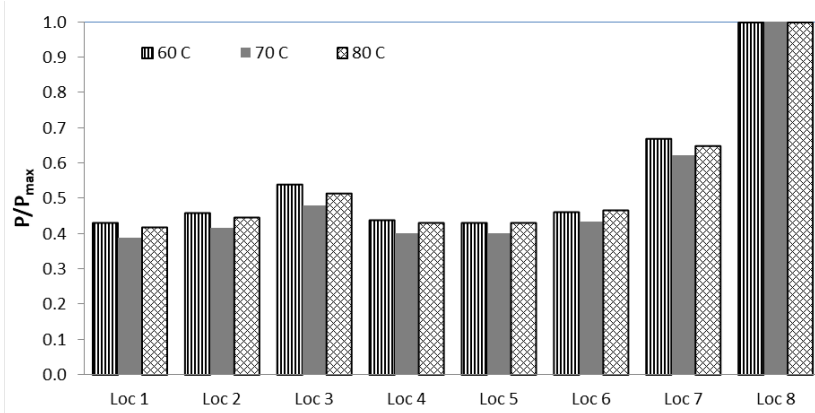
(b)
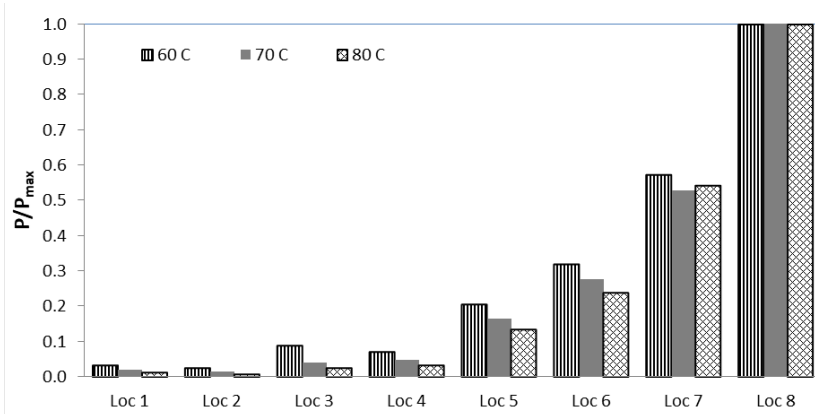
(c)

Figure 4. 8: Normalised P values for the three heating temperatures of the water bath: 60°C (lines), 70°C (solid) and 80°C (dots) for jars containing (a) water, (b) 10% sugar solution and (c) 3% agar solution. The Z-value considered in the calculations was z = 10°C and the reference temperature was T_{ref} = 80°C.
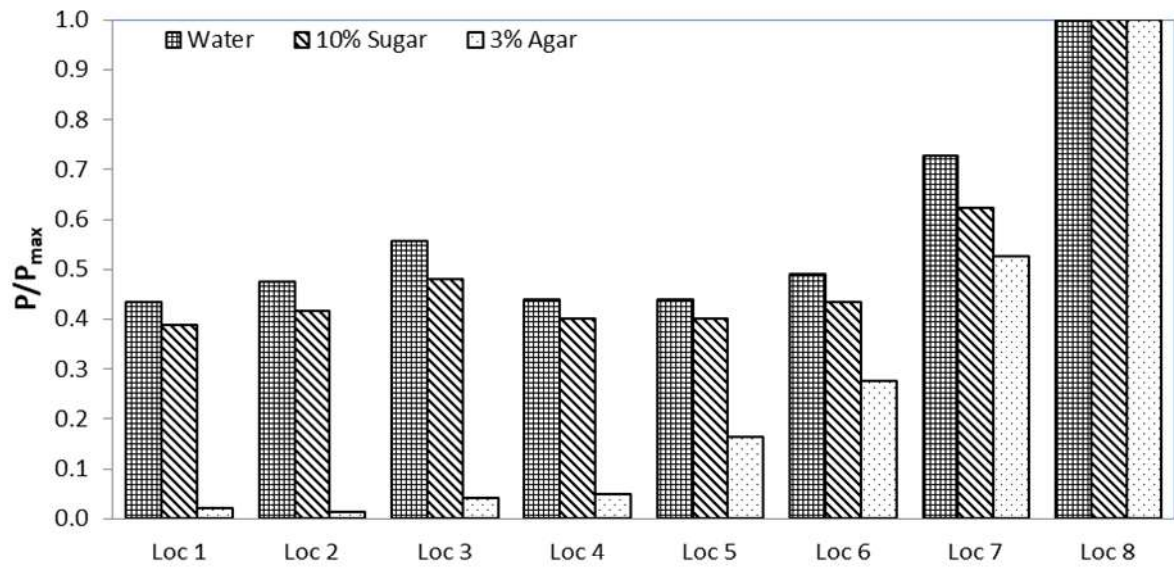
Figure 4. 9: Normalised processing values calculated under natural convection conditions in the water bath for three systems with different viscosity values: (squares) water, (lines) 10% sugar and (dots) 3% agar. The heating temperature was 70°C in all the cases. T_{ref} = 80°C, z value= 10

For the 3% agar solution, with a high viscosity, the system changes from being driven by convection to being driven by conduction, and exhibits much lower temperatures that lead to the lowest normalised P-values (P/P_{max}) of the three systems studied.

As corresponds to a conductive system, where temperature gradients increase in the radial direction, the calculated P/P_{max} values show increasing values as measurements points (locations 2, 4, 5 and 6) radially approach the wall of the jar.

The coldest point of water and 10% sugar systems was found at the same location (location 1) for all the water bath temperatures studied; for the 3% agar solution the

coldest point was located at the center (location 2). The different location for the coldest points is explained by the heat transfer mechanism dominant in each system (Singh and Rammasway, 2016), with the less viscous systems - water and the 10%(w/v) sugar solution – being driven by convection, and conduction governing heat transfer in the agar solution (the more viscous filling).

4.3.3 Effect of convection mode

Figure 4.10 shows process values calculated for forced and natural convection mechanisms in the water bath for jars containing: (a) water, (b) 10% sugar solution and (c) 3% agar solution. The heating temperature was 70°C in all cases.

The data presented in Figure 4.10 show the same behaviour for the three systems studied, with higher processing values obtained for forced convection conditions (due to mixing in the water bath), and the same trends observed for both forced and natural convection conditions: (i) increasing P/P_{max} values in the radial direction form the center to the wall of the jar in the agar system (ii) P/P_{max} values increasing in the axial direction for the water and sugar solution. However, at the center of the jar containing the agar solution the effect is minimal.
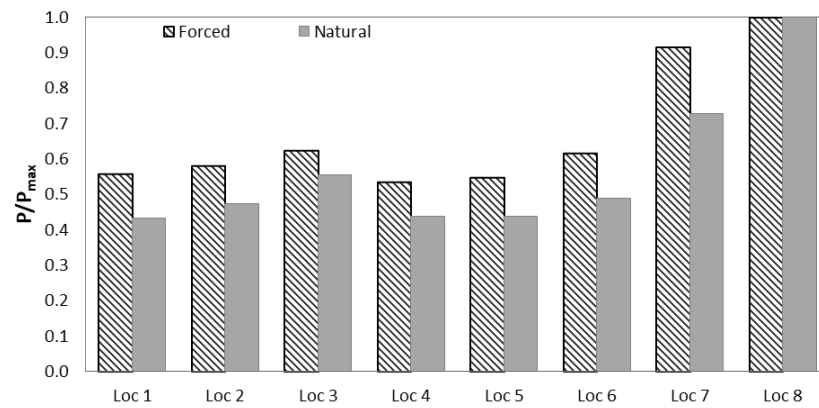
(a)
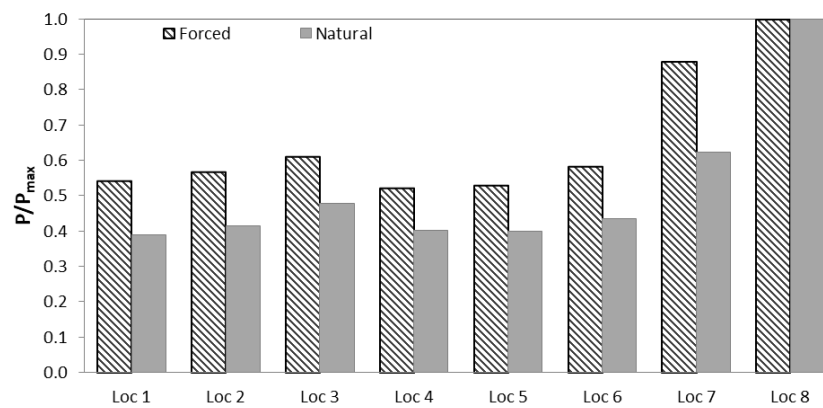
(b)
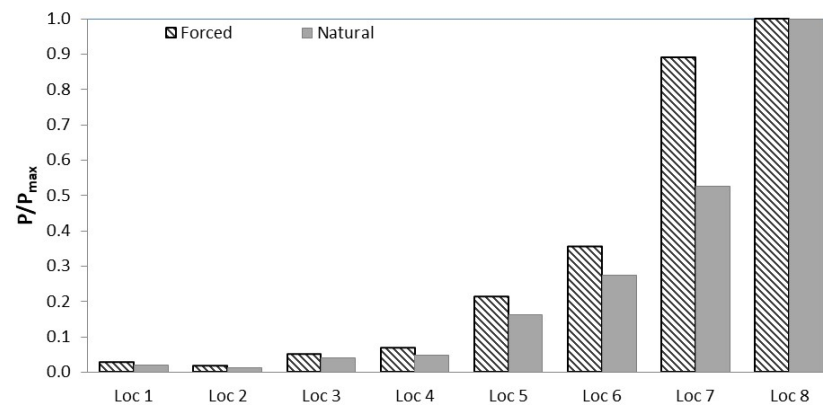
(c)

Figure 4. 10:Normalised process values for forced (pattern) and natural (solid) convection mechanisms in the water bath for jars containing: (a) water, (b) 10%(w/v) sugar solution and (c) 3%(w/v) agar solution. The heating temperature was 70°C in all cases. T_{ref} = 80°C, z value= 10.

4.3.4 Effect of Container size

Figure 4.11 shows the normalised P-values calculated for the systems with the lowest and the highest viscosity values – i.e. water and agar, respectively - for two different jar sizes: 330 ml and 660 ml. Data presented in Figure 4.12 (a) correspond to natural convection conditions in the water bath, while Figure 4.12 (b) shows P/P_{max} values resulting for forced convection conditions. The heating temperature was 70°C in both cases.

Large jars (660 ml) present lower process values for both water and a 3% agar systems.

The water system presents much higher normalised P-values than the 3% agar solution, consistently with the temperature profiles shown in Section 4.2.2 and the heat transfer mechanisms defining the dynamics of those systems – i.e. conduction for agar and convection for water.

The location of the coldest point of the jars has not been affected by the size of the container, being location 1 for water and location 2 for the agar solution.
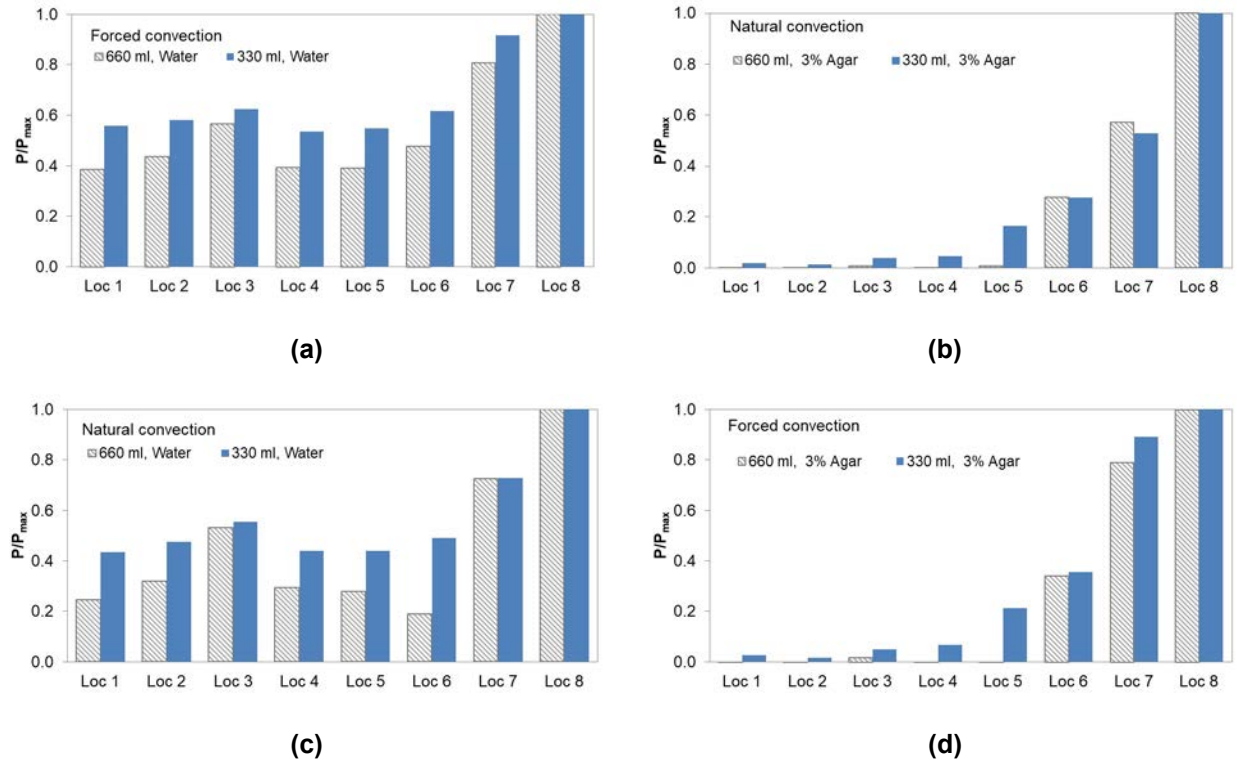
Figure 4. 11:- Normalised P-values for the systems with water and the solution of 3% (w/v) agar, for two different jar sizes: 330 ml and 660 ml. (a) natural convection condition in the water bath, (b) forced convection conditions in water bath. The heating temperature was 70°C in both cases. T_{ref} = 80°C, z value= 10.

** 1) location 1 is at the centre (R) and the bottom (1/4H),
2) location 2 is at the centre (R) and the half height (1/2H),
3) location 3 is at centre (R) and the top of jar (3/4H),
4) location 4 is at the ½ of radius(1/2R) and the half height (1/2H),
5) location 5 is at the ¼ of radius(1/4R) and the half height (1/2H),
6) location 6 is at the inside jar wall ,
7) location 7 is at the outside jar wall and,
8) location 8 is at water in water bath

4.3.5 Effect of percentages of head space

The normalised P-values calculated from the time-temperature profiles corresponding to the water system when the two different percentages of headspace (5% and 10%)

were considered are presented in Figure 4.12. The data slightly lower P/P_{max} values for the jars with 5% headspace than for the ones with 10% headspace. The lid of the jar (location B in this case) has the highest P/P_{max} values – as it is made from a high conductive material - while the lower process values correspond to the water surface (location 3 in Figure 4.12). Singh and Rammasway (2016) found that the headspace temperature increases rapidly due to lower heat capacity and viscosity of air, resulting in better heat transfer coefficients. This works also reports an effect of the can headspace on the heat transfer coefficient: higher headspace gave higher heat transfer coefficient due to a higher mobility of air.
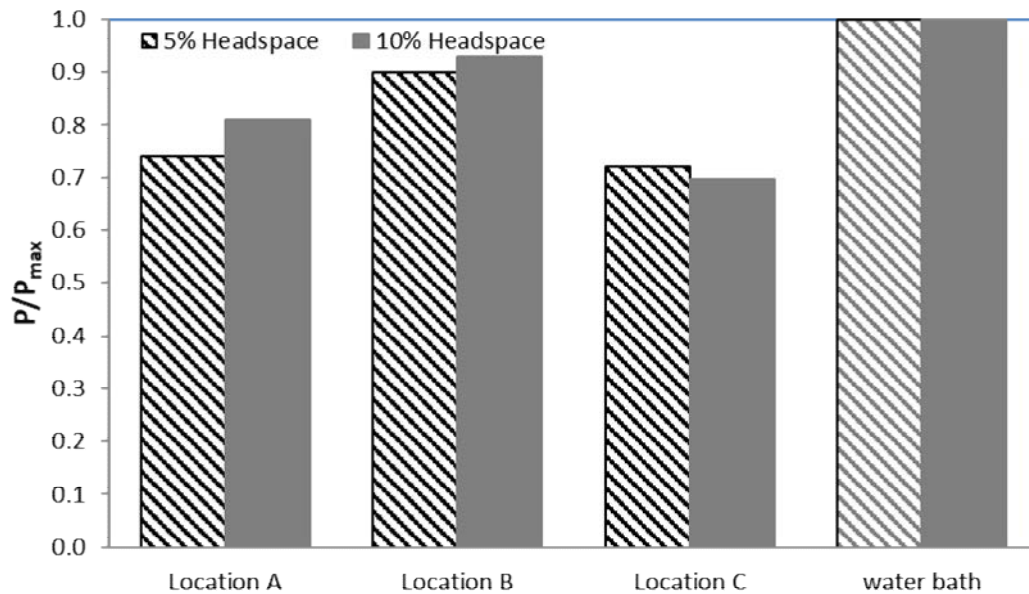
Figure 4. 12: Normalised P-values for two different percentages of headspace: 5% (w/v) and 10% (w/v). The heating temperature was 70°C in all the cases presented. T_{ref} = 80°C, z value= 10°C. P_{max}= 34.20 min

4.4 Application of TTIs in the water bath pasteurisation system

In this section, a validation study for the use of TTIs during the thermal experiments carried out in the water bath is presented. The BAA TTIs were placed in the same eight locations than in previous experiments, as shown in Figure 4.13, where locations for both thermocouples and TTIs are indicated. The container was subsequently positioned in the mixing water bath at different time intervals with varying temperature, as summarises in Table 3.3. The normalised P values were calculated too by integrating the temperatures obtained from the measured data and scaling using as reference the P value of the water bath (heating medium), and were then compared with the P/P_{max} values calculated from the thermocouple temperature readings.

Thermocouples Location Number	Thermocouples pointed position in a vessel
1	R,H/4
2	R,H/2
3	R,3H/4
4	R/2,H/2
5	R/4,H/2
6	Inner wall
7	Outer wall
8	Environment (water bath)
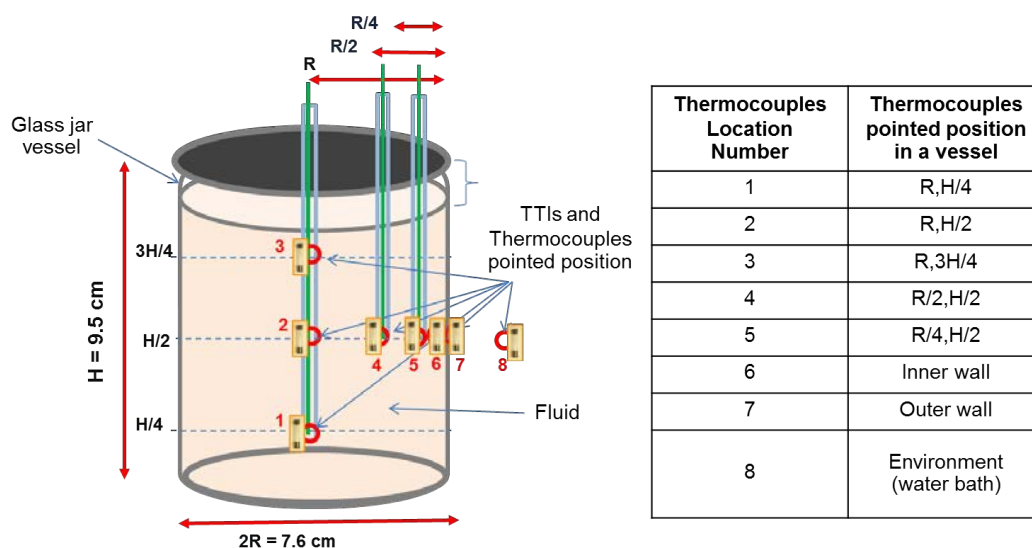
Figure 4. 13: Container thermocouples and TTIs set up.

(a)   (b)

(c)   (d)

(e)   (f)
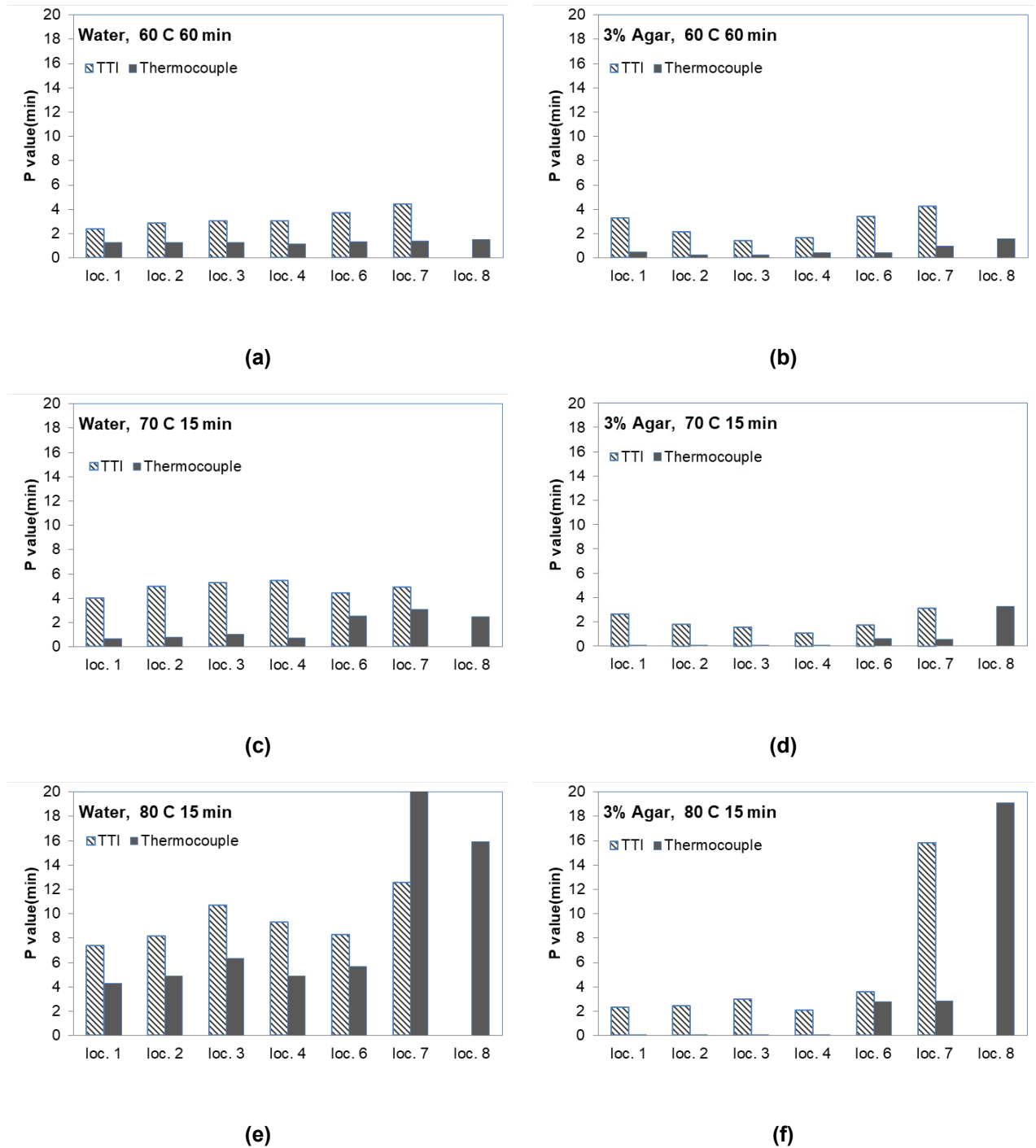
Figure 4. 14: Comparison of the process values calculated from the temperatures measured using thermocouples (solid) with those calculated employing the TTIs data (line) for different heating scenarios: heating temperature of 60°C during 60 min for (a) water and (b) 3% agar solution; heating temperature of 70°C during 15 min for (c) water (d) 3% agar solution and finally water bath at 80°C during 15 min for (e) water (f) 3% agar. T_{ref} = 80°C, z value = 8.9°C

Such comparison is presented in Figure 4.14, where larger P/P_{max} correspond in all cases to the TTIs. However, the differences between TTI and thermocouples are considerable larger than the usually accepted 10% experimental error, showing that either the TTI or the thermocouple data recovered form these experiments were not as accurate as expected.

4.5   Solid-liquid phase study

Nowadays an increasing number of commercial food products are made from a combination of liquid and solid ingredients, as for example soups or dipping sauces (D'addio et. al., 2014, Tolasa et. al., 2012). In this section, heat transfer - convection and conduction - in canned food is studied for such solid-liquid systems. Results obtained will be also used for comparison with the spray pasteurisation process presented in the next Chapter.

The experiments used fluids in a similar range of viscosity values than the food products usually found in these food mixtures, such as corn starch and guar gum, which were employed to study the effect of viscosity on thermal processes efficiency. The experimental set up is the one presented in Section 3.6, and also depicted in Figure 4.16. In all the experiments a container of 330ml volume was used and heated up in the water bath at a temperature of 70°C. During the experiments, the temperature was recorded at four different locations in the jar, as indicated also in Figure 4.16. Potato cubes of a volume of 1 cm^3, and always sit in the same positions, were employed as solid phase in this series of experiments.

Table 4.4 summarises the factors considered in the study of the two-phase system heat transfer (i) viscosity liquid phase, using four different solutions and (ii) solid/liquid fraction, considering either 10% or 50% (w/v). As in previous sections, temperature time profiles alongside with the corresponding P/P_{max} values will be presented and discussed.
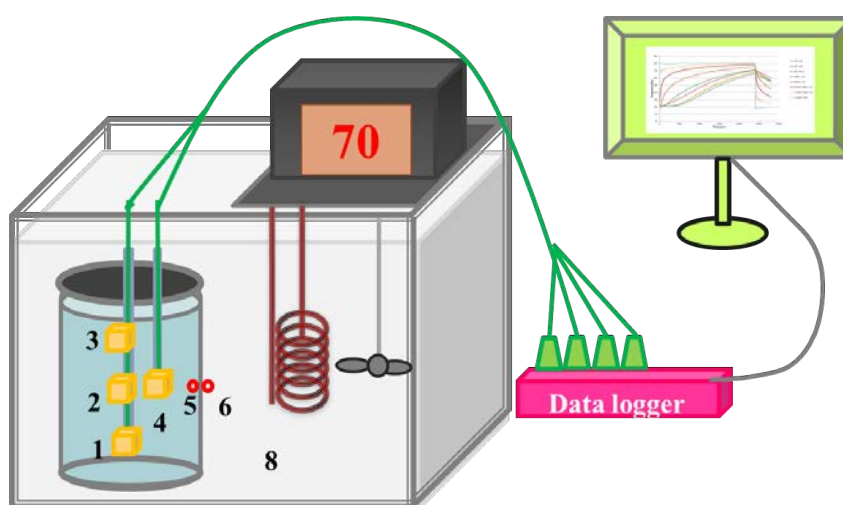
Figure 4. 15: Set up for the two-phase system in the water bath.

Table 4. 4: Two-phase experimental systems.

Carrier fluid	%(w/v) Potato Cubes
Water	10
	50
4% Corn starch	10
	50
4% Pre-gelatinised corn starch	10
	50
1% Guar	10
	50

4.5.1 Effect of Fluid viscosity

To study the effect of the filling fluid viscosity on the heat transfer rates of the water bath system, four different solutions – listed in Table 4.5 alongside the corresponding viscosity values - were employed. The viscosity of all the solutions was measured immediately after preparation, according to the procedure explained in Section 3.2.4, and the viscosity considered for water has been taken from Perry and Green(1999). All the data presented in Table 4.3 correspond to a temperature of 20°C.

Table 4. 5: Fillings employed in two-phase experiments and their viscosity values (at 20°C.)

Jar filling	Viscosity (Pa s)
Water	1.002x 10^{-3}
4% Pregelatinised corn starch	0.002
4% Corn starch	0.45
1% Guar	0.15

The temperature profiles obtained for each of the two-phase systems are presented in Figure 4.16 (a). Consistently with results shown in Section 4.2.2, the system with a water filling shows the fastest thermal response, with the slowest heat transfer rate corresponding to the more viscous liquid phase, i.e. the 4%(w/v) corn starch solution. As can be seen also in Figure 4.18, the 4% pregelatinised corn starch solution exhibits a behaviour close to the pure water, as viscosity values are similar in both systems.
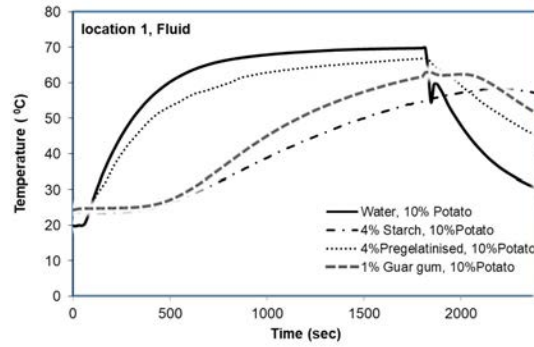
(a)
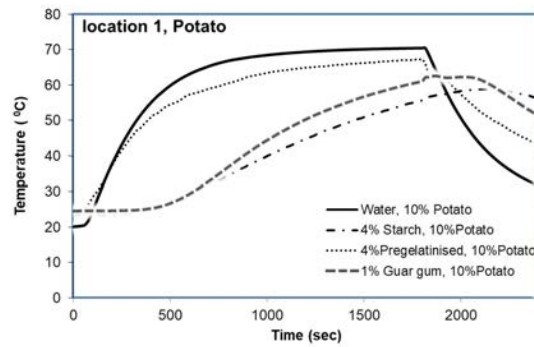
(b)
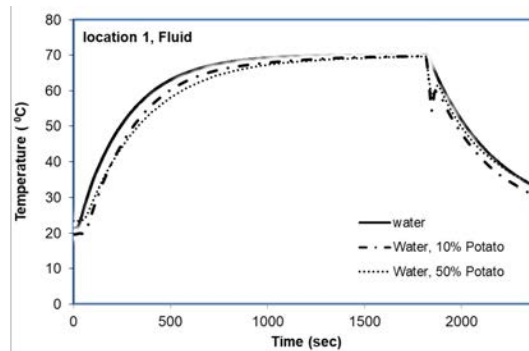
(c)

Figure 4. 16: Temperature profiles for the two-phase system for: (a) fluid temperature, (b) potato temperature and c) solid and non solid when the liquid phase presents different viscosity values: water (solid), 4%(w/v) starch (dotted-dashed), 4%(w/v) pregelatinised starch (dotted), and 1%(w/v) guar gum (dashed). The heating temperature was 70 ºC in all cases and the initial temperature of the two-phase filling was approx. 20 ºC. The temperature profiles shown correspond to the centre of the jar (location 1).

In between both viscosity bounds lies the 1 % guar gum, which showed a slightly faster heat transfer rate than the 4% starch solution in the first 800 seconds, that increased and after that initial stage until the end of the heating period over 1800s. Such behaviour is related to the temperature effect on the gelation bond of the guar gum, and effect that is not significant in the 4% corn starch solution. Overall more viscous fillings/liquid phases present a slower heat transfer rate than the low viscosity solutions.

Temperature-time profiles corresponding to the solid phase (the potato cubes) are also presented in Figure 4.16(b) that shows similar trends in heat transfer as in the fluid phase for all the systems.

Figure 4.17 shows the normalised process values calculated for each one of the systems using the temperature measurements showed above. As can be expected, the system with the highest viscosity – the 4% starch solution - presents smaller associated P/P_{max} values than the systems with lower viscosity (1% guar gum solution, a 4% pregelatinised starch solution and water).

It must be noted that all the process values obtained for the solid phase were slightly smaller than in the filling. Also, the solid phase seems to have no significant effect on the heat transfer mechanism through the liquid phase, as can be concluded from the comparison of the P values at different locations: coldest point still located at the bottom of the jar for the less viscous fillings and at the centre for the conduction-driven more viscous liquid phases.

4.5.2 Effect of solid/liquid phase fractions

In this subsection the effect of the fraction of solid phase present in the two-phase system is studied. Two solid/liquid fractions (w/v) were employed (i) 10% (ii) 50% and all the experiments were performed following the protocol defined in Section.
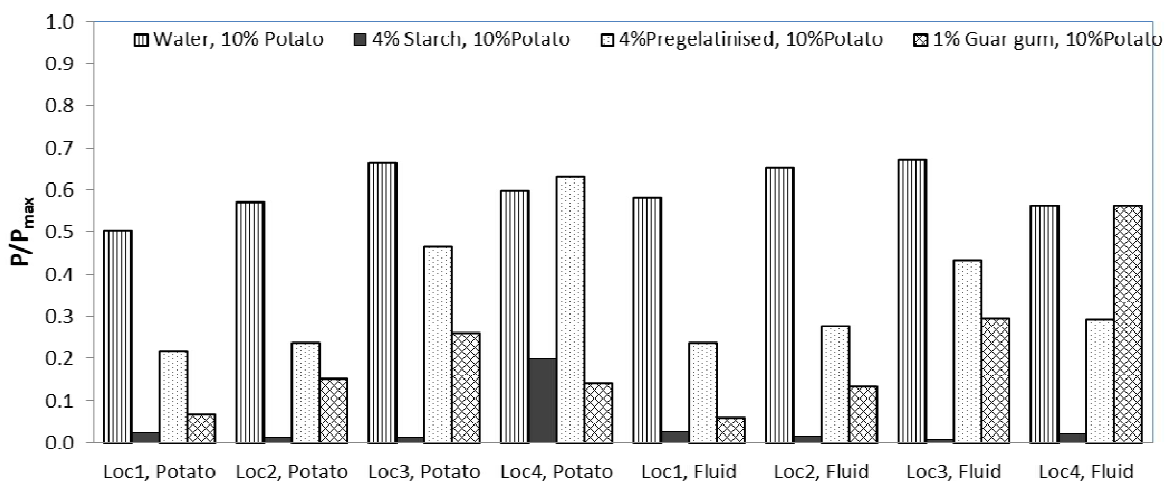
Figure 4. 17:   Normalised process values for both liquid and solid phases when the fluid filling presents different viscosity values: water (line), 4%(w/v) starch (solid), 4%(w/v) pregelatinised starch (dotted), and 1%(w/v) guar gum (diamond).
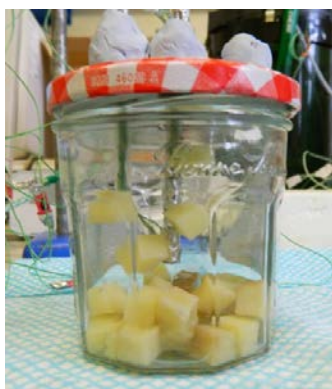
(a)   (b)

Figure 4. 18: Two-phase system with different solid/liquid ratios (w/v): (a) 10% and (b) 50% potato cubes in the 4% starch solution.

3.5.3. The liquid phase consisted of the four fillings used in the previous subsection, and for all the cases the experiments involved 30 minutes of heating followed by 10 minutes of cooling. The water bath heating temperature was 70 ^{0}C and temperature was recorded every 1 second, both in fluid and potato particles.

The temperature profiles recorded at location 1 (bottom of the jar) during this new series of experiments are presented in Figure 4.19. For water and for the 4% starch solution, Figure 4.19 (a) and (b) respectively, the results show that different solid-liquid fractions have no effect on the heat transfer dynamics of the liquid phase.

(a)   **(b)**

(c)   **(d)**
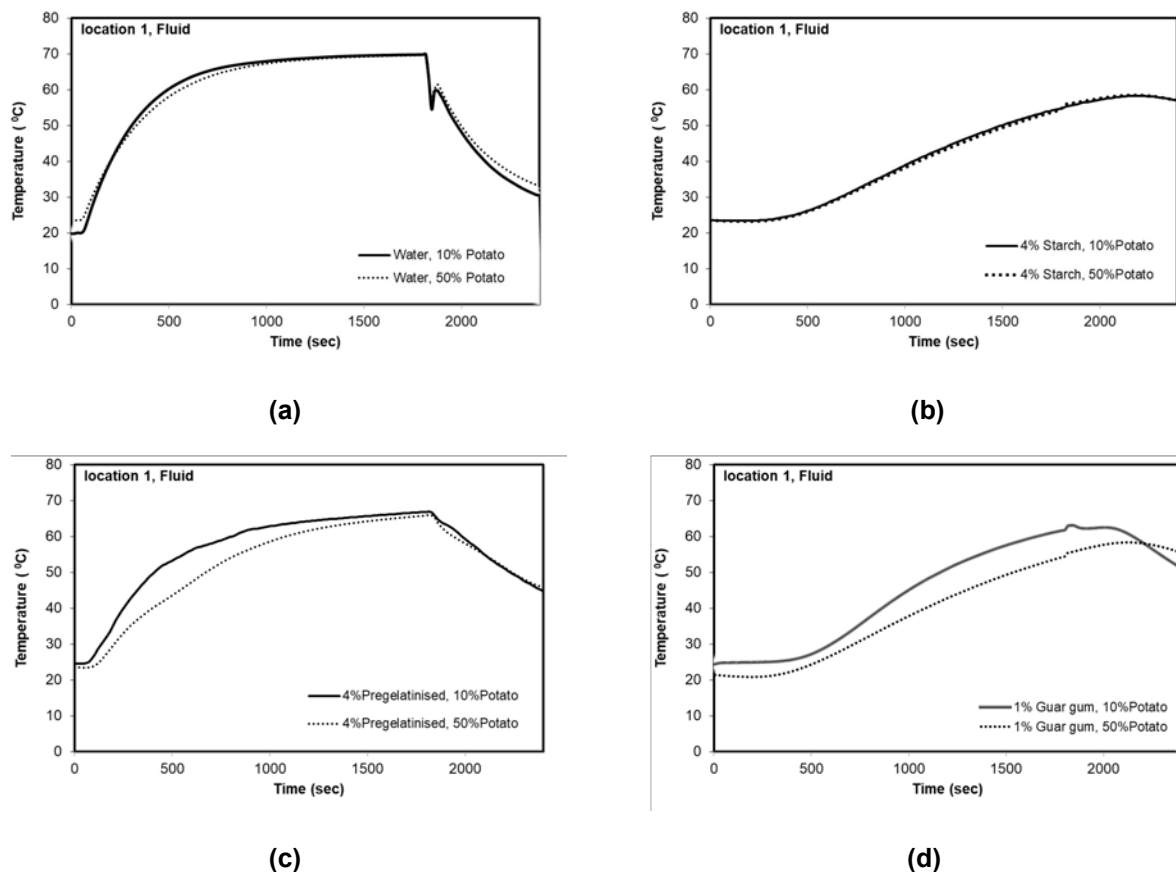
Figure 4. 19: Temperature time profiles for two different solid/liquid fraction systems: 10%(w/v) (solid) and (b) 50%(w/v) (dotted) using potato cubes as solid phase and (a) water, (b) 4%(w/v) starch, (c) 4%(w/v) pregelatinised starch (d) 1%(w/v) guar gum. The heating temperature was 70ºC in all cases and the initial temperature of the two-phase filling was approx. 20ºC. The temperature profiles shown correspond to the bottom of the jar (location 1) in fluid.

On the other hand, noticeable differences on the temperature values recorded in the filling and in the solid particles can be seen in the temperature profiles presented in Figure 4.19 (c) and (d) for the 4% pregelatinised starch and the 1% guar gum systems, respectively, with higher solid fractions (50%w/v) showing faster heating stages than the low solid fraction systems (10%w/v), and with temperature values around 4-7 ^{0}C lower in the latter ones.

Overall, these temperature trends show a significant effect of the solid/liquid fraction in those systems where conduction is the governing heat transfer mechanism, while such effect can be neglected in the less viscous and convection-driven cases.

Figure 4.20 shows the normalised process values (P/P_{max}) of the two potato contents – 10% (w/v) and 50% (w/v) potato – that were compared to study the effect of the solid fraction in the thermal response of the two phase system.

Figure 4.20 (a) presents the normalised process values corresponding to the system where water was employed as liquid phase. Very similar P/P_{max} values for both solid fractions were obtained, as the thermal response of the system was not affected by the increased solid fraction (see Figure 4.19). Similar process values were obtained for the two solid fractions in the 4% starch solution too - with the exception of location 4 where the values obtained must be affected by an error in the experimental measurement - as shown in Figure 4.20 (b). The higher differences in the normalised process values calculated for the two solid fractions where found in the 1% guar gum solution, as shown in Figure 4.20 (d); in the 4% pregelatinised 4% starch the effect of the solid fraction
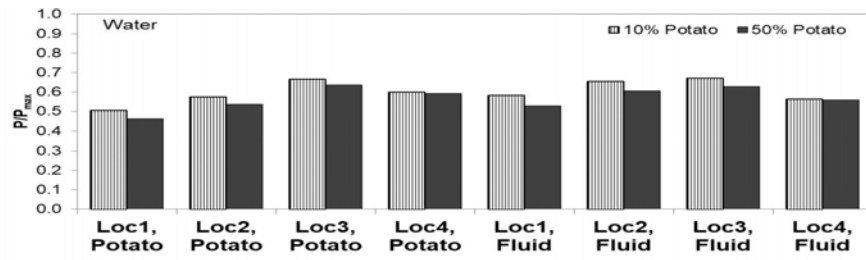
(a)
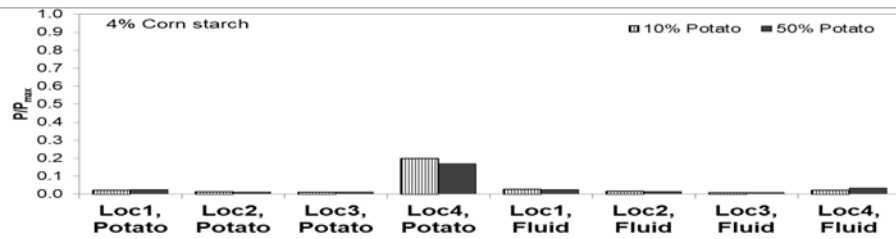
(b)
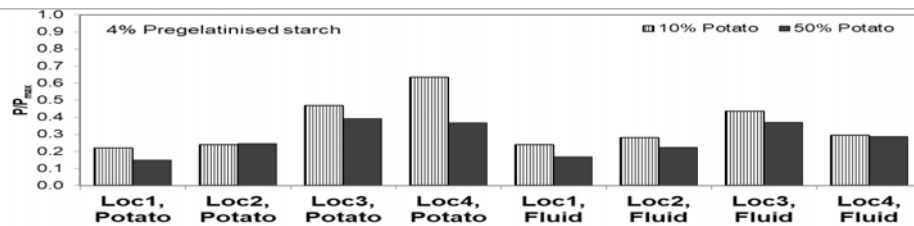
(c)
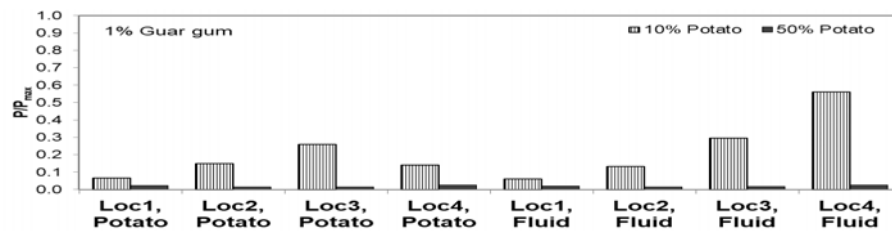
(d)

Figure 4. 20: Normalised process values calculated for the liquid phase when two different solid fractions were considered: 10%(w/v) (line) and 50%(w/v) (solid). Potato cubes were employed as solid phase in all cases, being the liquid phase is (a) water, (b) 4%(w/v) starch, (c) 4%(w/v) pregelatinised starch, (d) 1%(w/v) guar gum. The temperature profiles shown correspond to the bottom of the jar (location 1) in fluid.

Finally, in Figure 4.21 a comparison of the normalised process values (P/P_{max}) calculated for the fluid and solid phases in the four systems studied in this section is presented. Normalised P values corresponding to the water filling case – in Figure 4.21 (a) - present a very similar system behaviour, with close process values in both solid and liquid phases for all the locations where the temperature was measured. Again, the normalised processing values obtained must be influenced by the error of the experimental measurements – either caused by the accuracy of the thermocouples or by their misplacement – as temperatures in the solid are slightly higher in the solid than in the liquid phase.
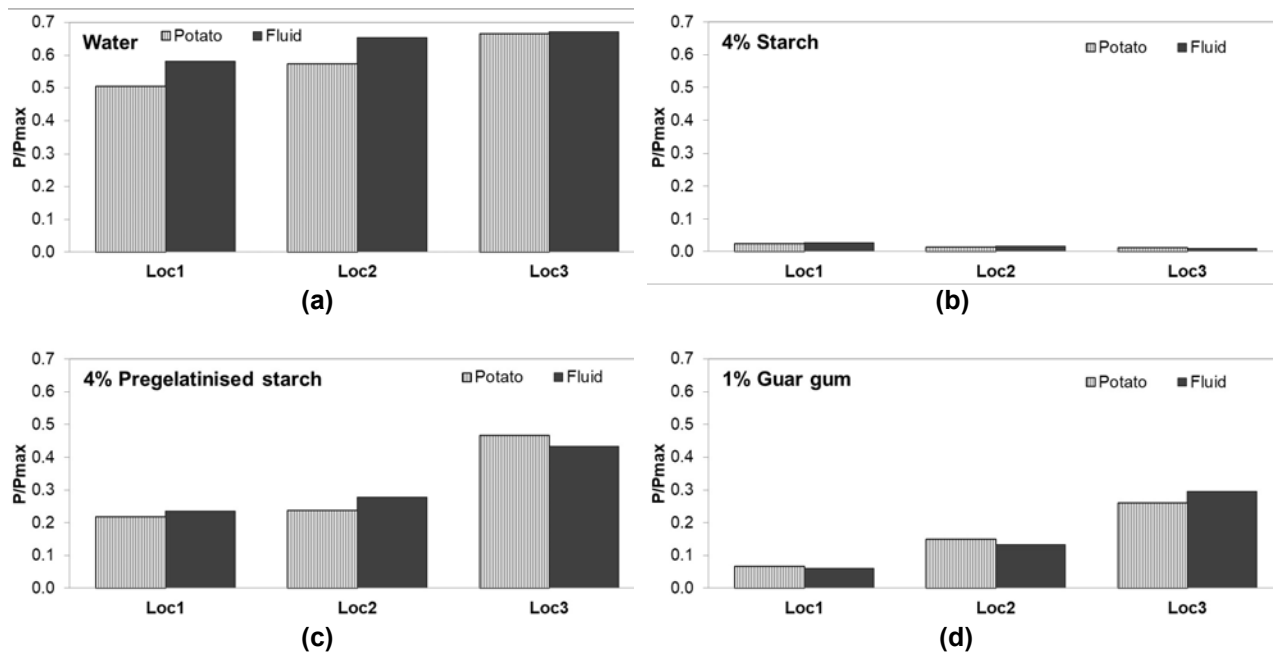
Figure 4. 21: Comparison of the normalised process values calculated for the fluid (solid) and potato (line) in a jar contain 10%(w/v) of potato cubes and (a) water, (b) 4%(w/v) starch, (c) 4%(w/v) pregelatinised starch, and (d) 1%(w/v) guar gum. The heating temperature was 70 ºC in all cases and the initial temperature of the two-phase filling was approx. 20 ºC.

4.6 Summary

In-container pasteurisation experiments have been conducted over a range of heating conditions, filling viscosities and container geometries using the water bath described in Section 3.5.2, with an acceptable reproducibility. These series of experiments have also included the study of a two-phase system, where potato cubes were employed as a solid phase while different fluids of various viscosities were used as the liquid phase.

The water bath system was chosen as a first approach to the study of the heating dynamics of spray pasteurisation systems, and it has been provided valuable information that can be correlated to the upper limit operation the spray tunnels, where mass flows are so high that heating rates become independent of the spray flow.

The thermal response of the systems pasteurised in the water bath has been represented by means of the temperature profiles recorded during each experiment at different locations, covering filling, container and environment (water bath). Normalised pasteurisation values were obtained by integrating in time those temperature profiles and using the maximum P value of the system – corresponding to the heating medium – as reference (see Section 3.4.5 for more details on these calculations).

Different pasteurisation values arose for the different conditions investigated (all P-values available in Appendix I), showing the range of heating rates defined by both filling and environment combinations. Viscosity of the filling, together with the convection moded in the water bath were revealed as the most influencing factors

affecting the heating rate of the process, also for the two-phase system. Overall, the following conclusions can be made:

•   Higher temperatures of the heating medium – water bath temperature increasing from 50°C to 70°C – resulted in higher pasteurisation values, for all the systems studied.

•   In all cases, an increase of the filling viscosity slowed down the heating dynamics, and consequently also affecting the processing values, which were found to be generally lower when the viscosity of the product was higher.

•   Under all the heating conditions and for all the fillings studied, the size of the container only had a small effect in the thermal response and subsequently in the process values calculated, as neither had the headspace volume.

Results presented on the performance of TTIs were conditioned by the quality of the experimental results, since as mentioned before in Section 4.4, the difference between the pasteurised values calculated using the TTI data were larger than expected when compared to the P values obtained using the temperature profiles measured with the thermocouples set.

Some observations must be made regarding the accuracy of the temperature recordings. Although all the experiments were conducted in triplicate and proved to be reproducible, inherent measurement errors – i.e. thermocouple reading and location errors together with thermal noise - could explain the results obtained for the two phase-system, where solid and liquid phases appeared to offer a very similar thermal response to the different pasteurisation conditions. The same reasoning would apply to the estimations of the heat transfer coefficient, where the calculated

standard deviations are significant. Note that the method employed to estimate the convective heat transfer coefficient in the water bath is extremely sensitive to thermal noise, and a certain temperature gradient between the points employed in the calculations would be desirable for higher accuracy.

However, the thermal response recovered from these series of experiments revealed the conditions where the two possible mechanisms governing heat transfer through the container filling – i.e. conduction and convection – were driving the heating dynamics. The results form this study will help in the understanding of pasteurisation processes exhibiting internally controlled heating dynamics, and they will be also valuable in the process of characterisation of the shower spray pasteurisation operations.

Chapter 5

Evaluation of mild thermal processes for food decontamination: Spray pasteuriser study

5.1 Introduction

Commercial spray pasteurizer systems as described in Chapters 1 and 2 use a falling spray of water as the heating medium. Chapter 4 has presented data for the analysis of heating in a water bath, showing the differences between different fluids and conditions. This chapter discusses the result of evaluation of a P value determination for mild thermal processes using a spray of water from nozzles and showerheads, using the thermocouples. The aims of this part of the work are to deliver variable temperature profiles for the mild thermal processes and study the effect results of this within and at the surface of pasteurised products. A new spray pasteurisation unit was designed and created in the university's workshop, and different types of nozzle (single jet and muti jet) used. A series of process conditions on both new showerheads using in a spray pasteuriser were studied, and the P values calculated.

This Chapter is organized into three main sections:

(i) In Section 5.2 the first nozzle, which had a 120-degree of angle of spray water, is studied. Results show the general trends for the effects of flow and food fluid.

However, because the nozzle had a very wide spread of spray water angle, nozzles that gave a new straight flow of water on to the vessel were developed.

(ii) Section 5.3, thus studies two different water flows with both a single jet nozzle and a showerhead.

(iii) Section 5.4 studies two-phase solid-liquid mixtures within the vessel.

The instrumentation of a showerhead experiment was set up as in Chapter 3 (Section 3.5.3) and shown in Figure 3.9 and Figure 3.10. The experimental set up is depicted in Figure 5.1 together with the position of the thermocouples employed to measure the temperature in the system.

Thermocouples Location Number	Thermocouples pointed position in a vessel
1	R,H/4
2	R,H/2
3	R,3H/4
4	R/2,H/2
5	Inner wall
6	Outer wall
7	Spray water
8	Environment (shower head)
9	Under vessel
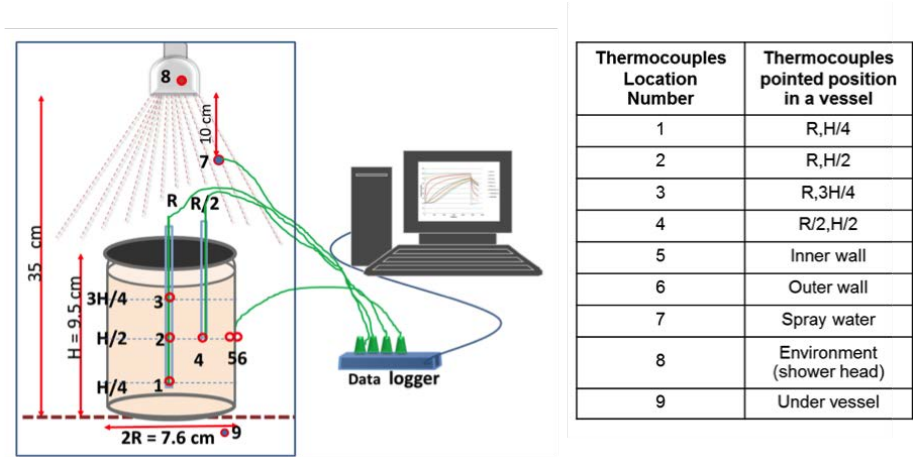
Figure 5. 1: Schematic of spray vessel and position

Temperature profiles were recorded for 60 minutes of heating time and 10 minutes of cooling time using seven calibrated thermocouples (type K) and data loggers (model: USB TC-08 Thermocouple Data Logger, Pico Technology, UK, having a temperature accuracy of ±0.5°C). Each temperature was recorded every 15 seconds.

The sample solutions were added into the containers at ambient temperature, with 5 %(v/v) headspaces. The containers were then placed into the spray pasteuriser unit and the results compared both the effects of different spray conditions and of different system viscosities and solid fractions.

5.2. Spray vessel design 1: A 120º spray shower set up.

This section presents the experimental results corresponding to the operation of a spray vessel with a showerhead pouring water up to an angle of 120º over the jar. A series of operation conditions have been studied, assessing the effect of the following process variables in the heat efficiency of the system:

- flow rate

- spray temperature

- viscosity of the filling fluid

Different heights for the nozzle, as well as different container positions and number of treated jars have been also considered to evaluate the effect of the vessel geometry.

Figure 5.2 compares the temperature profiles measured in (a) the water bath and (b) the spray vessel for a jar containing water. Measurements include also the jar environment.

The results for the experiment conducted in the water bath experiment show a relatively rapid heating of the jar filling, with the system reaching the water bath temperature around 1800s. The thermal response of the system was also fast during the cooling stage, with the temperature in all the measured points falling down to values close to 35ºC approx. 600 seconds after the jar was removed from the bath.

The spray vessel with the 120 spray nozzle exhibits a slower thermal response when compare to the water bath – it takes about 2100s to reach a temperature close to the 60°C while in the water bath that value is reached after only 900 seconds. After those first 2100 seconds the temperature in the spray vessel system keeps slowly increasing rate, maintaining values close to 65°C until the beginning of the cooling stage (around 3600s). The system does not reach the temperature of the shower spray due to the lower heat transfer compared to the water bath – there is both less mass of hot water providing heat to the system, and greater heat losses to the environment while spraying.

In both systems - water bath and spray vessel - the filling temperature profiles present the same behavior:

(i)   temperature increases with height, with location 3 identified as the hot spot;

(ii)   similar temperature values along the radial direction (locations 2, 4 and 5). This indicates that despite the difference in the heat transfer rate from the environment to the jar, convection is governing the heat transfer inside the container in both systems (hot water rises and replaced by cooler water from side of wall to the center of jar).
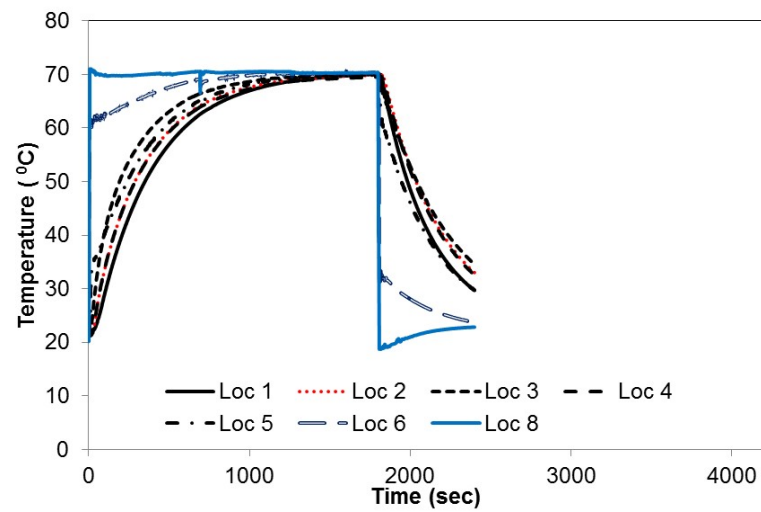
(a)
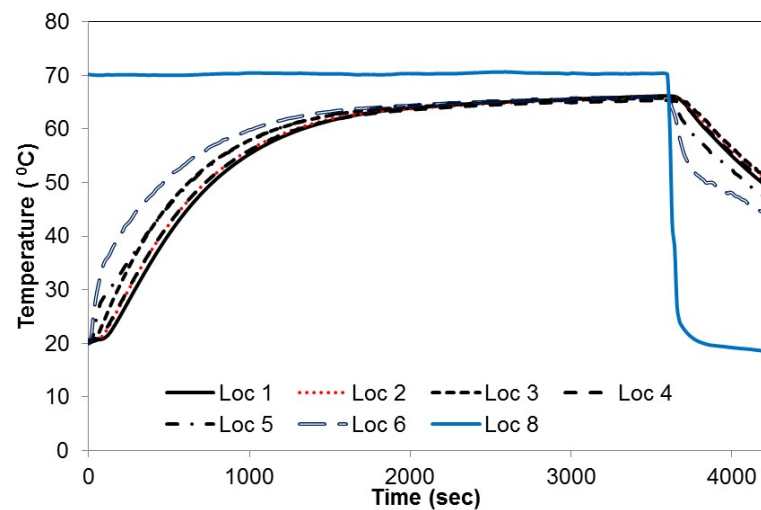
(b)

Figure 5. 2: Comparison of the temperature profiles measured for all the locations in the system (jar and its environment) in (a) water bath and in (b) spray vessel. The jars contained water in both cases, with bath and spray nozzle temperatures of 70°C. The filling was initially at room temperature (i.e. around 20°C). The data shown in (b) for the spray vessel corresponds to a mass flow rate of 1.09 l/min.

5.2.1 Effect of flow rate

Experiments were conducted (in triplicate) for three different flow rates (i) 0.53 l/min, (ii) 0.78 l/min, (iii) 1.09 l/min and water bath, and the resulting temperature profiles for four locations inside the jar are shown in Figure 5.3.

Heat transfer in the water bath is fastest in both location 1 and 2. The temperature profiles recorded for the 0.78 l/min and the 1.09 l/min flow rates are very similar, with a rapid heating between 100 and 1800 seconds and finally reaching temperatures close to the muti jet around 2500 seconds. On the other hand the lowest flow rate (0.53 l/min) shows a slower thermal response, with temperatures almost 20°C lower for times close to 1000 seconds. Overall, the results show clearly how the heat transfer rates increase with the flow rate. The similarity between the results of the two highest flow rates indicate that both are over the internally controlled limit, i.e that thermal conduction within the vessel is the slowest process.

Figure 5.4 compares the normalised process values (P/P$_{max}$) for all the locations where the temperature was measured during the flow rate experiments (processing values presented in Appendix II). As expected, the higher P/P$_{max}$ values correspond to rates of 0.78 l/min and 1.09 l/min, with values that are almost twice those corresponding to the lowest flow rate (0.58 l/min).

The values are significantly less than 0.1 showing the problems of getting good heat transfer (in compare to Figure 4.10) heat transfer from the water bath is studied.
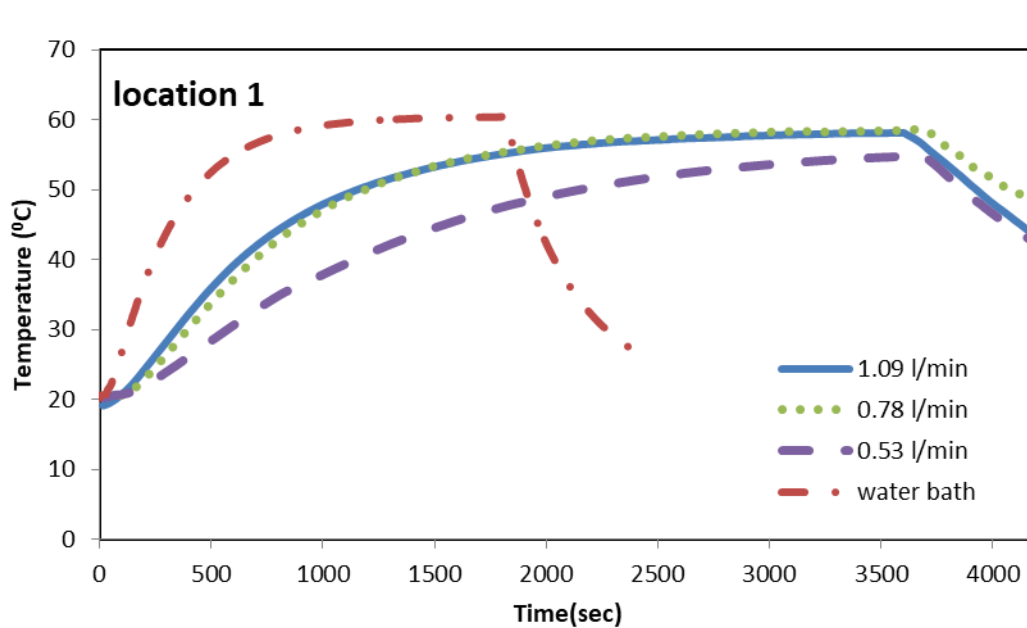
(a)
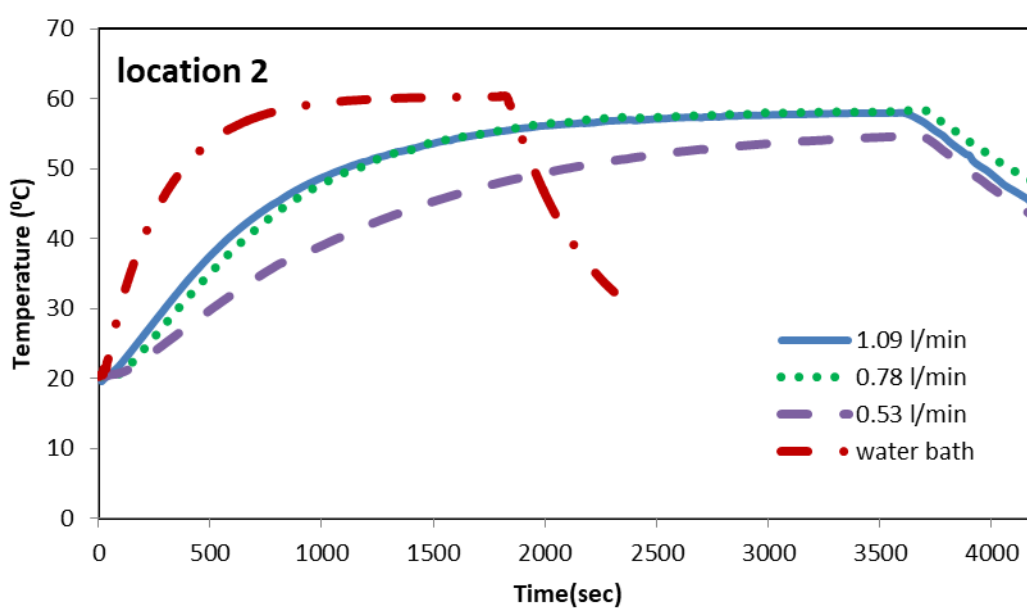
(b)

Figure 5. 3: Temperature profiles corresponding to two locations (a) location 1 and, (b) location 2 inside the jar for four different flow rate conditions: 0.53 l/min (dashed), 0.78 l/min (dotted) and 1.09 l/min (solid) and water bath (dashed and dotted) The temperature of the spray nozzle was 60°C , while the water filling the jar was initially at 20°C.
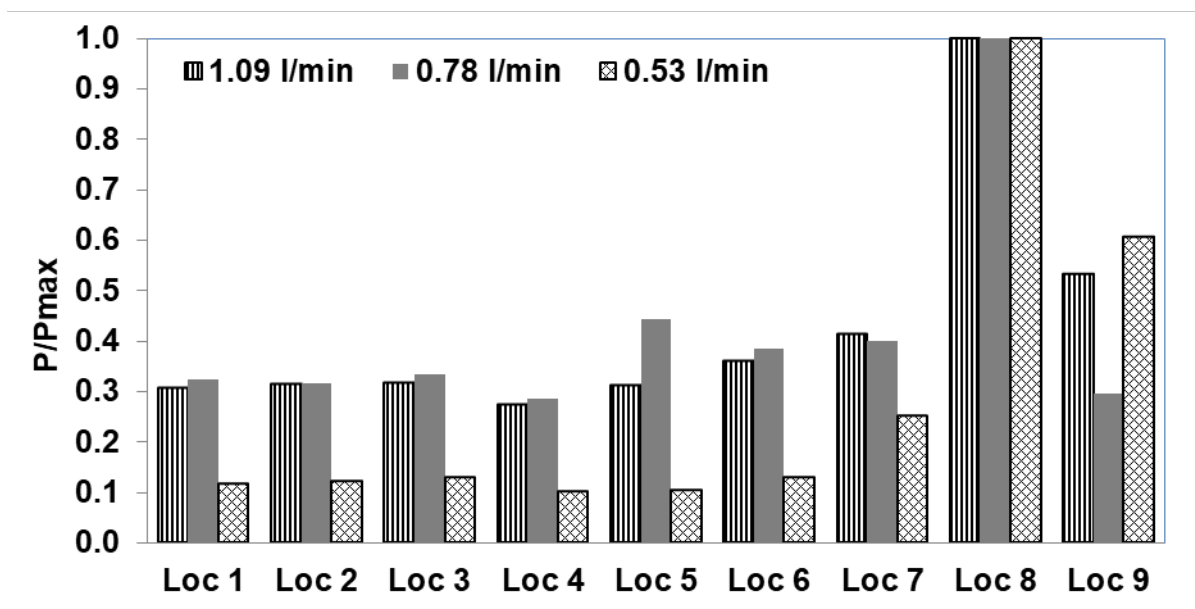
Figure 5. 4: Processing values for three different flow rate values: (a) 0.53 l/min (lines), (b) 0.78 l/min (solid) and (c) 1.08 l/min (diamond). The temperature of the spray nozzle was 60°C in all cases, with an initial temperature of the filling water of 20°C. The z-value considered in the calculations was z = 10°C and the value of the temperature reference used was T_{ref} = 70°C.

5.2.1.1 Convective heat transfer coefficients in the spray shower rig

Heat transfer coefficient values were calculated from the experiments with the aluminium block using the lumped capacitance method explained in Section 3.3 and are shown in Table 5.1. In order to calculate the Biot numbers for the experimental systems, a thermal conductivity of 0.58 W/mK was used for water *(Ramires, 1995)* and 0.26 W/mK for both starch solutions *(Fricke, 2001).* These are the relevant values at the starting temperature 21°C and it was assumed that thermal conductivity

does not change with temperature. The values of Biot numbers for the experimental set up involving the three test materials are also shown in Table 5.1.

Table 5. 1: Heat Transfer Coefficients and Corresponding Biot Numbers

Flow rates	0.1 kg/s	0.233 kg/s
Heat Transfer Coefficient $(W/m^2 K)$	1605	1619
Biot Number: Water	35.1	35.4
Biot Number: Starch Solutions	78.2	78.9

To check the order of magnitude of the heat transfer coefficients, a simplified correlation for heat transfer in falling films was used *(Euzen, 2004)* for a range of flow rates, and it could be confirmed that heat transfer coefficient values across the entire range of flow rates considered experimentally were in the correct order of magnitude. The Biot numbers across the large range are considerably greater than 0.1. It can therefore be concluded that across the considered experimental range, the process is internally controlled.

5.2.2 Effect of temperature

The effect of the spray temperature on the heating dynamics of the system was studied by running experiments using three different spray nozzle temperatures (i) 50°C (ii) 60°C and (iii) 70°C and jars containing water. The temperature profiles obtained from this series of experiments are presented in Figure 5.5, where the three systems show consistent trends in their thermal responses. Lower spray/tank temperatures resulted in lower filling temperatures; the highest temperature values are only 5°C lower than the spray temperature and correspond to the experiments

ran at 70°C. The driving force of the system is temperature, so higher temperatures

will lead to faster heat transfer rates.

(a)   (b)

(c)   (d)
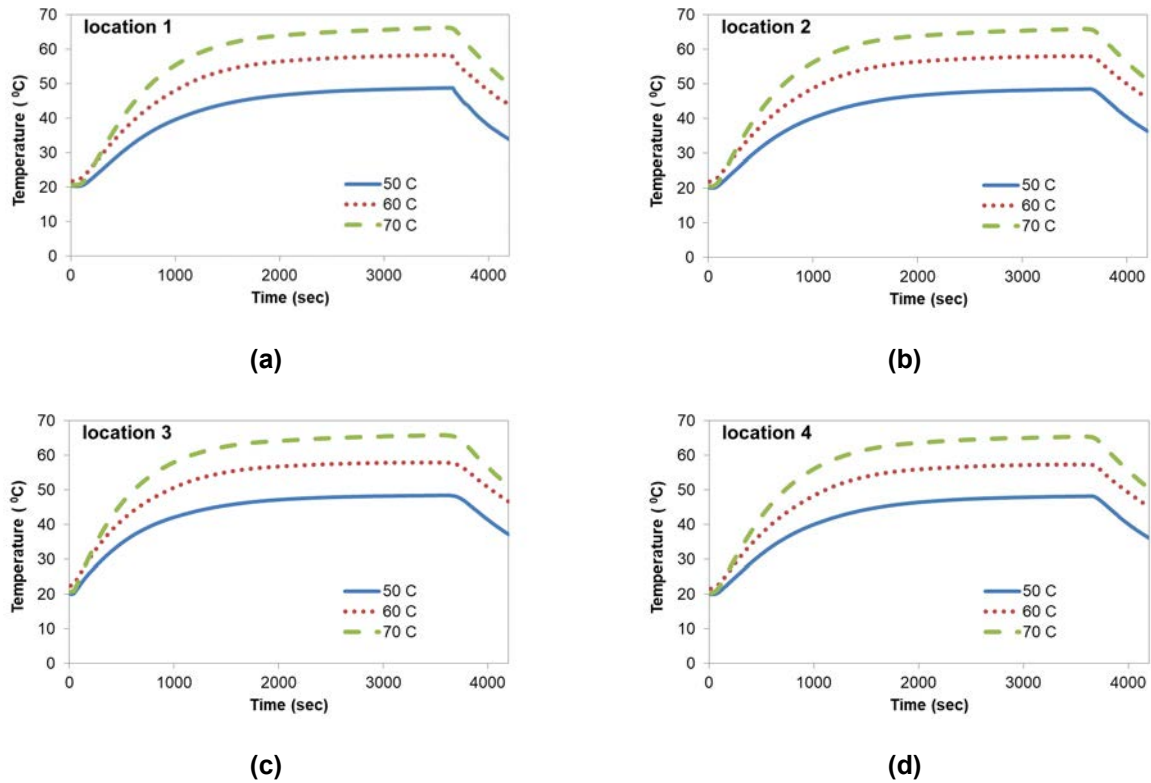
Figure 5. 5: Time-temperature profiles corresponding to four locations inside the jar (a) location 1,

(b) location 2 (c) location 3 and (d) location 4 for three different spray nozzle temperatures: (a)

50°C (solid), (b) 60°C (dotted) and (c) 70°C (dashed). The initial temperature of the water filling the

jars was 20°C. The data shown was measured for a mass flow rate through the nozzle of 1.09

l/min.
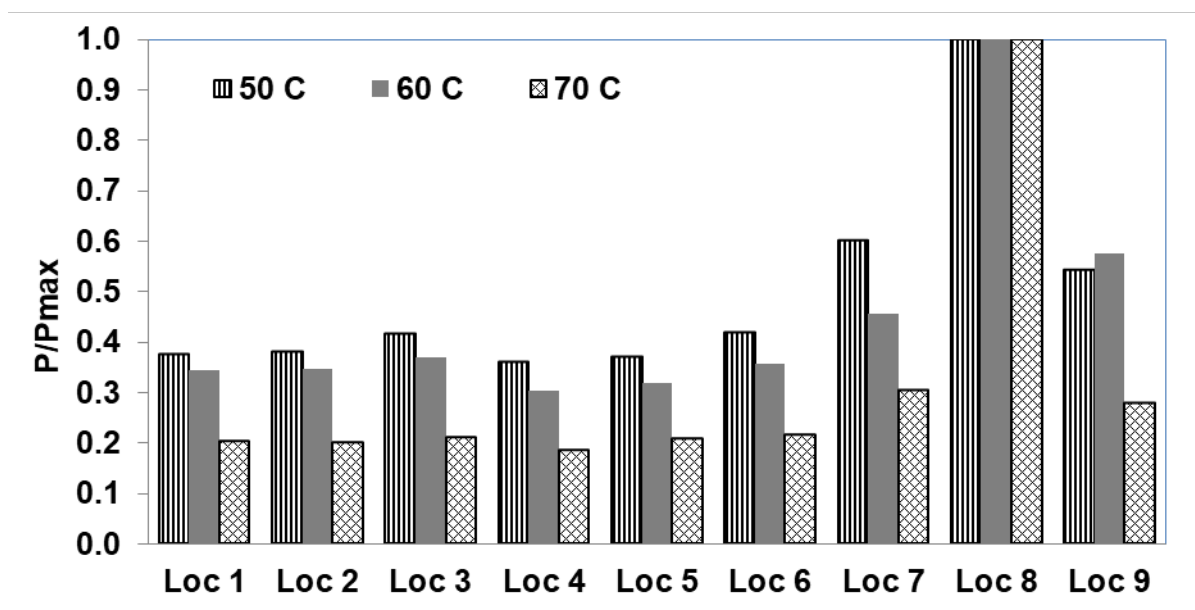
Figure 5. 6: Processing values calculated for three different spray nozzle temperatures: (a) 50°C (lines), (b) 60°C (solid) and (c) 70°C (out lined diamond) in a jar filled with water. The starting temperature was 20°C in all cases, and the Z-value considered in the calculations was z = 10°C. The reference temperature considered was T_{ref} = 70°C. The data shown was measured for a mass flow rate through the nozzle of 1.09 l/min.

5.2.3 Effect of solution viscosity

To study the effect that the viscosity of the filling has on the heat transfer rates of the spray vessels system, five different solutions were heat up in the vessel spray at a fixed flow rate of 1.08 l/min and with a spray nozzle temperature of 70°C. Table 5.2 lists the fillings used in this series of experiments, alongside their viscosity values.

Figure 5.7 shows the temperature profiles corresponding to five different fillings: water, 5%(w/v) pre-gelatinised starch, 5%(w/v) corn starch, 1%(w/v) guar gum and 3%(w/v) agar.

Table 5. 2: Fillings employed in the spray vessel experiments and their viscosity values.

Jar filling	Viscosity (Pa s)	Reference
Water	1.002×10^{-3}	Deen (2016)
5%(w/v) pre-gelatinised corn starch	1.96×10^{-3}	Telis et al (2007)
5%(w/v) corn starch	0.45	Mehuaden (2008)
1%(w/v) guar guam	0.75	This work
3%(w/v) agar	1450	Kasapis (2009)

The data shows:

 (i) For water, as in Figure 5.2 the temperature increases rapidly throughout the beginning of spraying process, and after 2800 seconds the heating rate slows down. The system temperature reaches 65°C over heating period for one hour.

(ii) The 5% (w/v) pre-gelatinised starch solution exhibits slightly slower heating dynamics, with a slower approach to the spray temperature after approx. 3000 seconds.

(iii) The temperature profile corresponding to the 1%(w/v) guar gum solution shows the same trend than water and the pre-gelatinised starch, but with a slower heating rate before 2000 seconds.

(iv) The 5% (w/v) starch and the 3% (w/v) agar solutions, present a similar behavior, with the slowest thermal responses and no cooling stage: i.e. heating is so slow that it continues after the external heating has stopped.

(v) Thermal responses were slower in those fillings with higher viscosity, in which conduction is mechanism driving heat transfer, in comparison with the fast heating show by water and the 10% sugar solution – system where convection is dominating heat transfer inside the jar.
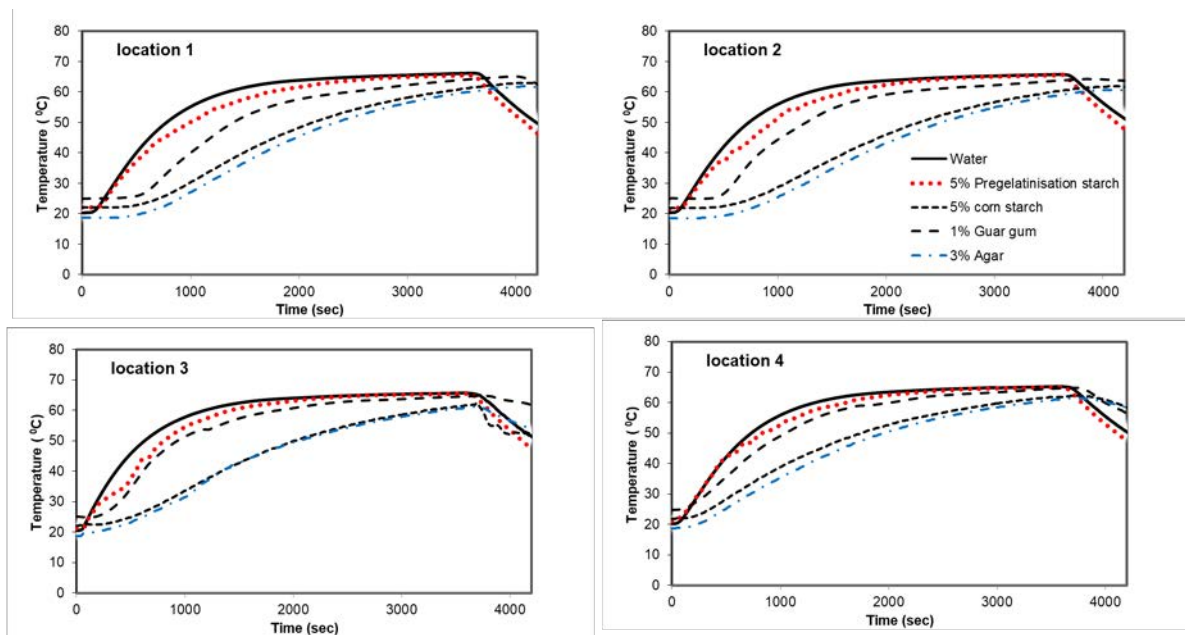
Figure 5. 7: Temperature profiles measured inside the jar for five fillings of different viscosity: water (solid), 5% (w/v) pre-gelatinised starch (dotted), 5%(w/v) corn starch (squares), 1%(w/v) guar gum (dashed), and 3%(w/v) agar (dash-dotted). The temperature of the spray nozzle was 70°C in all cases the shown, with an initial temperature of the fillings of approx. 20°C. The data corresponds to a mass flow rate through the nozzle of 1.09 l/min.
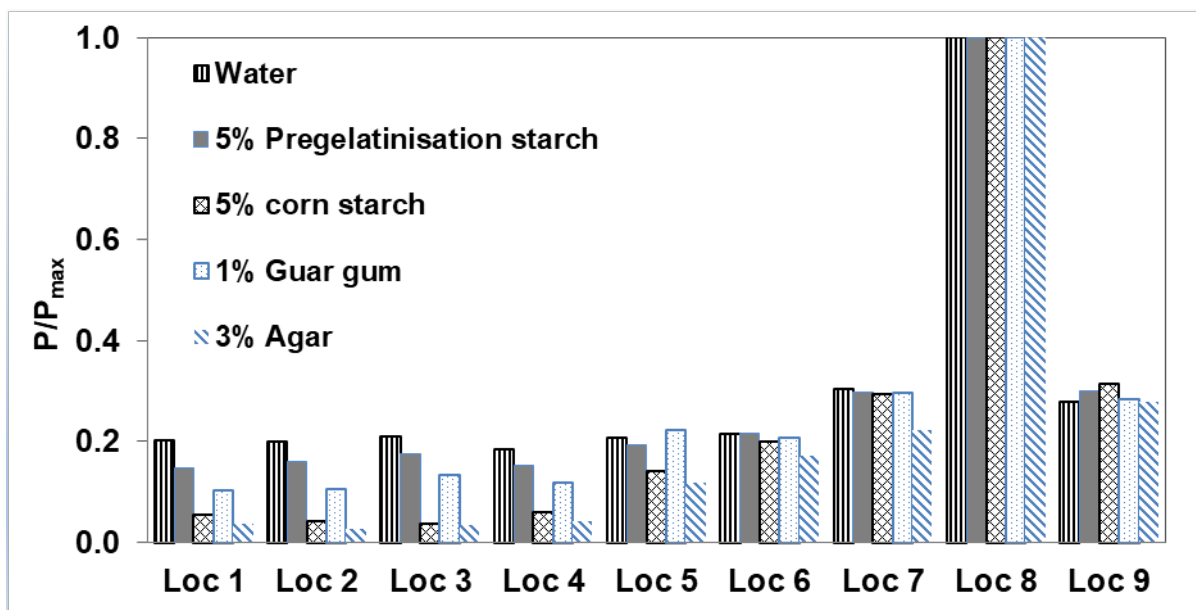
Figure 5. 8: Normalised P values for five different solution systems: water (line), 5%(w/v) pre-gelatinised starch (solid), 5%(w/v) corn starch (diamond), 1%(w/v) guar gum (dotted) and 3%(w/v) agar (wide downward). The spray nozzle temperature was 70°C in all cases, with a starting temperature for the filling of 20°C. The Z-value considered in the calculations was z = 10°C, T_{ref} =70°C. The data shown was recorded for a mass flow rate through the nozzle of 1.1 l/min.

The normalised P values for the five different solutions are presented in Figure 5.8. Data shows that the highest P/P_{max} values correspond to the system with the lowest viscosity – water. Lower heat transfer (as consequence of increasing viscosity values) results in lower P/P_{max} values, as can be seen in Figure 5.8 for the 3%(w/v) agar solution. Very low P values result from the processing of agar (*ca.* 0.05 as opposed to 0.2 for water for example).

5.2.4 Effect of nozzle position

In a real tunnel pasteuriser as shown in Chapter 1, a full load of jars passes through the tunnel to extend shelf life for the food by lowering the microbial load. However, there will be heat lost along the tunnel and over was conducted load of jars. A study of heat transfer in different positions inside a spray to understand its behavior and find out optimal location of can or jars. This section describes experiments shower there was an see the effect of:

(i)   relative position of nozzle and vessel

(ii)   height of vessel, and

(iii) container set up.

The jars were set up with thermocouples and temperatures were recorded as explained in Section 3.5.3.

5.2.4.1 Effect of holizontal distance between nozzle and container

It is not clear what effect the distance between nozzle and vessel will have on heat transfer behaviour and the heat lost in its environment. This experiment was set up with different locations of the jar in the pasteuriser rig unit as shown in Figure 5.10. There are four locations of the jar shown for four different holizontal distance position between the nozzle and a vessel systems; point 1 (25 cm), point 2 (18.5 cm.), point 3 (12 cm.), and point 4 (25 cm). The spray nozzle temperature was 60°C in all cases, with a flow rate of 0.78 l/min.
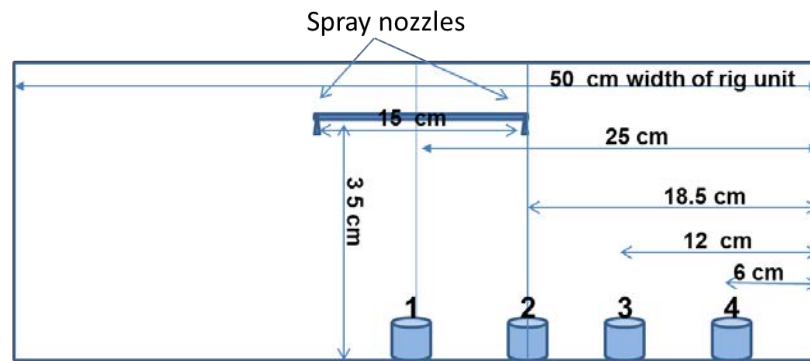
Figure 5. 9: Schematic of the distance between nozzle and vessel.

Figure 5.10 shows the temperature profiles obtained at four different locations in the jar for four different relative positions of nozzle and vessel.

- The distance between nozzle and vessel systems at point 4 gave the slowest heating profile, while at point 1 was the highest heating. However, the behaviour at point 2 and 3 had temperature profiles that were very similar.

- In all cases, the final temperature is reached at close to 56°C at the same time, after heating for 3000s.

- The data suggests, as expected, that the further the vessels are from the nozzle the slower the heating rate. This will be significant industrially in the case of effect of rows of can/jars or if the flow pattern is the pasteuriser is not uniform.
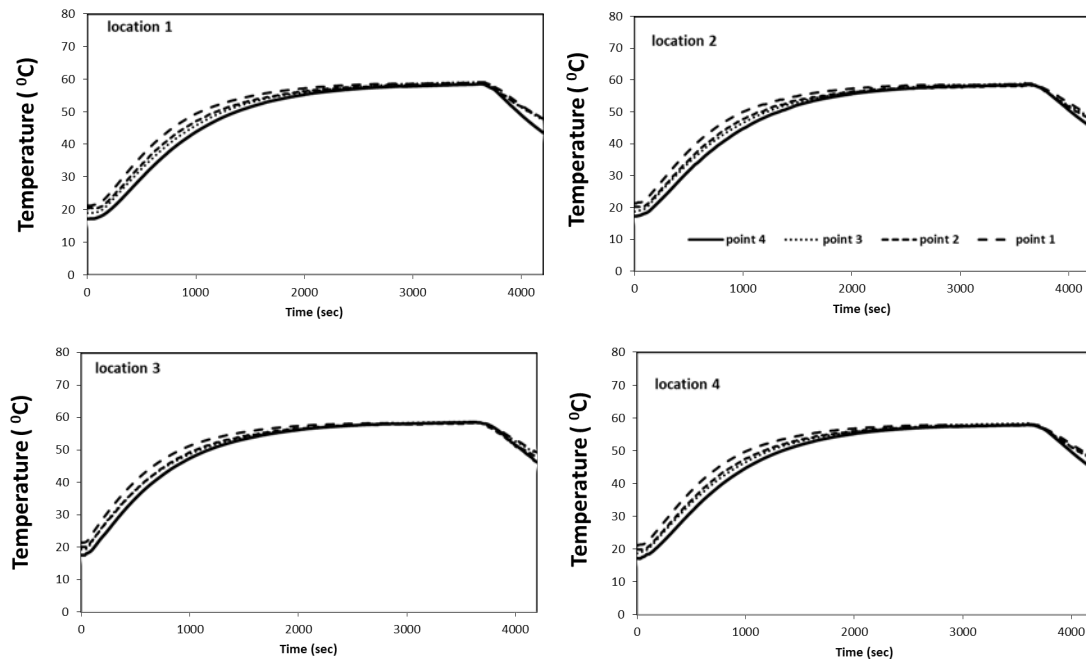
Figure 5. 10: Temperature profiles obtained at four locations in jar for four different relative position of nozzle and vessel: (a) point 1 (dashed), (b) point 2 (square dots), (c) point 3 (round dots), and (d) point 4 (solid). The temperature of the heating tank was 60°C, with a starting temperature around 20°C in all cases. The data shown was measured for a mass flow rate through the nozzle of 0.78 l/min.

Figure 5.11 presents the P/P_{max} values for the four different relative positions of nozzle and vessel. As seen in the temperature-time profiles in Figure 5.11, the distance between nozzle and vessel at point 4 gave the slowest heat transfer and the calculated P/P_{max} valued gave the lowest P values, whilst with the location at point 1 gave the highest P values. There were no significant differences between points 2 and 3.
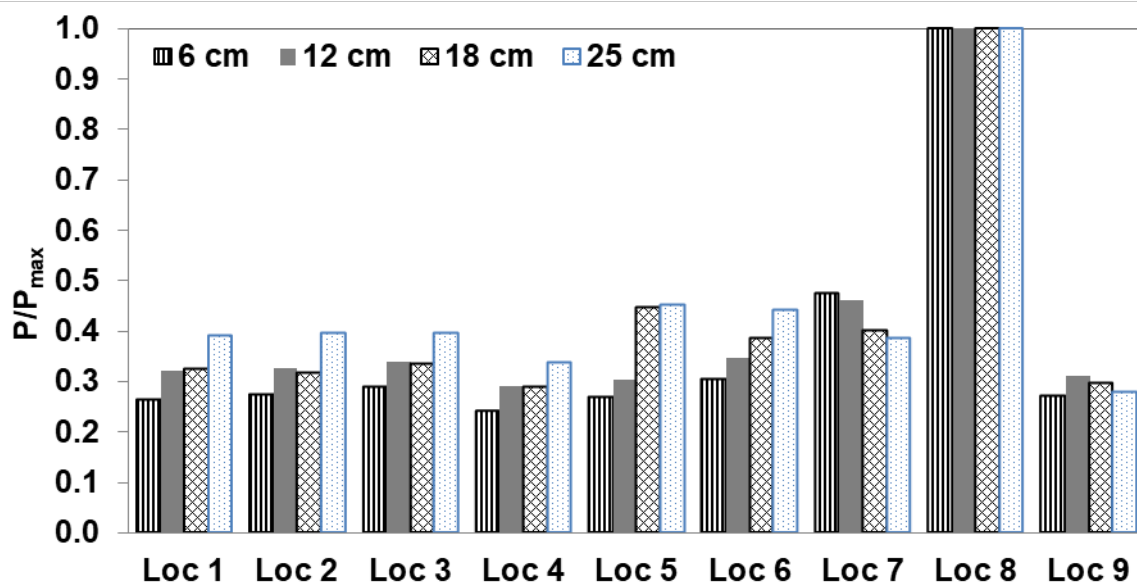
Figure 5. 11: the P/P$_{max}$ values for four different relative positions of nozzle and vessel: (a) point 1 (dots), (b) point 2 (diamond), (c) point 3 (solid), and (d) point 4 (line). The heating temperature was 60°C and flow rate 0.78 l/min in all cases. The starting temperature was 20°C, the z-value considered in the calculations was z = 10°C and T$_{ref}$ = 70°C.

5.2.5 Effect of vertical distance between nozzle and container

The other assumption about the effect of nozzle position on heat transfer was the effect of the height between a nozzle and jar. The experiment then was set up with various locations of jar in a pasteuriser rig unit as shown in Figure 5.12.   Three heights (18.6 cm, 26.8 cm, and 35 cm.) between nozzle and jar were studied. The spray nozzle temperature was 60°C in all cases. The spray nozzle flow rate was 0.78 l/min. The temperature was recorded for every 15 seconds.
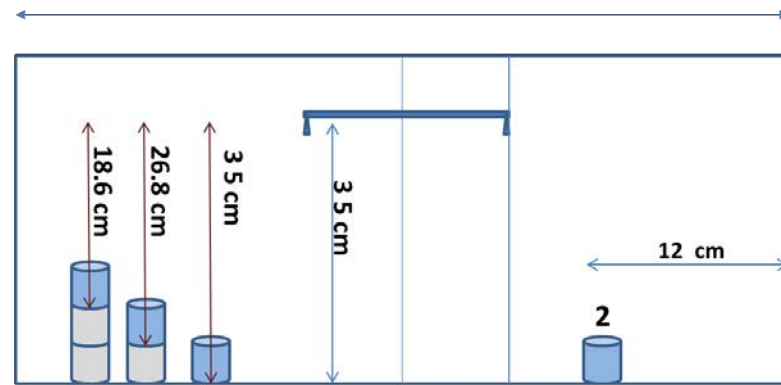
(a)
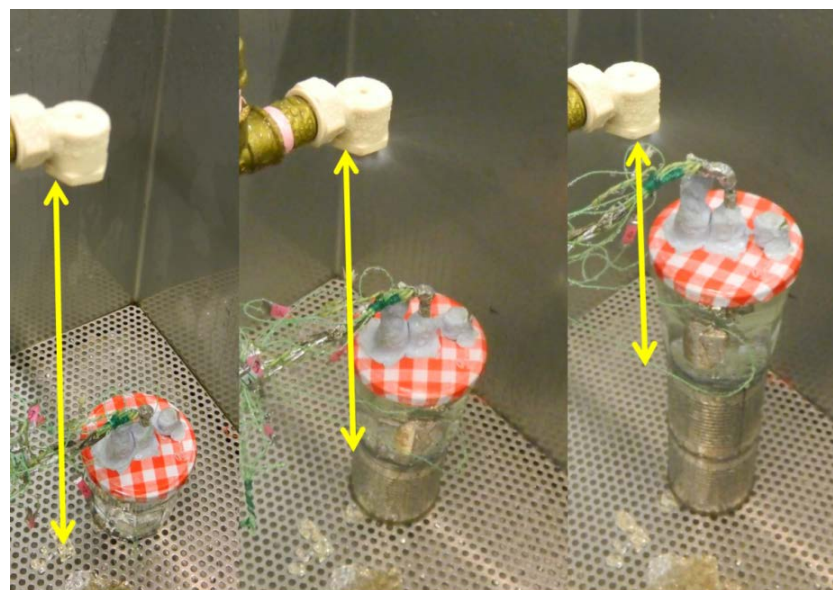
(b)

Figure 5. 12: Schematic of the distance variations between nozzle and jar.

Figure 5.13 shows the time-temperature profiles for the three different distances between nozzle and jar studied: (a) 35 (dashed), (b) 26.5 (dots) and (c) 18.6 (solid) cm. The figure shows that:

The 18.6 cm distance gave the fasest heating profile, while for a distance between nozzle and jar of 26.8 cm the heating temperature profile obtained showed the slowest values.

- slightly differences in the temperatures of the jar locations 1, 2, and 4 (radial distribution) were found when the smallest and biggest distances between nozzle and jar were compared.

- On the contrary, it seems that the falling height of the spray had a certain rising effect on the temperature profiles register at location 3 (the top of jar).

- In all cases, the systems reached the their highest temperature value about 57°C after heating for 2800s.

- It was found that different distances between nozzle and jars had no uniform effect on heat transfer.

(a)

(b)

(c)

(d)
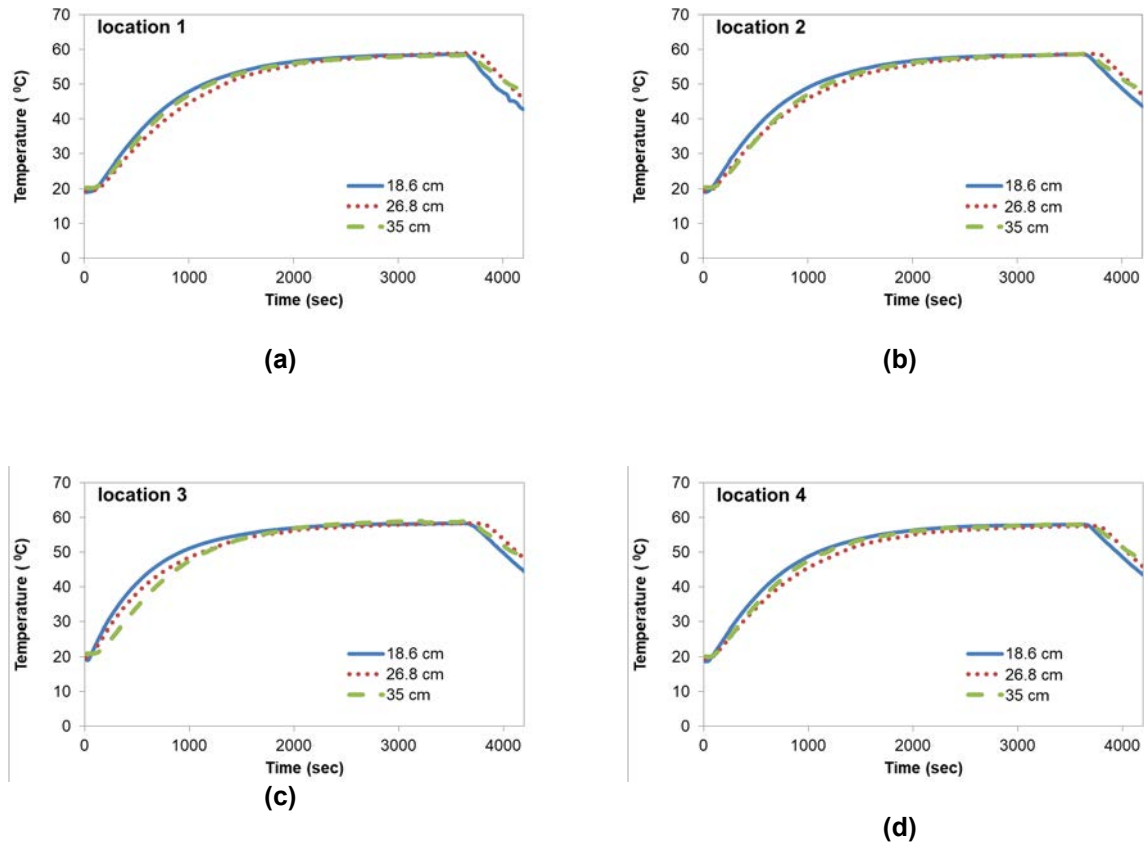
Figure 5. 13: Time-temperature profile for three different heights of the nozzle with respect the jar top: (a) 35 cm (dashed), (b) 26.5 cm (dots) and (c) 18.6 cm (solid). The jars contained water initially at a temperature of 20°C. The temperature of the heating spray approx. was 60°C and its flow rate was 0.78 l/min in all cases.

Figure 5.14 shows the P/P_{max} values for the three different heights of the nozzle (see Appendix II for the P values without normalisation). The z-value considered in the calculations was $z = 10°C$ and the reference temperature considered was $T_{ref} = 70°C$.

Accordingly to the temperature-profiles showed in Figure 5.13, the P/P_{max} values for the 18.6 cm distance between nozzle and jar were the highest ones, whilst those calculated for the 35 cm distance were the lowest ones.
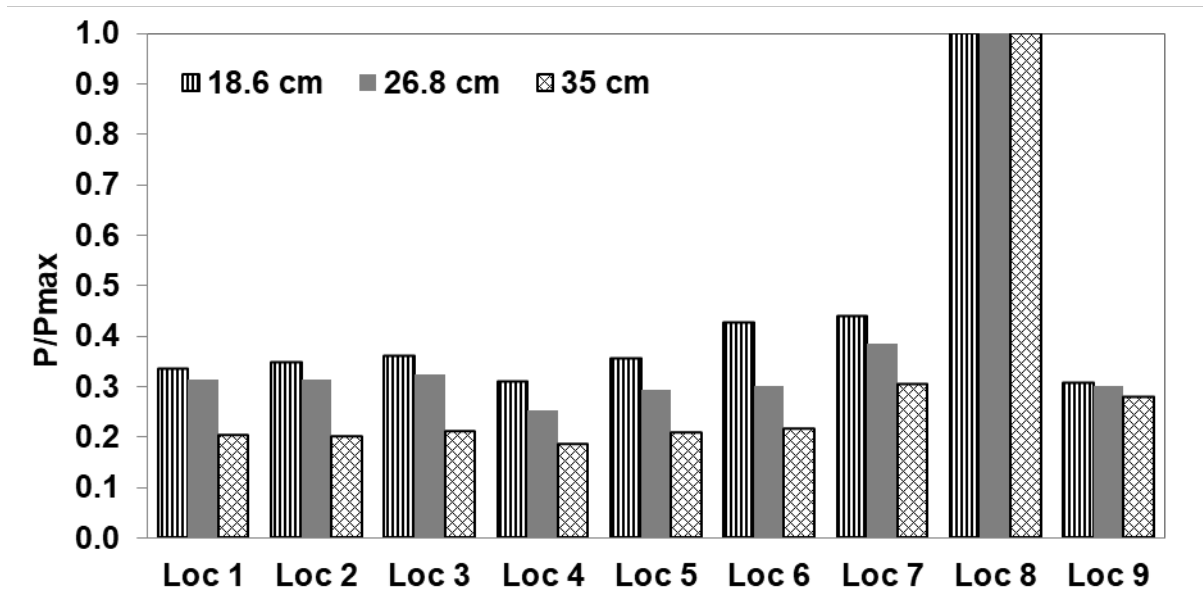
Figure 5. 14: Normalised pasteurisation values for three different heights of the nozzle: (a) 35 cm (line), (b) 26.5 cm (solid) and (c) 18.6 cm (out lined diamond). The z-value considered in the calculations was z = 10ºC, and the reference temperature was T_{ref} = 70 ^{0}C.

5.2.6 Container set up

The last set of tests to assess the effect of the nozzle position on heat transfer of the system looked at different container set ups: i.e. different number of jars (1, 2, 3, 4, and 9) inside the pasteuriser rig unit, as shown in Figure 5.15. The spray nozzle temperature was 70ºC in all cases, with a flow rate of 0.78 l/min, and temperatures were recorded every 15s. In a commercial tunnel, jars are close together, and this might affect heating condition.
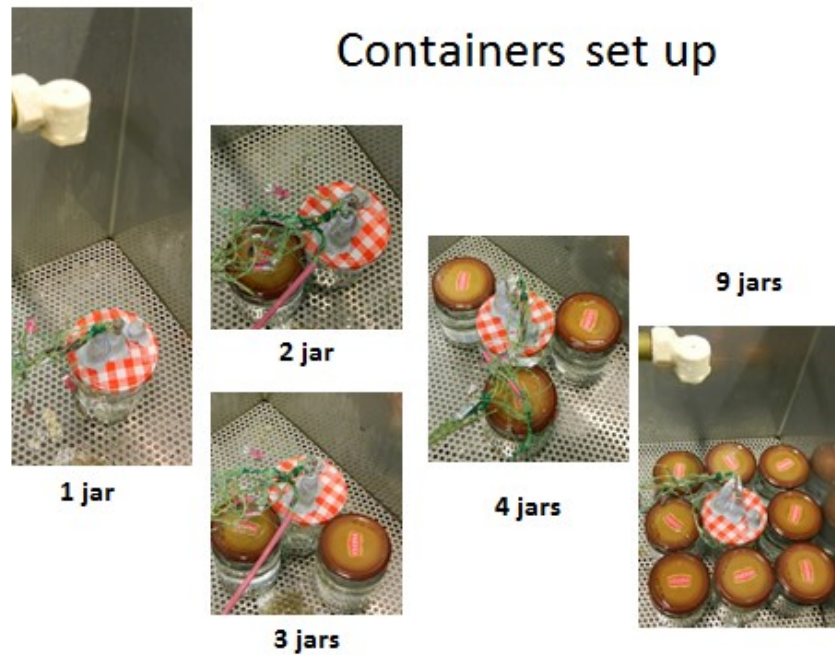
Figure 5. 15: Pictures of the spray rig showing the disposition of the system for different jet arrangements.

Figure 5.16 shows the temperature profiles obtained for the five different container set ups compared in the spray system: 1 jar (black solid), (b) 2 jars (red dots), (c) 3 jars (black squares), (d) 4 (dashed) and 9 (dashed-dotted. It this graph it can be seen that:

(i) The single container set up gave the most rapid heating profile, while the 9 containers set up was the lowest heating temperature profile.

(ii) As the number of containers in the set up increased, the rate heat transfer decreased.

(iii) In all cases (but the 9 jars set-up), the final system can reach the temperature at similar times; although the heat transfer rate depend on a number of jars, all them reached the highest temperature (approx. 65°C) after 3200s.

In the 9 jars set up the maximum temperature reached is lower than in the other jar arrangements studied. This might be due to the amount of water supplied to each jar being insufficient for heating - as noted in Chapter 2, the supply of insufficient amount of heat will significantly reduce the heating rates

(a)   **(b)**

(c)   **(d)**
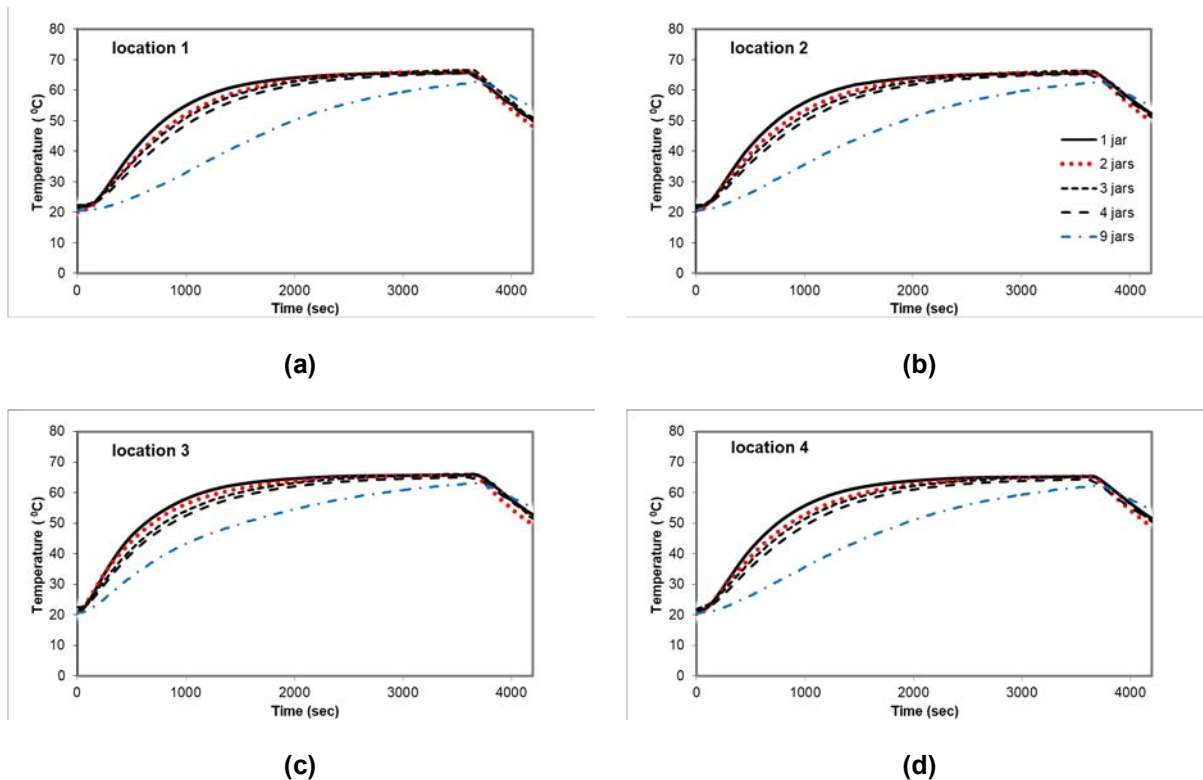
Figure 5. 16: Temperature profiles obtained for heating temperatures at four different locations inside the jar in container set up consisting of: (a) 1 jar (black solid), (b) 2 jars (red dots), (c) 3 jars (black squares), (d) 4 jars (dashed) and 9 jars (dashed-dotted). The heating temperature was 70°C and the mass flow rate was 0.78 l/min. The starting temperature was around 20°C.

In Figure 5.17: the normalized P values for these five different container set ups are shown. It would be expected that:

(i) The single container set up resulted in the highest P values, while the 9 containers set up was the lowest P values follow as temperature-time profile in Figure 5.16.

(ii) As the number of containers in the set up increased, P values decreased.

(iii) However, the 2 and 3 containers set up were not significantly different in normalised P values.

Conclusions that can be drawn from these experiments are:

- P/P_{max} values increase with the temperature of the heating medium and the liquid flow rate.

- Similarly, P P/P_{max} values increased as viscosity of the food decreased.

- However, the normalised P values decrease when the number of jar increased.

- P/P_{max} values at a separation of nozzle and jar of height of 18.6 cm are the highest; however, P values at the height of 18.6 cm and 35 cm are almost the same.

- A target of 70°C for 5 min is achievable with an optimal design using rate 70 °C of 30 min.

- There is a strong effect of viscosity on the system internal temperature but this only weakly affects the surface.
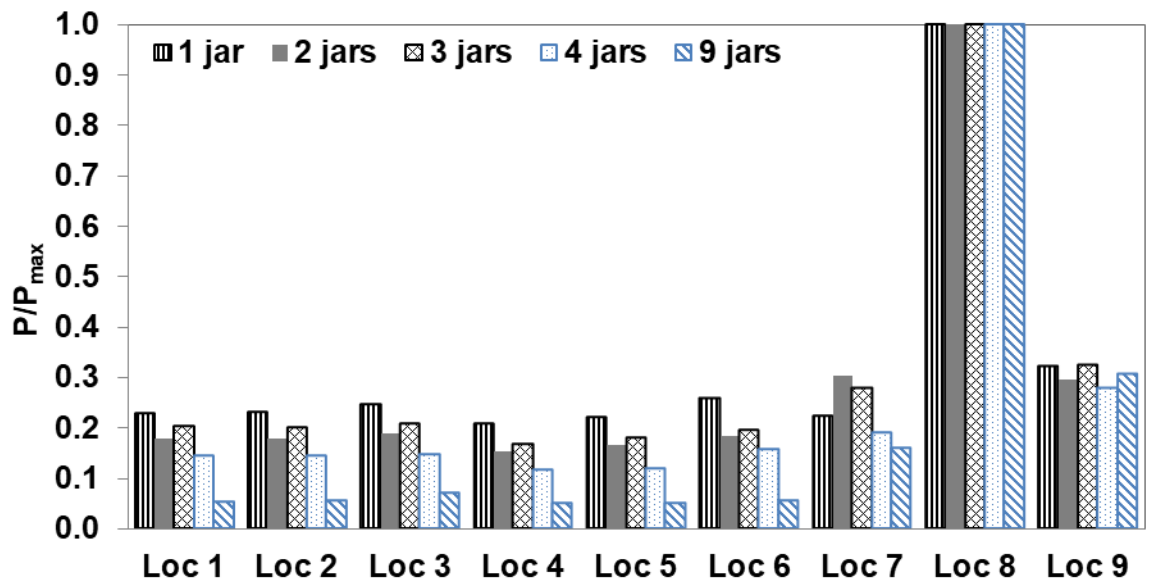
Figure 5. 17: Normalised P values for five different container set up systems: (a) 1 jar (line), (b) 2 jars (solid), (c) 3 jars (out lined diamond), (d) 4 jars (dots) and (e) 9 jars (wide downward). The z-value considered in the calculations was z = 10°C and T_{ref} = 70 °C.

5.3   Spray vessel design 2: Straight water flow nozzle set up

In Section 5.2 the efficiency of a nozzle that spraying in a 120-degree wide angle on the heat transfer in jar during pasteurisation was investigated, and results were showed how parameters such as the location of jars affect heat transfer. However, this 120-degree nozzle presented a wide spray distribution, and this might be affect the heat lost between nozzle, vessel and its environment.

To identify how much heat could be lost, two other types of nozzle were studied for comparison: (i) a single jet nozzle and (ii) a straight-line showerhead, both shown in Figure 5.18 (a) and (b) respectively. The single jet nozzle represents a very straight vertical flow, in which all the liquid reaches directly to the top of a vessel, and the showerhead was representative as a raining flow onto a vessel.   The experiment

was set up and experiments carried out as detailed in Section 3.5.3.   The experimental set up is the same as shown previously in Section 5.2.

(a)   (b)

Figure 5. 18: New showerheads: (a) single jetsingle jet and (b) Multi jet.

Table 5. 3: Experiment plan for the spray experiments conducted with the single jet and the shower head nozzles.

Type of Nozzle	Flow rate (l/min)	Filling
Single jet	0.92 - 1.91	water
		5% corn starch
Muti jet	0.98 - 1.71	water
		5% corn starch

Table 5.3 shows the parameters studied:

(i) Effect of a spray flow rate (0.92 and 1.91 l/min for single jet nozzle and 0.98 and 1.78 l/min for a muti jet nozzle).

(ii) Effect of type of nozzle.

(iii) Effect of viscosity of food fluid (water and 5%(w/v) corn starch).

All experiments were conducted for 60 min heating and 10 min cooling. The heating temperature at the nozzle was 70°C and temperature was recorded every 15 seconds.

5.3.1 Time temperature profile

Figure 5.19 compares the time - temperature profiles between two nozzles measured at eight locations in both jar and its environment. For both nozzles, the behaviour of the system was very similar:

(i) There was slow heating at the centre of the jar locations 1, 2 and 3.

(ii) However, the temperatures were very similar for all the locations along the axial direction: bottom (location 1), half height (location 2) and top of the jar (location 3). This behaviour is not similar to the water bath experiments, in which the temperature decreased from top to bottom of jar (see Chapter 4).

(iii) The temperature profile was lower from the centre of jar (location 2) to side of jar (location 4) (which was the slowest point) but increased from to inner wall of jar (location 5) and the outer wall of jar (location 6).

(iv) The temperature in the jar could not reach the heating temperature; jar temperatures were 2-3°C lower, showing heat losses in the spray system.
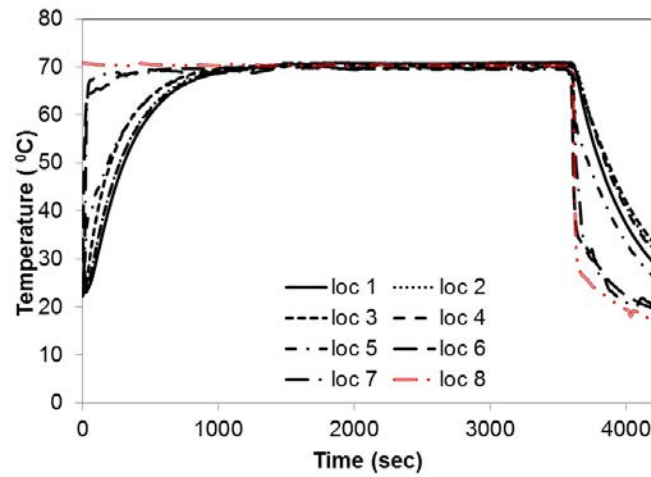
(a)
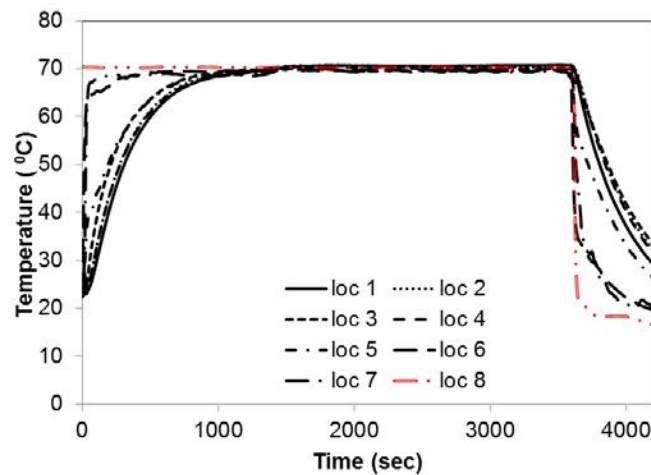
(b)

Figure 5. 19: Temperature profiles measured for eight locations in the system (jar and its environment) under a spray pasteuriser unit using 2 different nozzle (a) single jet (maximum flow rate at 1.91 l/min) and (b) muti jet (maximum flow rate at 1.78 l/min). The jars contained water and heating nozzle temperatures of 70°C. The filling was initially at room temperature (i.e. around 20°C).

5.3.2 Effect of flow rate

The data of Figure 5.20 show temperature profiles for two different flow rates (minimal flow rate and maximum flow rate) for each type of nozzle (single jet nozzle and muti jet). The research found that there were the same behaviour in all experiments, for all flow rates at nozzle and kind of nozzle, with faster thermal responses for maximum flow rate treatments.

(a)

(b)

(c)
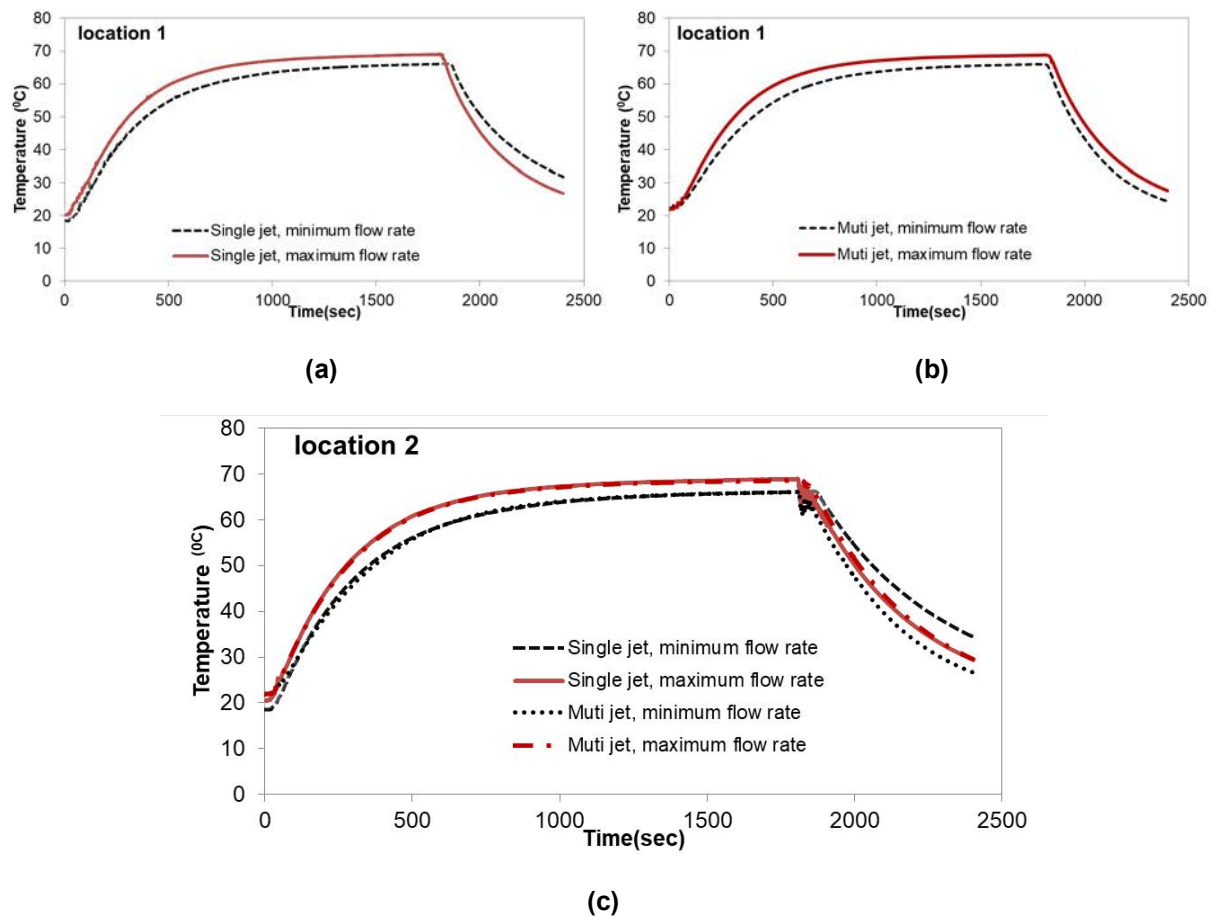
Figure 5. 20: Temperature profiles for two different flow rate of conditions: minimum flow rate (dashed) and maximum flow rate (solid) for two types of nozzle: (a) single jet nozzle and (b) multi jet, and (c) single jet and muti jet. Temperature of the heating spray was 70°C, while the water filling the jar was initially at approx. 20°C

As example, system in Figure 5.20(a) – single jet nozzle with maximum flow rate condition – where the temperature rapid reaches values close to the nozzle temperature during initial heating period (800s); for the minimum flow rate the water in the jar reached the same temperature values after about 1000s.

Showerhead and single jet nozzle showed very similar thermal responses, for both maximum and minimum flow rates, with temperatures in the jars between 2-5°C lower than the heating temperature.

Figure 5.21 presents the normalized P values for minimal flow rate (solid) and maximum flow rate (line) for each type of nozzle: (a) single jet and (b) muti jet.

- For both types of nozzles, the normalised P values increased with the flow rate. There is a higher heat transfer rate for the maximum flow rate, as seen in Figure 5.20.

- Following the trend seen in the temperature profiles, there are no significant differences between the pasteurization values in the radial direction, contrary to what was found for the water bath experiments in Chapter 4.

- Also in the water bath the jar was completely immersed in the heating medium (water), and the thermal transfer in occurred through from top and walls of the jar, resulting in P values that decreased accordingly from the top to the bottom of the jar.

(a)

(b)
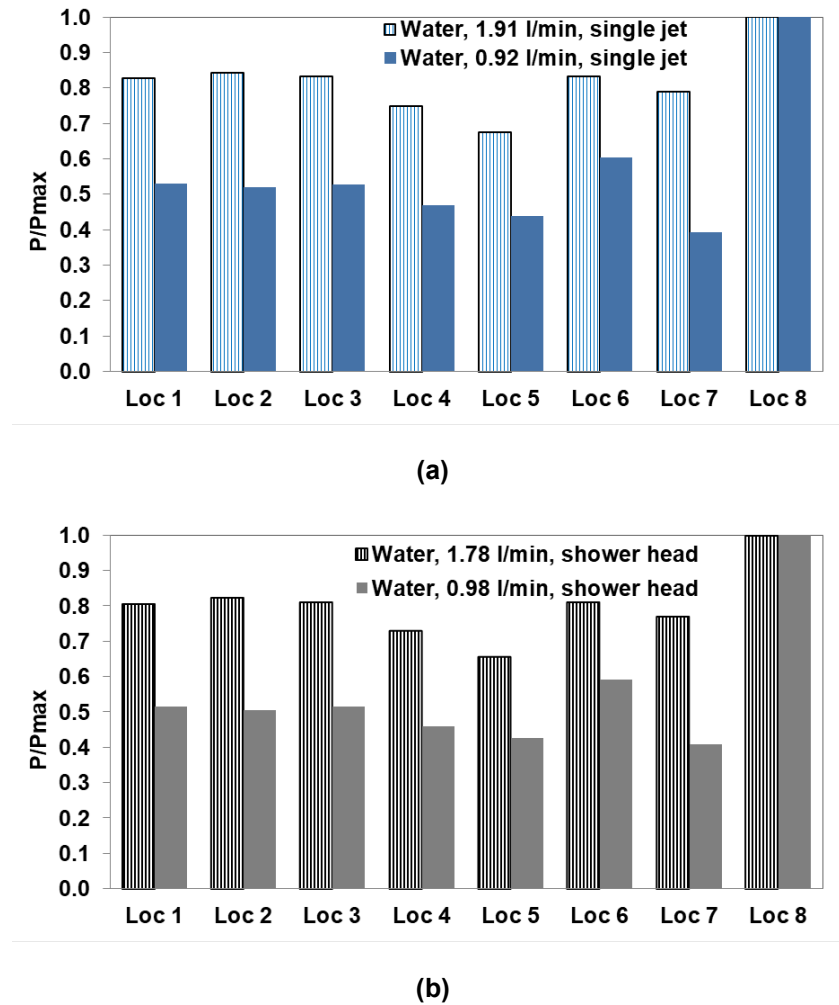
Figure 5. 21: **Normalised P values for two different flow rate of conditions: minimal flow rate (solid) and maximum flow rate (line) for each type of nozzle: (a) single jet and (b) muti jet. The z-value considered in the calculations was z = 10°C and the reference temperature was T_{ref} = 70°C. P_{max} = 65 min.**

On the other hand, in the spray system - for both single jet and muti jet - the jar was sat under the rain shower with water falling directly to some point of the jar lid, and then flowing down on the side of the jar as a thin falling film. The heat transferred from the falling film is subjected to losses (evaporation) and as the mass of water involved in the heating process is much less than in the water bath, the heat transfer rate is slower in this case. As a result too, there was a change in the location of the

coldest point of the filling, from location 1 in the water bath to location 4 in the spray shower system.

5.3.3 Effect of type of nozzle

The data from Figure 5.22 shows the comparison of temperature time profiles between the two different type of nozzle at the minimum and maximum flow rate. Both nozzle systems gave essentially identical temperature-time profiles for all flow rate conditions, presented in Figures 5.22 (a) and (b).

Comparison between three different nozzles - a single jet (flow rate at 0.92 l/min), a showerhead (flow rate at 0.98 l/min), and a 120^0 (flow rate 1.09 l/min) nozzle) - is shown in Figure 5.22 (c). Overall, the data collected in these experiments showed that:

(i)   The single jet and the showerhead had no significantly differences in the temperature-time trends in both location 1 and 5.

(ii)   The temperature for both the single jet and the showerhead nozzles increases rapidly in the beginning of spraying process up to 1200 seconds, and after that the heating rate slows down. The system temperature reaches around 67°C at the end of heating period.

(iii)   The 120° nozzle presents a significantly slower heating than the single jet and the muti jet nozzles, with a slower approach to the spray temperature after approx. 2000 seconds. The highest temperature that the system reached is around 65°C

(a)

(b)

(c)
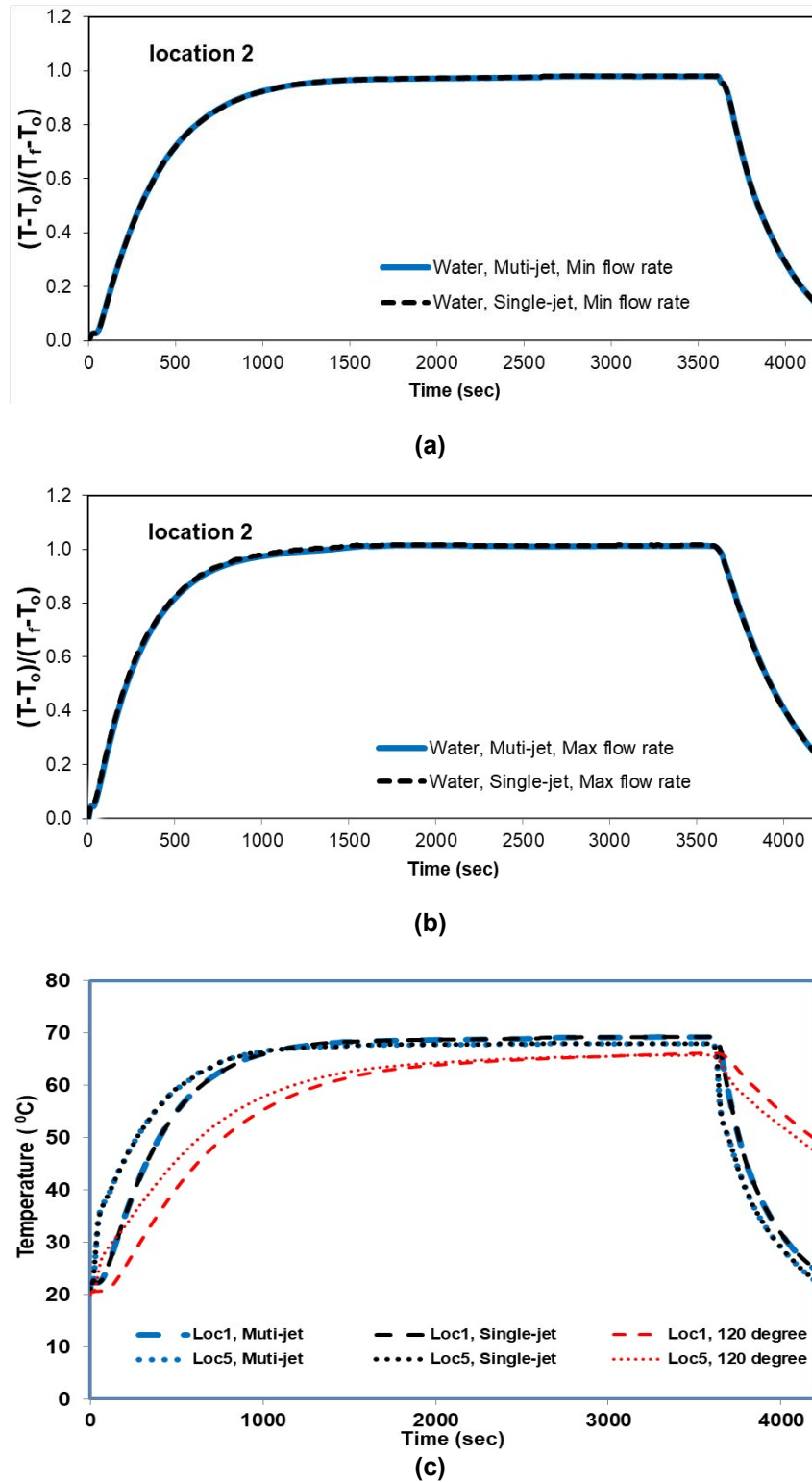
Figure 5. 22: Temperature-time profiles for the three different types of nozzle. A comparison between single jet (dashed) and muti jet (solid) is shown in (a) for the lowest flow rate and in (b) for the maximum flow rate. The three nozzles: multi jet (blue), single jet (black) and the 120^0 nozzle (red) are shown in (c) for locations 1 (dashed) and 5 (solid).
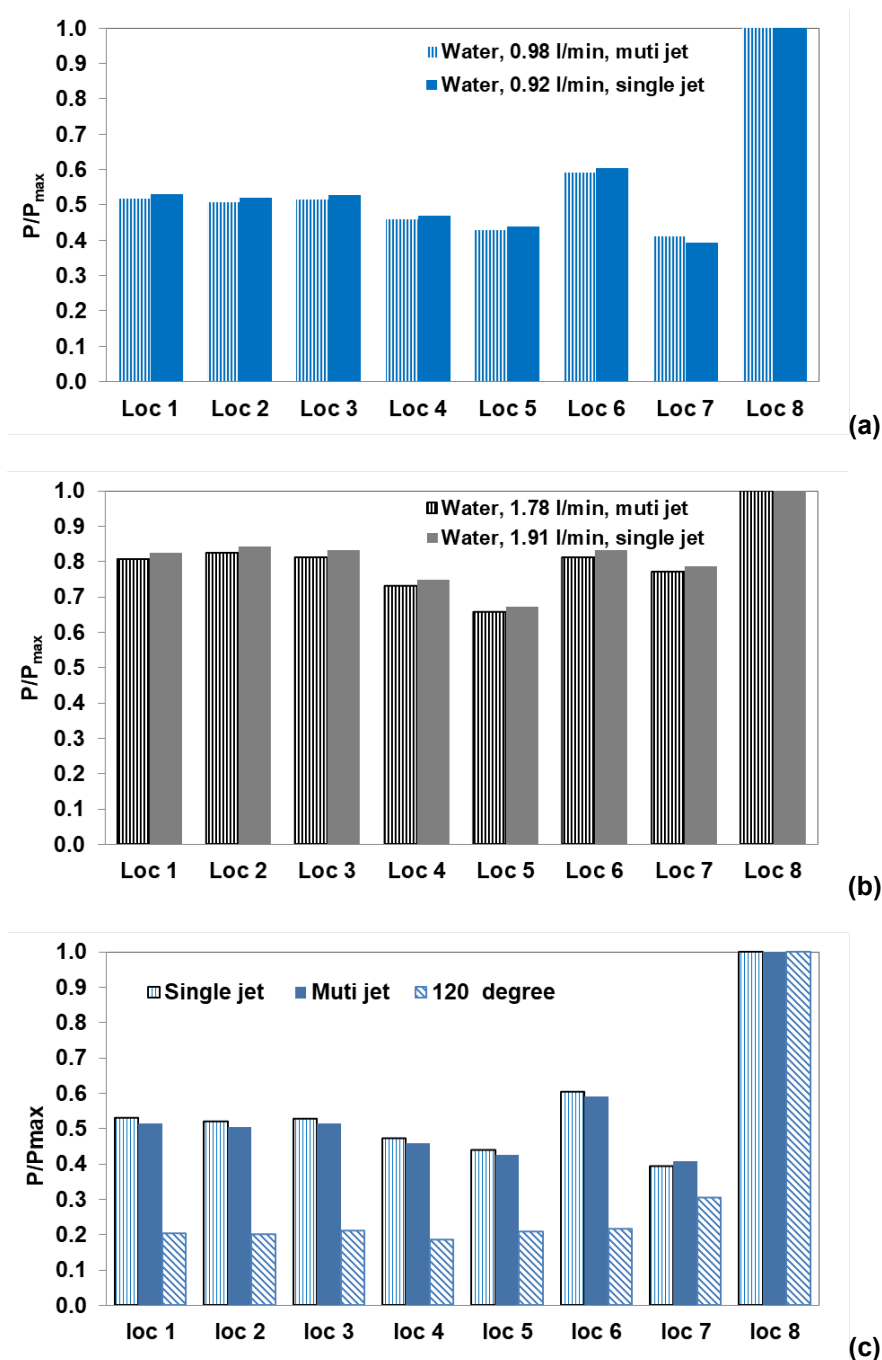
Figure 5. 23: Normalised P values were calculated for two different type of nozzle system: (a) single jet (solid), and (b) a muti jet (line) for (a) the minimum flow rate, and (b) maximum flow rate. The z-value considered in the calculations was z = 10°C and the reference temperature was T_{ref} = 70°C. P_{max} = 65 min.

Figure 5.23 shows the normalized P values calculated for the single jet nozzle and the showerhead. There was no significant difference between P-values for the shower and single jet nozzle. Figure 5.23(c) compares the P/P_{max} values for the three different nozzles used in this work, showing that the normalised P-values of the 120° nozzle are lower (almost half) than the other nozzles. All the calculated P values for the spray system are given in Appendix II).

5.3.4 Effect of solution viscosities

Figure 5.24 shows time-temperature profiles for two different solution viscosities - water and a solution of 5% (w/v) starch - for each type of nozzle (single jet nozzle, and muti jet). The data shows:

(a) For water, (i) the system rapidly reaches a uniform temperature after about 1000s; (ii) there is rapid cooling after the jar is removed from the spray.

(b) For a solution of 5% starch, the dashed graph shows (i) a very slow thermal response: the system temperature is still approaching the water bath set point by the end of experiments; (ii) there is slightly slow cooling stage.
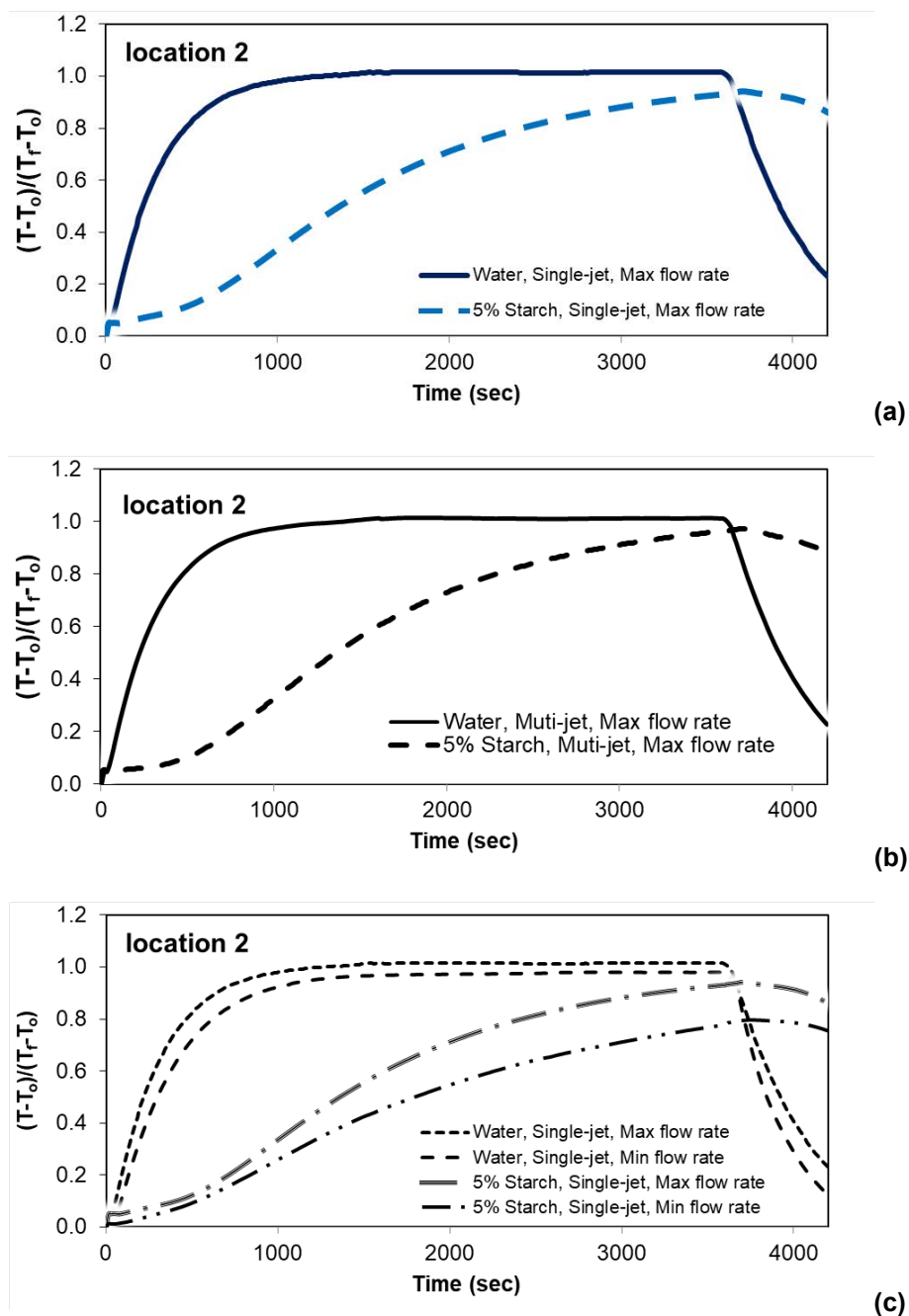
Figure 5. 24: Temperature-time profiles for two different solution viscosities: (a) water (solid), and (b) a solution of 5%(w/v) starch (dashed) for (a) single jet nozzle, and (b) muti jet nozzle, (c) single and muti-jet. Temperature of the heating nozzle was 70°C , while the water filling the jar was initially at approx. 20°C.

The data from Figure 5.25 shows that the viscosity of the solution has affected the P/P_{max} values for both types of nozzle (single jet and showerhead). The lowest viscosity system (water) demonstrates with its higher P-values that the more viscous systems (as the 5% starch solution studied here) will need longer times to achieve the desired decontamination, i.e. targeted equivalent treatment.

Conclusions for this section that can be drawn from these experiments are:

- For both single jet and muti jet, as the flow rate increased the P values increased as well, with a uniform pattern across the jars.

- There was no effect of the type of nozzle on the heat transfer in the system – although the 120° nozzle used in earlier sections showed that poor spray can reduce both the heat supplied to the system and the rate of heating.

- P/P_{max} values decreased when the solution viscosity increased – in all cases the process is controlled here by in-pack behaviour.

(a)

(b)
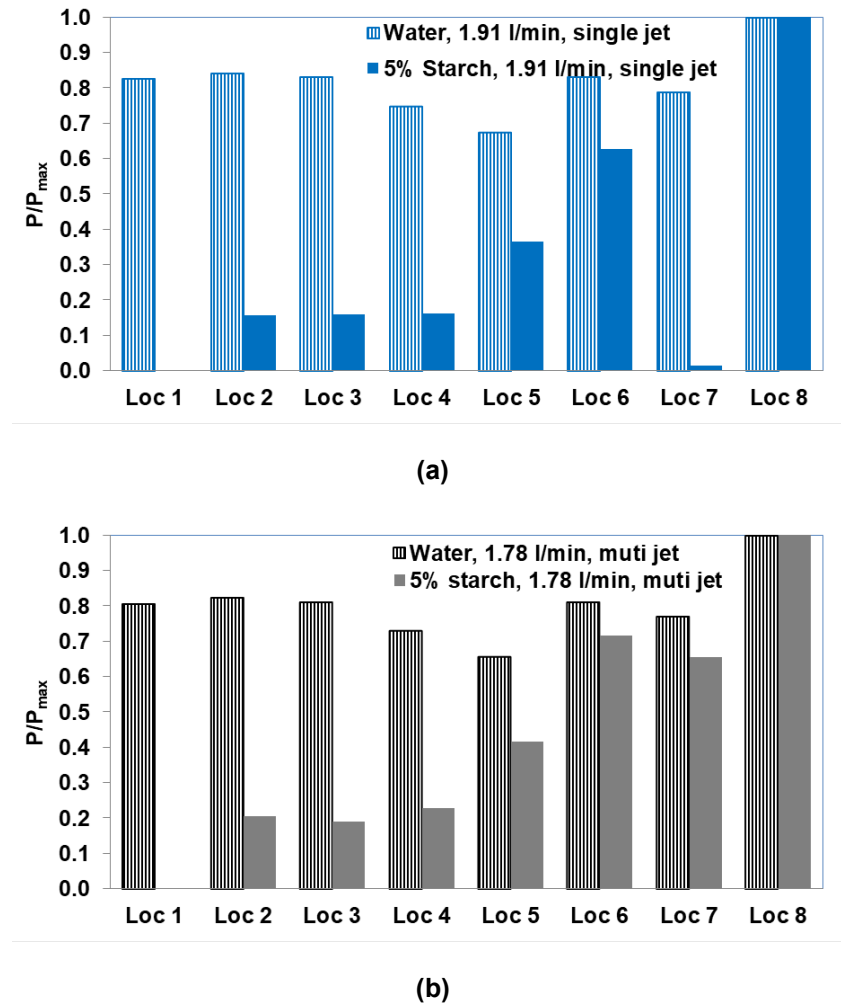
Figure 5. 25:   Effect on the normalised P values of the solution viscosity: water (line) and a solution of 5% starch (solid) for (a) single jet nozzle and (b) muti jet. The z-value considered in the calculations was z = 10ºC and the reference temperature was T_{ref} = 70ºC. P_{max} = 65 min.

5.4 Two phase solid liquid phase study

The previous experiments in Sections 5.2 and 5.3 have studied spray head conditions using single phase of solutions. In fact, most of the products made by the food industry and sold in jars, such as, soup, sauces, such as salsa or kurma sauce are two phases –liquid solid solution which they usually added some small pieces of vegetables like potato, carrot or corns. Particle size can vary from a few mm to

perhaps a cm scale. Therefore, the heat transfer behavior for two phase foods under the spray head conditions was of interest and it has been investigated through a series of experiments using the three nozzles: 120º spray head, single jet and the showerhead.
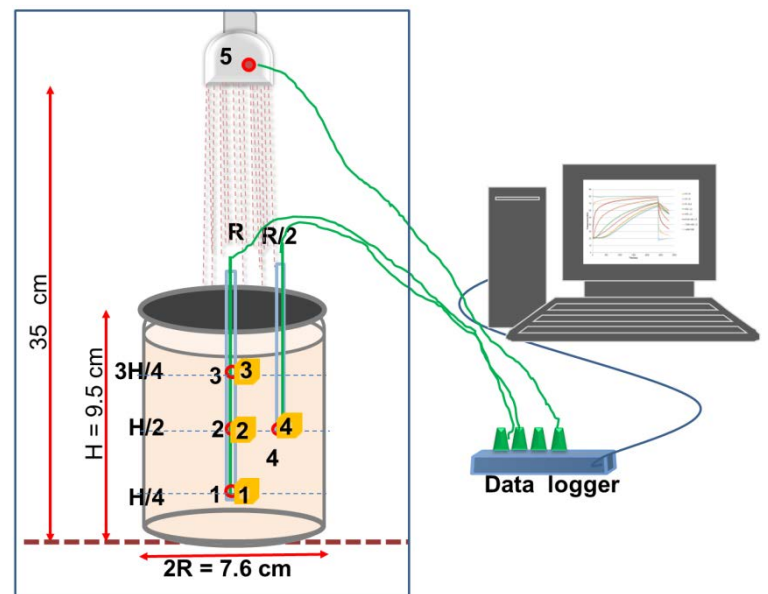
Figure 5. 26: Schematic of 2 phase test set up in spray pasteurizer

5.4.1 Two-phase study using 120-degree spray head

The experimental plan for the two-phase study using the 120-degree spray head is given in Table 5.4.

Table 5. 4: Two phase study using 120 degree spray head experiments; round (75.2 mm height x 85.8 mm diameter) and hexagonal (86.0 mm height X 9.40 mm diameter) jar, as shown in Figure 5.28.

Treatment	Geometry of jar	Carrier fluid	% 1 cm^3 potato cubes
1	Round	water	10
2	Round	water	50
3	Round	5% corn starch	10
4	Round	5% corn starch	50
5	Hexagonal	water	10
6	Hexagonal	water	50
7	Hexagonal	5% corn starch	10
8	Hexagonal	5% corn starch	50

Table 5.4 shows that the parameters studied here were:

(i) Effect of solid-liquid fraction (10 and 50 %(w/v)),

(ii) Effect of viscosity of food fluid (water, and 5%(w/v) corn starch),

(iii) Effect of geometry of packages

The experiment set up and protocols were described in Section 3.5.3, and a schematic of the spray unit is presented in Figure 5.26 for illustration. As in previous sections, all the experiments conducted involved 60 minutes of heating followed by 10 minutes of cooling. The heating temperature of the spray flow was 70°C, with a

mass flow rate of 1.09 l/min. the temperature in the system (jar and environment) was recorded every 15 seconds.

330 ml Round Jar   330 ml Hexagonal Jar

Figure 5. 27: Picture of the two different jars employed in the two-phase experiments: round (left) jar and hexagonal jar (right).

5.4.1.1 Temperature time profiles

Figure 5.28 shows temperature time profiles for a round jar containing (a) water and (b) 5%(w/v) starch solution with 10%(w/v) potato cubes in 9 locations both in solution (black) and potato (red).

For water:

(i) Fluid temperature is higher than potato temperature in all locations (1-4) and 4-5°C different from the beginning of the heating stages and become closer in the end of process. And temperature slow decreased in cooling stage if compared with single phase as shown in Figure 5.2.

(ii) The coldest point was found at the bottom of the jar (location 1). Temperature values increase with height (hot spot at location 3, top of the jar), while there are no significant temperature gradients in the radial direction (similar temperature profiles at locations 2, 3 and 4). The observed heating dynamics correspond to a system where convection drives heat transfer in the product: the filling water is heated, then expands and rises being replaced by cooler water, from the side of wall to the center of jar.

For 5% starch:

(i) The system has similar trends in the temperature-time profiles as water, in which fluid temperature is higher than potato temperature about 2-3°C different

(ii) The temperature of fluid and potato in the 5% starch systems are closer than in water systems – overall the heat transfer rates are slower.

(iii) The coldest point was found at the center of the jar (location 2).
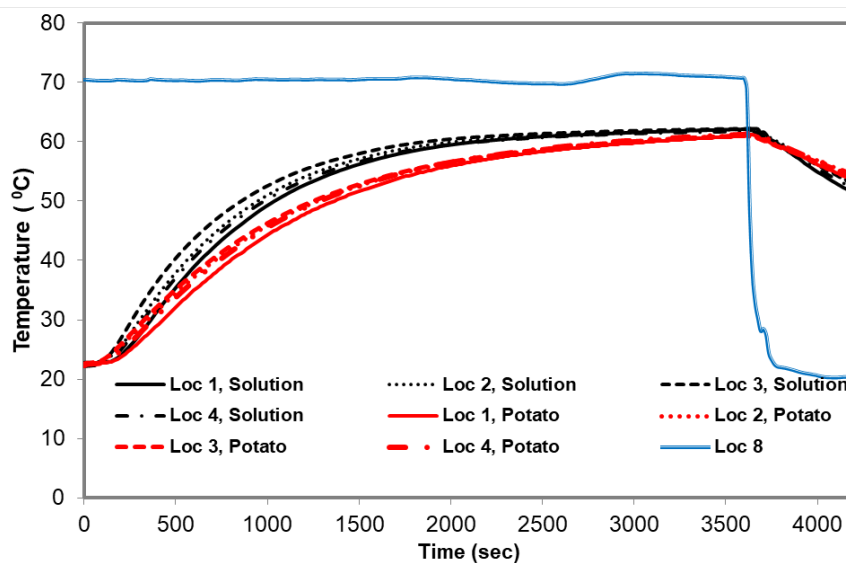
(a)
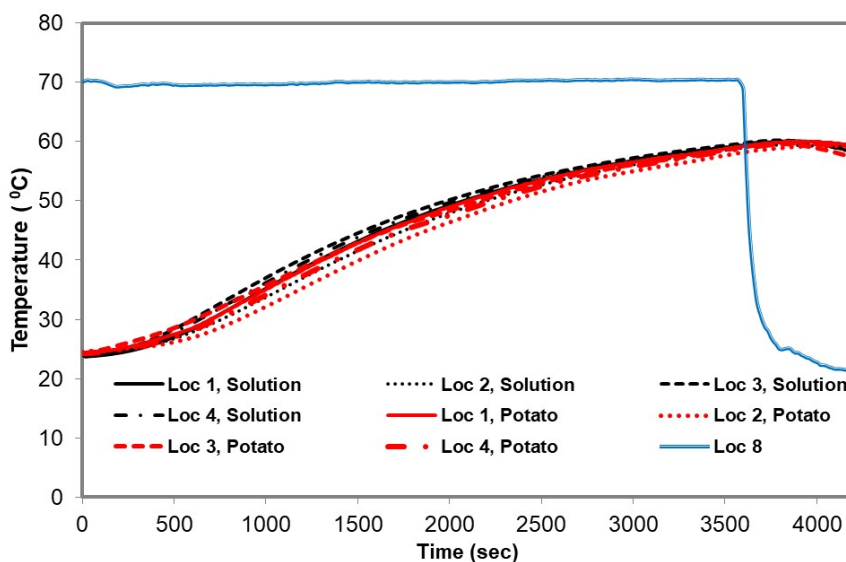
(b)

Figure 5. 28: Temperature time profiles for a round jar containing (a) water and (b) 5%(w/v) starch solution with 10%(w/v) potato cubes in nine locations both in solution (black) and potato (red) using 120 degree spray nozzle. Temperature of the heating nozzle was 70°C, while the water filling the jar was initially at approx. 20°C. Nozzle flow rate 1.09 l/min.

5.4.1.2 Effect of solid-liquid fraction

Figure 5.29 shows temperature time profiles for the effect of two different fractions of potato: 10% (w/v) and a 50% (w/v) potato cubes in both water and starch. Using a round jar in eight locations it was found that:

- For a water filling, the high solid fraction (50%w/v) had slightly more rapid heat transfer than the low solid fraction (10%w/v), and there was 1-2°C difference between high and low solid fractions.

- For the 5% starch solution filling, the results showed no effect of solid-liquid fraction in terms of heat transfer behavior, both in fluid and particles.

The normalised P values (P/P_{max}) for the two different fractions of potato (10% (w/v) and 50% (w/v) potato) in water and 5% starch solution are shown in Figure 5.31. Data shows that:

- For water, in Figure 5.30(a), the normalised P values increased when the solid-liquid fraction increased. P/P_{max} values of fluid were higher than those for the potato in all the jar locations (1-4). The coldest point was found at the bottom of the jar (location 1).

- For a 5% starch solution shown in Figure 5.30(b), there were no significant differences between the P/P_{max} values in this case. These results confirm that there was no solid-liquid fraction effect on the thermal response of the system, as seen in the Figure 5.29.
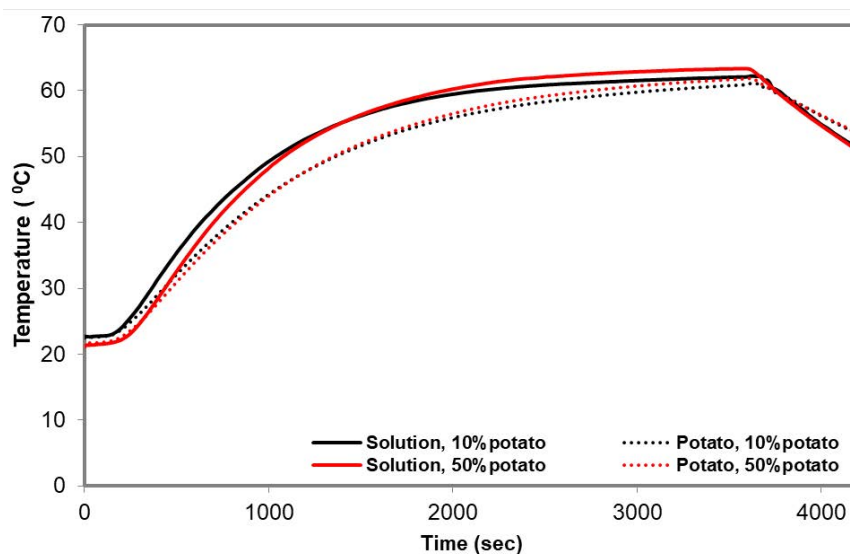
(a)
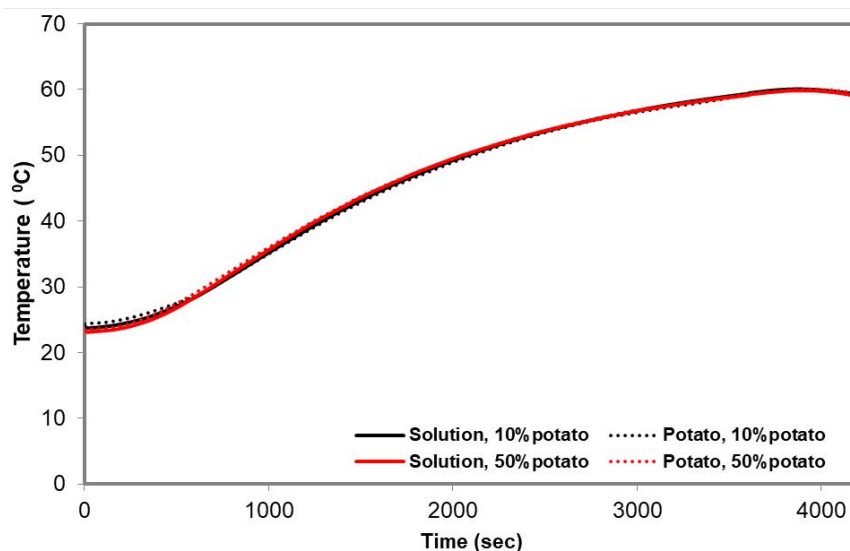
(b)

Figure 5. 29: Temperature-time profiles recorded at location 1 for two different fractions of potato: (a) 10% (w/v) (black), and (b) 50% (w/v) potato cubes (red) in both fluid (solid line) and potato (dotted) using a round jar in eight locations: (a) water and (b) 5% starch. Temperature of the water at the heating nozzle (120 degree spray nozzle) was 70°C, while the water filling the jar was initially at approx. 20°C. Nozzle flow rate 1.1 l/min.

(a)

(b)

Figure 5. 30: Normalised P Values for two different factions of potato 10% (w/v) (solid) and 50% (w/v) potato (dotted) for (a) water, and (b) 5%(w/v) starch solution using a round jar with thermocouples in eight locations. The z-value used in the calculations was z = 10°C and the reference temperature considered was T_{ref} = 70°C.

5.4.1.3 Effect of viscosity of food fluid

Figure 5.31 further illustrates the temperature time profiles for the effect of two different viscosities of solution: water and a 5% starch solution. As would be expected, water (low viscosity) has a faster thermal response than a 5% starch

solution in both fluid and solid particles about 5-8°C different at the heating period over 3600 seconds. The thermal transfer for water gave a rapid increase in temperature heating stage for 2500 seconds. The heat transfer in the fluid is higher than in the solid particle, because of the convective mechanism in the fluid, but conduction mechanism in the solid.

However, the thermal transfer for both in fluid and solid in a 5% starch solution system almost the same trends. This because heat transfer in a high viscous solution is slower than in low viscous solution; the liquid behaves more as a solid, so the whole system is controlled by thermal conduction, giving smaller thermal convection modes in this figure. The 50 % solid fraction had similar temperature time profiles as the 10% solid-liquid fraction.

In Figure 5.32 the corresponding normalised P values for the two fluids studied: water and a 5% starch, and the two fraction of solid phase (10% potato, and 50% potato) are presented. P/P_{max} values for water are two times higher than P values of a 5% starch solution in a 10% solid liquid fraction, and 2.5 times higher in a 50% solid liquid fraction. The percentages of potato had no effect on P/P_{max} values in the 5% starch solution (high viscosity), with P values in both in fluid and solid almost the same.
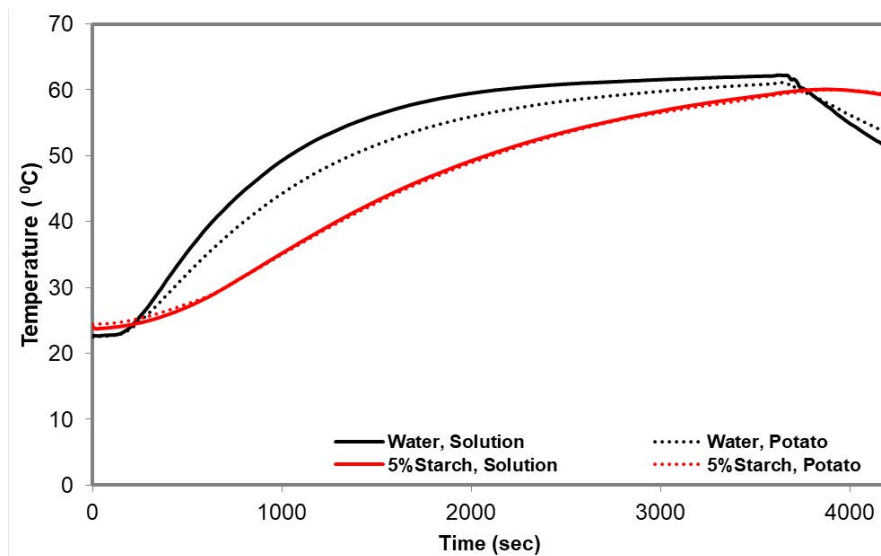
(a)
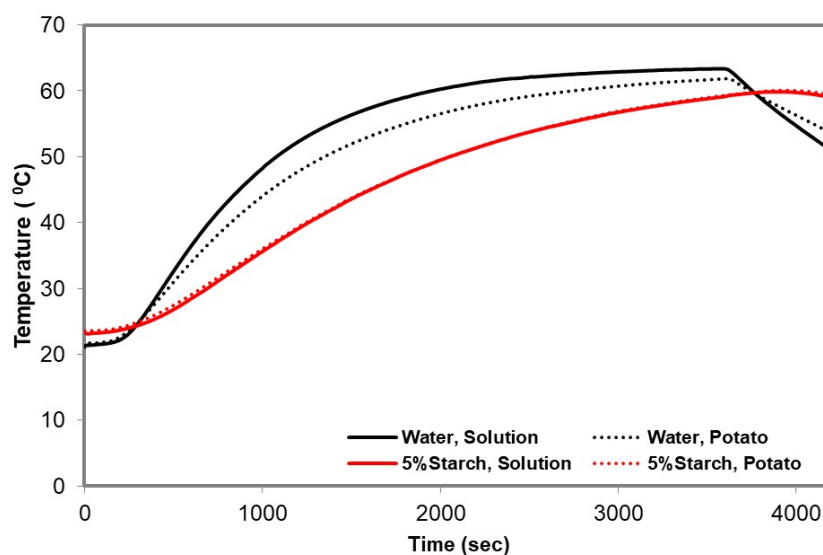
(b)

Figure 5. 31: Temperature-time profiles for the two-phase system with fluids being either water (black) or 5% starch solution (red) measured in the round jar at location 1: (a) 10% (w/v) potato and (b) 50% (w/v) potato. Temperature of the heating nozzle (120 degree spray nozzle) was 70°C , while the water filling the jar was initially at approx. 20°C. Nozzle flow rate 1.1 l/min.

.
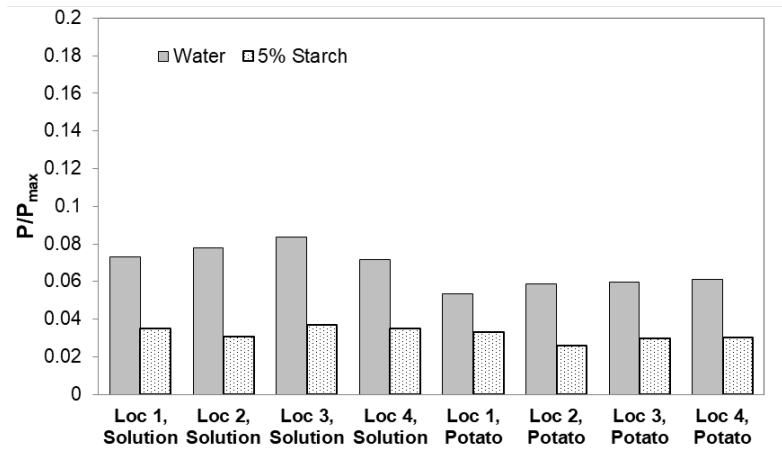
(a)
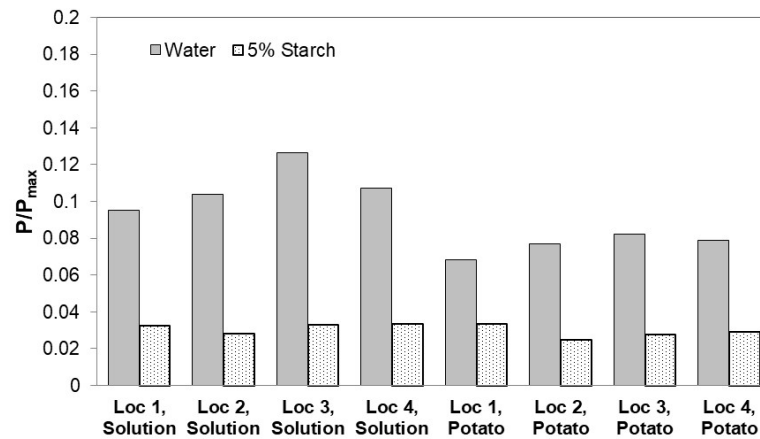
(b)

Figure 5. 32: P values effect of two viscosity of food fluid: (a) water (solid), and (b) a 5% starch (dotted) in two different systems; (a) 10% (w/v), (and (b) 50% (w/v) potato. The z-value considered in the calculations was z = 10°C and the reference temperature was T_{ref} = 70°C.

5.4.1.4 Effect of geometry of packages

Figure 5.33 shows temperature-time profiles for two different package geometries: (a) round (black), and (b) hexagonal (red).

For 10% solid liquid fraction (Figure 5.33(a)): the thermal transfer of hexagonal jar is slower than that for the round jar in the first 1200 seconds of heating system. Then the heat transfer rate became faster rate. There was a few degree Celsius of difference at the end of heating stage over 3600 seconds, which may reflect slightly different heating temperatures. Temperature of the heating fluid was around 2-4°C higher than the temperature of solution in both jar geometries.

For 50% solid liquid fraction (Figure 5.33(b)), the data shows similar heating behaviour for both type of geometry of jar as shown in a 10% solid liquid fraction system. After 2000 seconds of heating, there was no significant different at the end of heating stage for both hexagonal and round jar.

Figure 5.34 shows the corresponding P/P_{max} values for the two different geometries of the package: round and hexagonal jars. For 10% potato, the P/P_{max} values of round jar are lower than the normalized P values obtained for the hexagonal jar by ca. 2-1.5 times, with the lowest P/P_{max} values corresponding to location 1 (bottom of jar) for both jars. For 50% potato, the normalised P values of round jar were again slightly lower than P values of hexagonal jar times in all locations, and the coldest point was the same location as in a 10% solid fraction, i.e. at location 1. The results showed there was a small effect of the jar geometry on the P values, with the hexagonal jar giving higher P values.
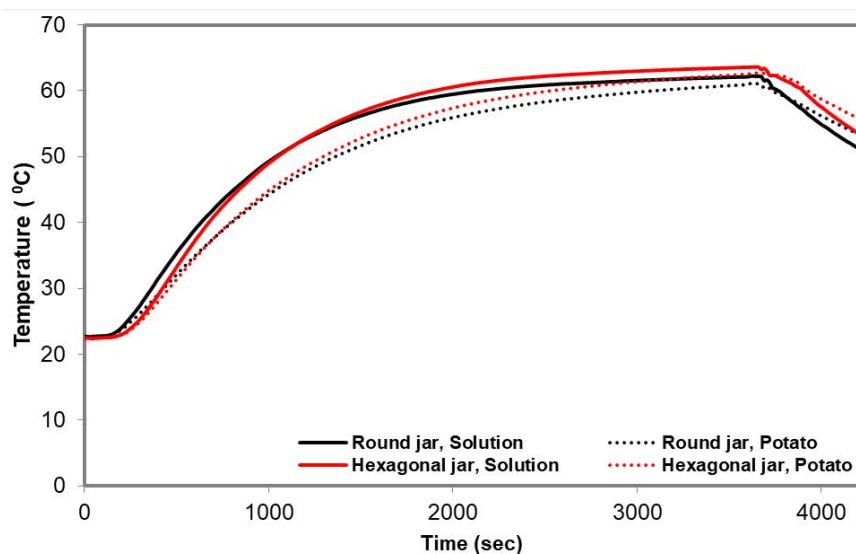
(a)
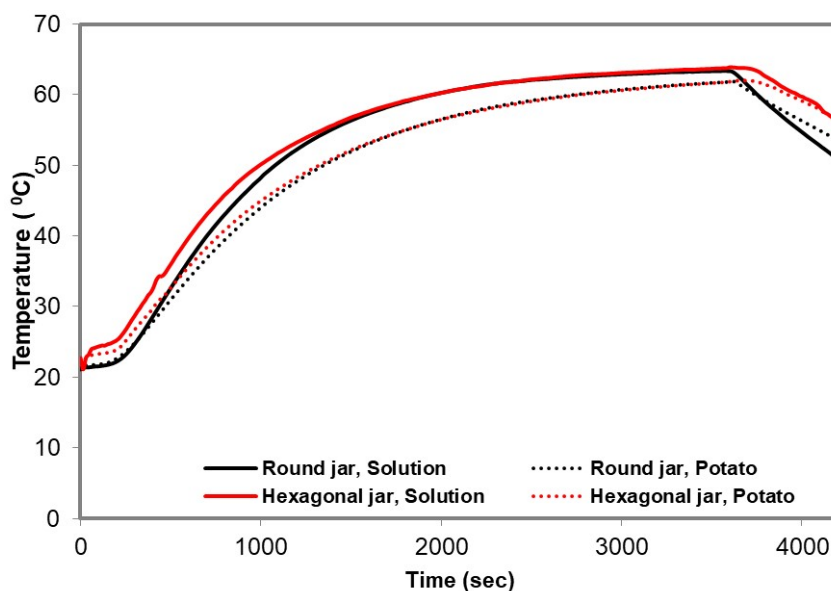
(b)

Figure 5. 33: Temperature-time profiles recorded at location 1 for two different package geometry: (a) round (black), and (b) hexagonal (red) both in fluid (solid line) and potato (dotted) for solid fractions of (a) 10% (w/v) potato and (b) 50% (w/v) potato. Temperature of the heating water was 70°C, while the water filling the jar was initially at approx. 20°C. Flow rate was 1.1 l/min through the 120-degree spray nozzle.

(a)

(b)
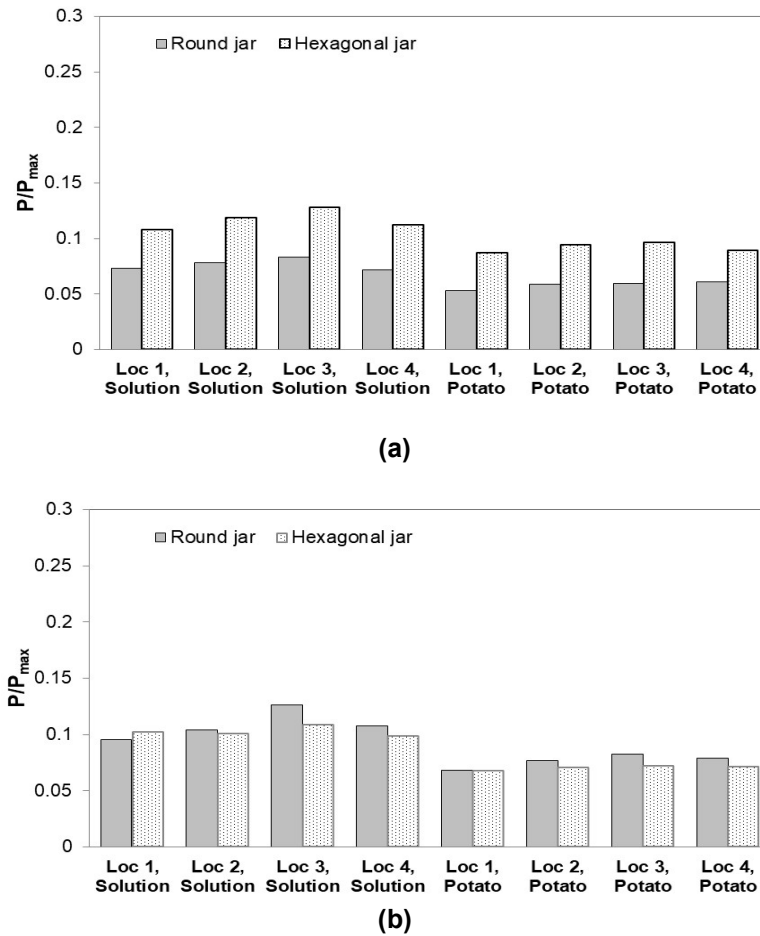
Figure 5. 34: Normalised P values obtained for round (solid) and (b) hexagonal (dotted) jars in using (a) 10% (w/v) potato and (b) 50% (w/v) potato as solid phase. The z-value considered in the calculations was z= 10°C and the reference temperature was T_{ref} = 70°C.

This section has shown that in a low solids fraction system and for low solution viscosities, the P values increased as %solid fraction of the food increased; this reflected the reduced convection effects that are possible in a high solid fraction. However, for the high viscosity fluid, where conduction is the primary mechanism, there is no effect of %solid liquid fraction. High viscosity of fluid results in lower P/P_{max} values than low viscosity. Few normalized P values of round jar are lower than P/P_{max} values of hexagonal jar.

5.4.2 Two-phase study using single jet nozzle

In the previous study in Section 5.3.3 on effect of type of nozzle, it was found that there were no significant differences between a single jet nozzle and a showerhead, as can be seen in Figure 5.23. Therefore, the single jet nozzle was chosen to be used in this section. The highest solid liquid fraction of 50%(w/v) was also selected for this section studied because (i) the coldest point is as same location than in the low solid liquid fraction and (ii) there are more effects of heat transfer in the higher solids fractions.   So this section will describe experiments that study heat transfer mechanism in a two-phase mixture using the single jet nozzle.

To study the effect of flow rate on the heat transfer of the solid-liquid system, the following condition were parameters were considered:

(i)   Effect of solution viscosity (water and a 5% starch solution) and

(ii)   Effect of four different flow rates.

Table 5. 5: Parameters for the two-phase experiments using the single jet nozzle.

Flow rate (l/min)	Fluid carrier	% of 1 cm^3 potato cubes
0.92 ± 0.03	Water and 5%(w/v) starch	50%
1.91 ± 0.03	Water and 5% (w/v)starch	50%
2.56 ± 0.03	Water	50%
10.57 ± 0.10	water	50%

5.4.2.1 Temperature time profile

Figure 5.35 shows temperature time profiles for a jar containing (a) water and (b) 5% (w/v) starch solution with 50%(w/v) potato cubes both in solution (black) and potato (red). Data shows that:

- For water: the coldest point was found at the bottom of the jar (location 1). Temperature values increase with height (hot spot at location 3, top of the jar), while there are no significant temperature gradients on the radial direction (similar temperature profiles at locations 2, 3 and 4). The observed heating dynamics correspond to a system where convection drives heat transfer in the product: the filling water is heated, then expands and rises being replaced by cooler water, from the side of wall to the center of jar.

- For 5% starch: the temperature of the fluid and potato are closer than in the water system, being higher in the liquid phase (about 2-3°C) than in the potato measured points. As corresponds to a system where conduction governs the heat transfer in the liquid phase, the coldest point was found at the center of the jar (location 2).
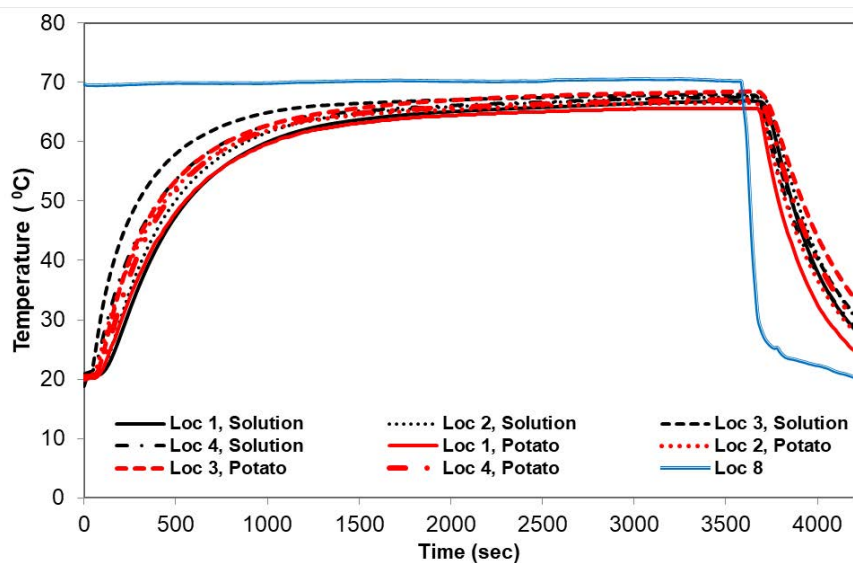
(a)
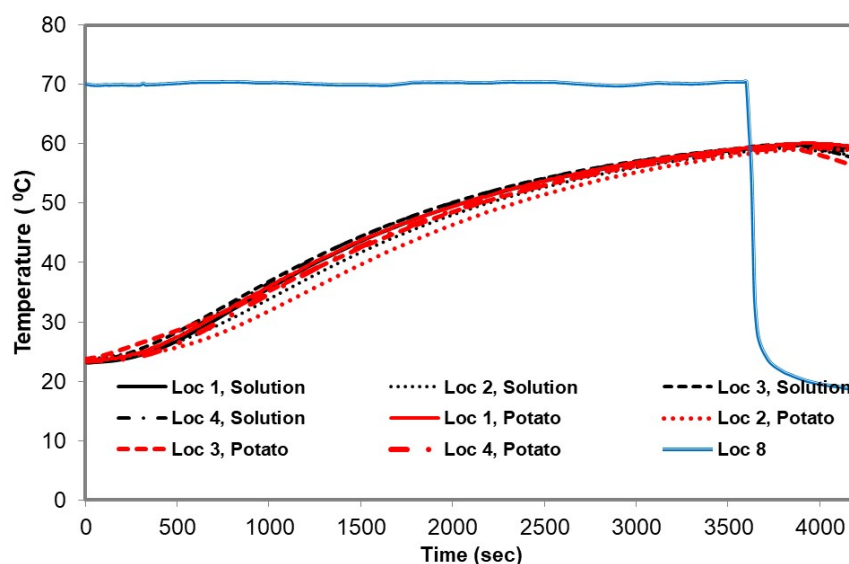
(b)

Figure 5. 35:   Temperature-time profiles for a jar containing   (a) water and (b) 5%(w/v) starch solution with 50%(w/v) potato cubes both in solution (black) and potato (red) using the single jet nozzle. Temperature of the heating nozzle was 70ºC, while the water filling the jar was initially at approx. 20ºC. Nozzle flow rate 0.92 l/min.

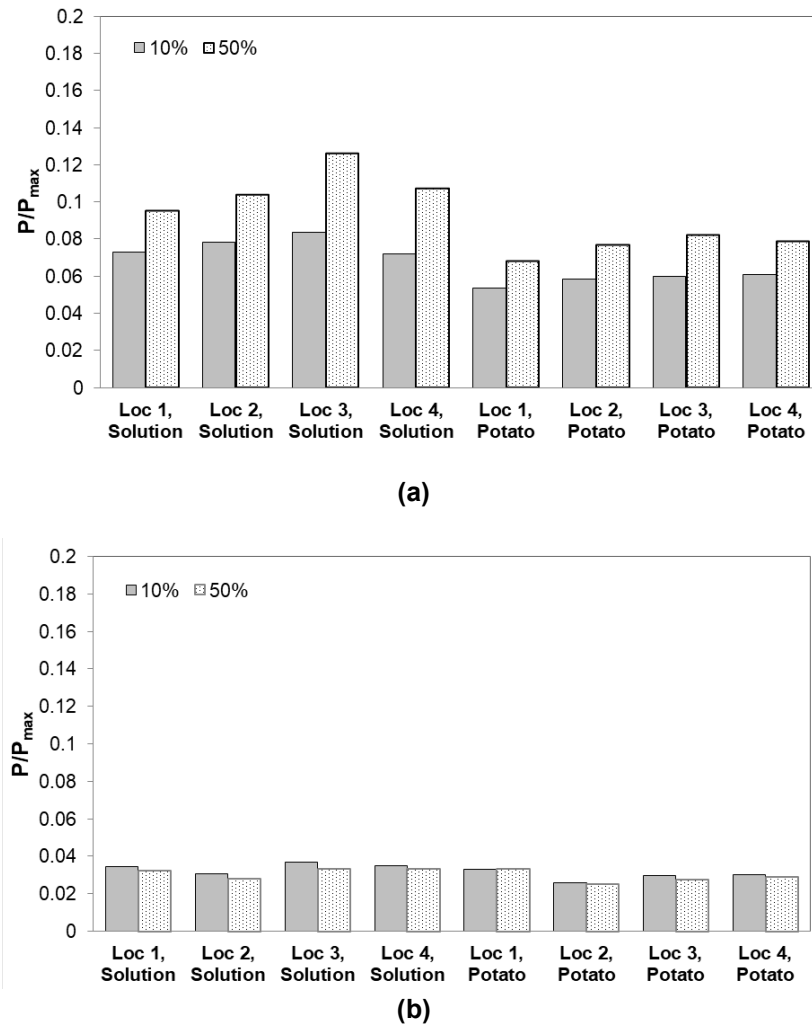## 5.4.2.2 Effect of viscosity of food fluid

Figure 5.36 illustrates the temperature-time profiles for effect of two different viscosities of solution: water and a 5% starch solution. Water (low viscosity) has a faster thermal response than a 5% starch solution, in both fluid and solid particles with a difference of about 5-8°C at the heating period over 3600 seconds. The heat transfer dynamics for water presents a rapid increase in the beginning of the heating stage below 1500 seconds, with the heat transfer rate in the fluid being higher than in the solid particles. This because convection mechanism is driving heat transfer in the fluid, while conduction is the dominant mechanism in the solid.

On the other hand, the thermal response for both in fluid and a solid in the 5% starch solution show almost the same trends, as would be expected in a system where the dominant heat transfer mechanism in both solid and liquid (but viscous) phase is conduction. This graph also shows that the 50 % (w/v) solid fraction had similar temperature time profiles than the 10% solid-liquid fraction.

Figure 5.37 shows the normalized P values obtained that show the effect of viscosity in the fluid phase. The P values of water double the P values corresponding to the 5% starch solution for the two-phase system with 10% of solid fraction, and there are >2.5 times in the system with 50% solid fraction.

It was found that the percentage of potato had no effect on the P values of the two-phase system with the 5% starch solution (high viscosity) as fluid, being the P values of at all locations, both in fluid and solid phases almost the same.
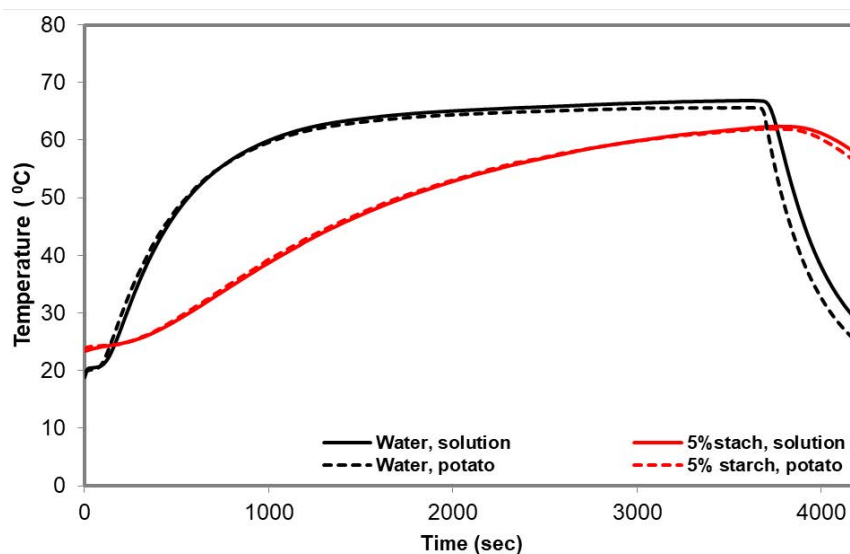
Figure 5.36: Temperature-time profiles at location 1 for two different fluid phase viscosities: water (black) and a 5% starch solution (red), both in the fluid (solid) and potato cubes (dotted). Temperature of the heating spray was 70°C, while the water filling the jar was initially at approx. 20°C. Nozzle flow rate 1.1 l/min.
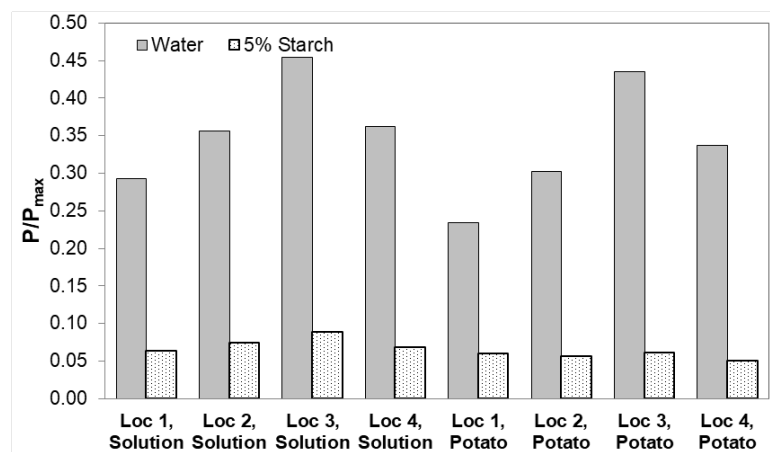
Figure 5.37: Normalised P values effect for water (solid) and the 5% starch solution (dotted) in a 50% (w/v) potato fraction system. The z-value considered in the calculations was z = 10°C and the reference temperature was T_{ref} = 70°C.

5.4.2.3 Effect of flow rate

Figure 5.38 shows the temperature-time profiles recorded when four different flow rates (0.92 l/min, 1.91 l/min, 2.56 l/min, and 10.57 l/min) were used in the experiments. The profiles corresponding to the fluid phase are presented in Figure 5.38(a), where is shown that the thermal response for the 10 l/min flow is slightly faster in the first 1200 seconds of the process. At this point, temperatures for this flow rate are about 2°C, 2.5°C, and 6°C higher than in the 2.56 l/min, 1.91 l/min and 0.92 l/min flow rates, respectively. It can be seen also that the 1.91 l/min and 2.56 l/min flow rates have a very similar behaviour. Same trends on heat transfer for the potato cubes were found that are shown in Figure 5.38(b).

Figure 5.39 shows the normalized P values for the four flow rates compared, showing that the higher P/P_{max} values correspond to the higher flow rates. It also reported that normalised P values of the solid phase are lower than the corresponding fluid phase, as expected from the temperature profiles.
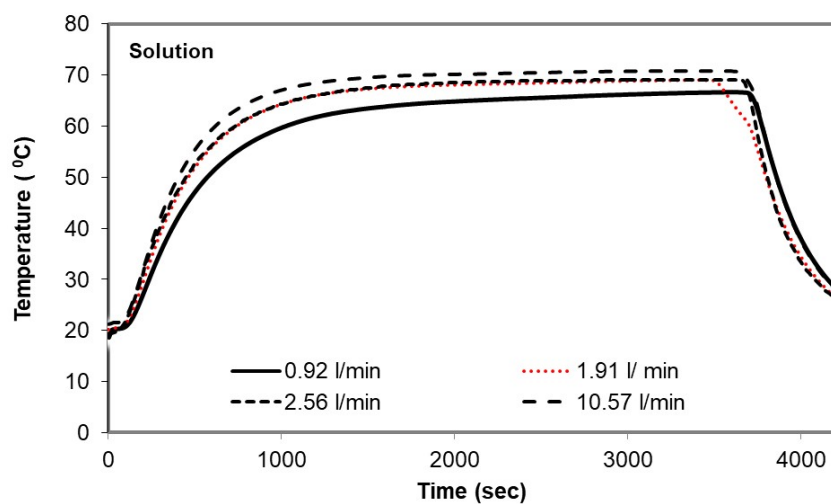
(a)
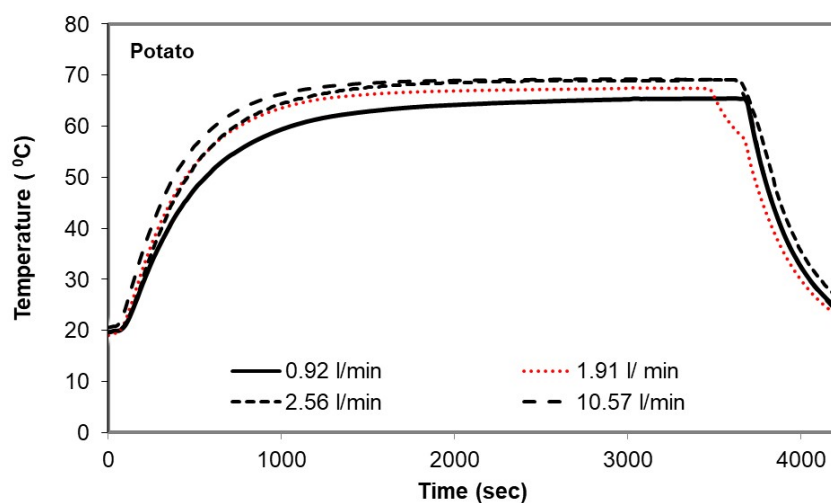
(b)

Figure 5. 38: Temperature-time profiles effect of four different flow rate: both in fluid (solid) and potato (dotted) using a round jar at locations 1. Temperature of the heating nozzle (120 degree spray nozzle) was 70°C , while the water filling the jar was initially at approx. 20°C.
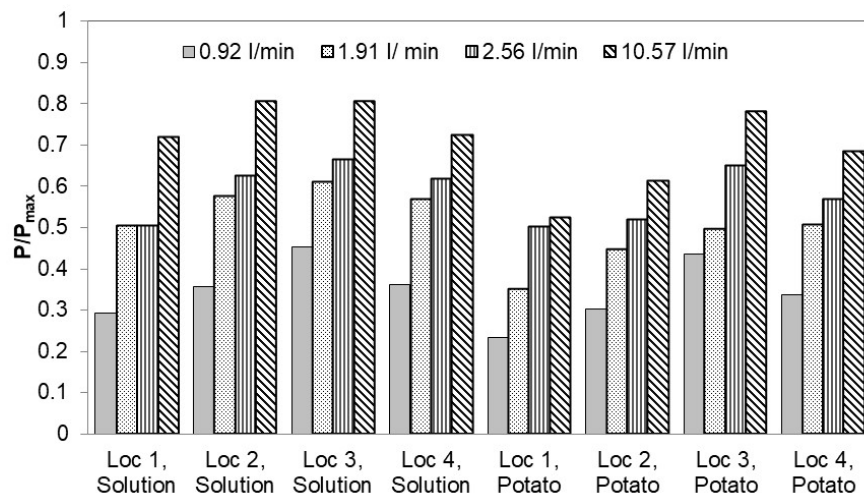
Figure 5. 39: Normalised P values at location 1 for the four flow rates studied both in the solution and in the potato cubes when a round jar was used. The z-value considered in the calculations was z = 10°C and the reference temperature was T$_{ref}$ = 70°C.

5.4.2.4 Effect of nozzle type

Figure 5.40 compares the temperature time profiles between the 120^0 and the single jet nozzle. It is shown that:

- The single jet nozzle has a faster thermal response than the 120° nozzle in both fluid and solid particles, with temperatures about 10-18°C higher.

- The heat transfer rate for single jet nozzle increased rapidly in the beginning of the heating stage before the 1500 seconds.

- The heat transfer dynamics for the single jet nozzle are very similar in both solid and fluid phases.

In Figure 5.41 the P/P$_{max}$ values for the two types of nozzle for a 50% (w/v) potato fraction system are shown. The normalized P values of single jet nozzle are more

than 1.5-2 times higher than the P/P$_{max}$ values of the 120° nozzle at location 1,2 and 4 and higher than 3.5 times at location 3. This because at the top point of jar (location 3), the spray water flow directly onto top of lid jar, while for the other points heat is transferred from the falling film and passes though the jar wall and thus not so efficient.
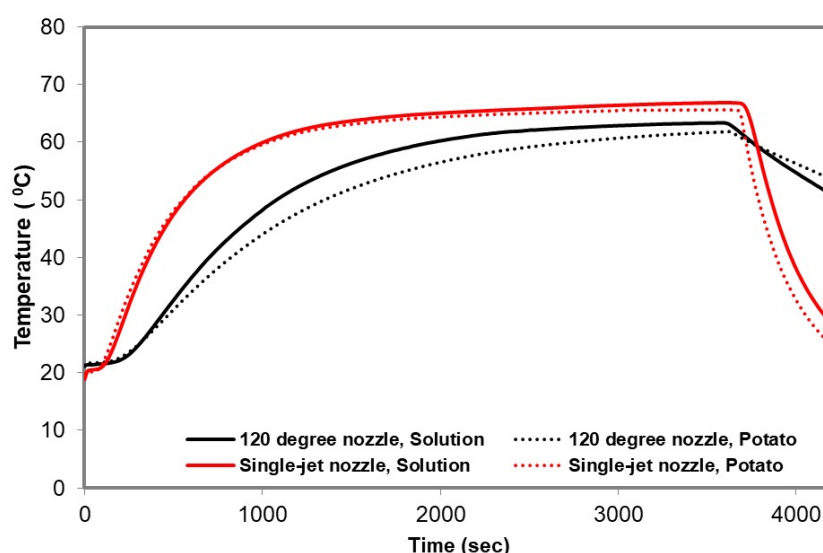
Figure 5. 40: Temperature-time profiles at location 1 comparing the 120 degree nozzle (black) and the single jet (red) nozzles in the 50% (w/v) potato fraction system. Fluid phase is plotted using solid lines, while the potato profiles are the dotted lines. Temperature of the heating water was 70°C, while the water filling the jar was initially at approx. 20°C. The flow rate was 1.0±0.1 l/min.
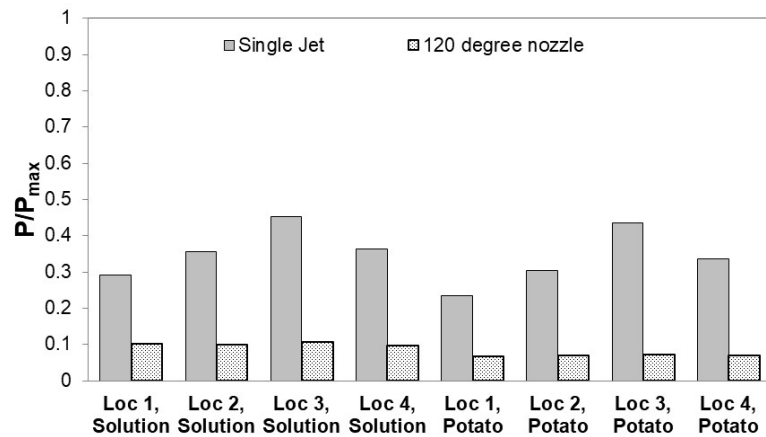
Figure 5. 41: Comparison of the P/P$_{max}$ between the single jet (solid) and the 120 degree nozzle (dotted) nozzle in the 50% (w/v) potato fraction system. The z-value considered in the calculations was z = 10°C and the reference temperature was T$_{ref}$ = 70°C. P$_{max}$ = 64.75 min.

Conclusions of this section were:

- P values increased as flow rate of the food increased in a low solution viscosity system.

- High viscosity of fluid gives a lower P value than low viscosity.

5.5 Summary

Chapter 4 investigated the heating dynamic in a water bath, in terms of the differences in temperature and P-value calculated for different fluids and process conditions. The results have been used as the basis for this section. This chapter has focussed on the evaluation of a time temperature history for mild thermal processes using spray of water from nozzles and muti jets, using thermocouples.

The aims of this chapter were (i) to measure variable temperature profiles for the mild thermal processes and (ii) to study the effect of process factors on the results of this within and at the surface of pasteurised products. A new rig, (a spray pasteurisation unit) was designed and built, and different types of nozzle (single jet and muti jet) were used and studied as process conditions, with P/P_{max} values measured.

There are three main sections of work

(i)   Preliminary work used a spray with a 120-degree of angle of spray. The effect a wide range of process variables on the heat efficiency of the system were studied: flow rate, spray temperature, viscosity of the filling fluid, different heights for the nozzle, different container positions and number of treated jars. The results showed simllar general trends as previous work for the effects of flow and fluid.

(ii)   The nozzle had a very wide spread of spray water angle, which resulted in high heat losses. Two alternative nozzles, one without spray, with the flow falling straight onto the vessel directly, and a showerhead were developed and investigated.

(iii)   The parameters studied were spray flow rate (0.92 and 1.91 l/min for single jet nozzle and 0.98 and 1.78 l/min for a muti jet nozzle), type of nozzle, and viscosity of food fluid (water and 5 %(w/v) corn starch).

(iv)   two-phase solid-liquid mixtures within the vessel were also studied in terms of the effect of solid-liquid fraction (10 and 50 %(w/v)), viscosity of food fluid (water, and 5%(w/v) corn starch), and geometry of packages.

Conclusions that can be drawn from these experiments are:

- P/P_{max} values increase with the temperature of the heating medium and the liquid flow rate for all cases.

- Similarly, for all type of nozzles studies, P P/P_{max} values increased as viscosity of the food decreased. In all cases the process is controlled here by in-pack behaviour.

- However, the normalised P values decrease when the number of jar increased.

- P/P_{max} values at a separation of nozzle and jar of height of 18.6 cm are the highest; however, P values at the height of 18.6 cm and 35 cm are almost the same.

- A target of 70°C for 5 min is achievable with an optimal design using rate 70 °C of 30 min.

- There is a strong effect of viscosity on the system internal temperature but this only weakly affects the surface temperature

- For both single jet and muti jet, as the flow rate increased the P values increased as well, with a uniform pattern across the jars.

- For solid liquid system, a lower solids fraction system and for lower solution viscosities, the P values decreased as %solid fraction of the food increased; this reflected the reduced convection effects that are possible in a high solid fraction. While no effect of %solid liquid fraction for high viscosity fluid, which conduction dynamics. However, High viscosity of fluid results in lower P/P_{max}

values than low viscosity. Few normalized P values of round jar are lower than P/P$_{max}$ values of hexagonal jar.

- The single jet nozzle was chosen to be used in a two-phase mixture studied instead a muti jet because (i) the coldest point is as same location than in the low solid liquid fraction and (ii) there are more effects of heat transfer in the higher solids fractions. The results presents P values increased as flow rate of the food increased in a low solution viscosity system. High viscosity of fluid gives a lower P value than low viscosity, as same as previous work result trends.

Chapter 6

Conclusions and Future Work

6.1 Conclusions

This thesis describes an experimental study of the thermal and spray pasteurisation performance of glass vessels. The type of system studied is relevant to the common industrial problem of glass jars of product being pasteurised in a spray tunnel; such tunnels are used both to pasteurise products that were not pre-pasteurised, and to 'top-up' pasteurisation for products that have been pasteurised but are then filled into jars that have not been. There are some industrial issues with the formation of mould or the growth of bacteria around the headspace or lid of some jars as a result of incomplete pasteurisation.

The literature on spray pasteurisation and on thermal transfer into packs has been briefly reviewed. Generally it would be expected that heat transfer is slowest within the packs, i.e. that either convection (in low-viscosity systems) or conduction (for high viscosity products) is the controlling process. It is important that the spray is correctly designed, and that there are no regions of low water flow rate. Models for the process show that under some conditions of very low flow there is insufficient heat provided, so the heating rate is unacceptably slow. Conversely, at too high a flowrate the supply of heat might be too large – this could lead to excessive pumping and heating costs.

It is possible to monitor heating in a number of different ways – thermocouples are the easiest method, in that they give a direct read out of temperature that can be added to the equation that describes microbial inactivation and give a prediction of the effect of the process. Time-temperature indicators are small tubes or packets of heat-sensitive enzyme that can be placed in a food product and then passed through the process; when assayed, the difference between initial and final value is a measure of thermal treatment. TTIs are more complex that thermocouples to use in static situations, but are ideally suited to cases where the product is passed through a real system.

A series of experiments were designed to test the response of vessels to sprays, using a variety of experimental setups. In all cases a series of thermocouples were places in specified positions inside a glass jar, filled with one of a variety of fluids, ranging from water to highly viscous CMC. Two types of heating medium were used; a heated water bath and one of a series of spray heads.

The results demonstrated that

(i)   In all cases studied the heat transfer was primarily controlled by the internal behaviour of the system. The greatest effect on the overall heating rate was given by the viscosity of the system – the highest viscosity gives a response that is much closer to the case where the system behaves as if it were a solid.

(ii)   However, external flow or temperature had some effect; heating in the water bath was in all cases faster than heating from the range of sprays used;

(iii)   The type of spray used and the distribution of the spray had an effect, both in the rate of heating and the final temperature. With a diffuse (120°) spray, the heating rate was slower and the final heating temperature lower than when better directed sprays were used.

(iv)   When particles were made part of the model product, the heating rate slowed, even in water, reflecting the barriers to mixing and convective heat transfer. In highly viscous systems, the lag between liquid and solid temperature was very small; in these systems, most of the heat flow is due to conduction.

P values were calculated on the basis of thermocouple measurements – it was found that for the low P-values studies here TTIs did not appear accurate. Experiments tended to use lower heating temperatures than would be needed for pasteurisation as the aim of the experiments was simply thermal monitoring. Data is often plotted as the ratio P/P_{max}, where the P_{max} is calculated from the temperature of the bath or spray, and represents the effect of the heating temperature for the whole process time.

The data shows that:

- In all cases, as would be expected, when the heating medium temperature was higher, for example when the system temperature increased from 50°C to 80°C, higher pasteurisation values resulted.

- An increase of the filling viscosity slowed the heating dynamics of the system, and consequently also affected P/P_{max} values, which were lower when the viscosity was high.

- In the water bath, for all the heating conditions and for all the fillings studied, the size of container and headspace volume had no significant effect on the thermal response and subsequently in the ratio P/P_{max} values calculated,.

- For the spray system, P/P_{max} values increase with the temperature of the heating medium and the liquid flow rate. However, the normalised P values decrease when the number of jars increased.

- A target of 70°C for 5 min is achievable with an optimal design using rate 70 °C of 30 min.

- In all cases, for solid liquid systems for lower solution viscosities, the P values decreased as %solid fraction of the food increased; this reflected the reduced convection effects that are possible in a high solid fraction. No effect of %solid liquid fraction on P values was seen for high viscosity fluids, demonstrating conduction dynamics. High viscosity of fluid results in lower P/P_{max} values than low viscosity.

- The single jet nozzle was chosen for use rather than the muti jet because (i) the coldest point is as same location than in the low solid liquid fraction and (ii) there are more effects of heat transfer in the higher solids fractions. The results presents P values increased as flow rate of the food increased in a low solution viscosity system. High viscosity of fluid gives a lower P value than low viscosity.

Overall the work has shown that it is possible to study spray heating using thermocouples and calculate P values in the same way as has been done for retorting systems. The data show how the thermal pattern can be identified from the experiments, and that it is possible to obtain pasteurisation. The experiments offer the basis for a more complete study of spray pasteurisation and possible optimisation.

6.2 Future work

This work has studied spray pasteurisation and presented investigations of the various factors that affect thermal transfer into packs. However there some future studies that can be suggested here:

- Comparison of the monitoring method with other possible method such as the enzymatic TTI, to obtain better evaluation of mild thermal processes for food pasteurisation.

- TTIs would enable experiments to be done on process lines. Before then it would be useful to study on a small scale the effects of spray pasteurisation factors such as different types of nozzle, a wider range of process heating conditions and the integrated P values that result.

- This work is used a cold- filled method in the packs studied, this is should be enough data for laboratory scale. Hot- filling is generally used in real pasteurising process industry condition and this should be studied to compare with this cold filling.

- The pilot plant or full-scale experiments would be interesting to study – here TTIs would be very valuable as thermocouples would be difficult to use in a moving situation. Such work would also use different types of food and package as cans, plastics or pouches instead of the glass jar in this work and would be representative of other surface pasteurised food factory problems.

- The modelling mathematics for this work can be more developed - it would be useful to identify the optimal positions predicted by the model and whether these conditions are found on real plant.

References

Abdul Ghani A.G., Farid M.M. Numerical simulation of solid–liquid food mixture in a high pressure processing unit using computational fluid dynamics. Journal of Food Engineering 80(4) 1031-1042.

Aganovic K., Grauwet T, Kebede B.T., Toepfl S., Heinz V., Hendrickx M., Van Loey A. (2014). Impact of different large scale pasteurisation technologies and refrigerated storage on the headspace fingerprint of tomato juice. Innovative Food Science & Emerging Technologies 26, 431-444.

Akterian S.G. (1996). Studying and controlling thermal sterilization of convection-heated canned foods using functions of sensitivity. Journal of Food Engineering 29(3–4), 329-338.

Augusto P.E.D., Cristianini M. (2011). Numerical evaluation of liquid food heat sterilization in a brick-shaped package. Procedia Food Science, Vol.1, 1290-1294.

Awuah G.B., Ramaswamy H.S., Simpson B.K. (1995). Comparison of two methods for evaluating fluid-to-surface heat transfer coefficients. Food Research International 28(3), 261-271.

Awuah G.B., Ramaswamy H.S., Economides A. (2007). Thermal processing and quality: Principles and overview. Chemical Engineering and Processing: Process Intensification 46(6), 584-602.

Barigou M. , Fairhurst P.G., Fryer P.J., Pain J.-P. (2003). Concentric flow regime of solid–liquid food suspensions: theory and experiment. Chemical Engineering Science 58 (9),1671-1686.

Barigou M., Mankad S., Fryer P.J. (1998). Heat transfer in two-phase solid-liquid food flows: a review . Food and Bioproducts Processing 76(1), 3-29.

Berk Z. (2013). Chapter 18. Thermal Processes, Methods and Equipment. Food Process Engineering and Technology (Second Edition).

Bhuvaneswari E., Anandharamakrishnan C. (2014). Heat transfer analysis of pasteurization of bottled beer in a tunnel pasteurizer using computational fluid dynamics. Innovative Food Science and Emerging Technologies 23, 156–163.

Boz Z., Erdogdu F. (2013). Evaluation of two-dimensional approach for computational modelling of heat and momentum transfer in liquid containing horizontal cans and experimental validation. Food and Bioproducts Processing 91(1), 37-45.

Cariño-Sarabia A., Vélez-Ruiz J.F. (2013). Evaluation of convective heat transfer coefficient between fluids and particles in suspension as food model systems for natural convection using two methodologies. Journal of Food Engineering 115(2), 173-181.

Chen G., Campanella O.H., Peleg M. (2011). Calculation of the total lethality of conductive heat in cylindrical cans sterilization using linear and non linear survival kinetic models. Food Research International 44(4), 1012-1022.

Cuesta F.J., Lamúa M., Alique R. (2012). A new exact numerical series for the determination of the Biot number: Application for the inverse estimation of the surface heat transfer coefficient in food processing. International Journal of Heat and Mass Transfer 55 (15–16),4053-4062.

D'Addio L., Di Natale F. , Budelli A., Nigro R.(2014). CFD Simulation for the pasteurization of fruit puree with pieces. Chemical Engineering Transactions 39, 1699-1704.

Dilay E., Vargas J.V.C., Amico S.C., Ordoñez J.C. (2006). Modeling, simulation and optimization of a beer pasteurization tunnel.   Journal of Food Engineering 77(3), 500-513.

Eckert E.G. , Goldstein R.J., Patankar S.V., Pfender E., Ramsey J.W., Simon T.W. , Sparrow E.M. (1982). Heat transfer - a literatute review of 1981. International Journal of Heat and Mass Transfer 25(12), 1783-1812.

Erdogdu F., Tutar M. (2012). A computational study for axial rotation effects on heat transfer in rotating cans containing liquid water, semi-fluid food system and headspace. International Journal of Heat and Mass Transfer 55(13–14), 3774-3788.

Erdogdu F., Uyar R. and Koray Palazoglu T. (2010). Experimental   comparison   of natual convection and conduction heat transfer. Journal of Food Process Engineering 33, 85–100.

Escudero-López, B., Cerrillo, I., Gil-Izquierdo, Á., Hornero-Méndez, D., Herrero-Martín, G., Berná, G., Medina, S., Ferreres, F., Martín, F., Fernández-Pachón, M.-S. (2016).   Effect of thermal processing on the profile of bioactive compounds and antioxidant capacity of fermented orange juice. International Journal of Food Sciences and Nutrition 67 (7), 779-788.

Fairhurst P.G., Barigou M., Fryer P.J., Pain J.-P. (1999). Particle Passage Time Distributions in Vertical Pipe Flow of Solid–Liquid Food Mixtures. Food and Bioproducts Processing 77(4), 293-301.

Fellows P.J. (2009) 12 - Pasteurisation, In Woodhead Publishing Series in Food Science, Technology and Nutrition, Woodhead Publishing. Food Processing Technology (Third edition).

Funami T., Kataoka Y., Omoto T., Goto Y., Asai I., Nishinari K. (2005). Food hydrocolloids control the gelatinization and retrogradation behavior of starch. 2b. Functions of guar gums with different molecular weights on the retrogradation behavior of corn starch. Food Hydrocolloids 19 (1), 25-36.

Ghani A.G.A., Farid M.M., Chen X.D., Richards P. (2001). Thermal sterilization of canned food in a 3D pouch using computational fluid dynamics. Journal of Food Engineering 48(2), 147-156.

Goff H.D. (2013). Chapter 9 – Dairy Product Processing Equipment. Handbook of Farm, Dairy and Food Machinery Engineering (Second Edition).

Gogou, E., Katapodis, P., Christakopoulos, P. & Taoukis, P. S. (2010). Effect of water activity on the thermal stability of Thermomyces lanuginosus xylanases for process time-temperature integration. Journal of Food Engineering, 100, 649-655.

Guiavarc'h, Y. P., Dintwa, E., Van Loey, A.M., Zuber, F. T., & Hendrickx,M. E. (2002b). Validation and use of an enzymatic Time Temperature Integrator to monitor thermal impacts inside a solid/liquidmodel food. Biotechnology, 18, 1087−1094.

Guiavarc'h, Y., Deli, V., Van Loey, A., Hendrickx, M., (2002a). Development of an enzymic time–temperature integrator for sterilization processes based on Bacillus licheniformis α-amylase at reduced water content. Journal of Food Science 67, 285–291.

Guiavarc'h, Y., Sila, D., Duvetter, T., Van Loey, A. and Hendrickx, M. (2003). Influence of sugars and polyols on the thermal stability of purified tomato and cucumber pectinmethylesterases: a basis for TTI development. Enzyme and Microbial Technology, 33: 544–555.

Guiavarc'h, Y., Van Loey, A., Zuber, F., Hendrickx, M. (2004). Bacillus licheniformis α-amylase immobilized on glass beads and equilibrated at low moisture content: potentials as a time and temperature integrator for sterilization processes. Innovative Food Science and Emerging Technologies 5, 317–325.

Hauge S.J., Wahlgren M., Røtterud O-J., Nesbakken T. (2011). Hot water surface pasteurisation of lamb carcasses: Microbial effects and cost-benefit considerations. International Journal of Food Microbiology 146(1), 69-75.

Hendrickx, M., Maesmans, G., De Cordt, S., Noronha, J., Van Loey, A. and Tobback, P. (1995). Evaluation of the integrated time–temperature effect in thermal processing of foods. Critical Reviews in Food Science and Nutrition, 35(3): 231–262.

Hendrickx, M. E., Weng, Z., Maesmans, G., and Tobback, P. (1992) Validation of time temperature integrator for thermal processing of food under pasteurisation conditions. International of Food Science and Technology 27, 21-31.

Holdsworth, D.S. and Simspson, R. (2007). Thermal processes of packaged foods. Food Engineering Series. Springer.

Horn C. S., Frank, M., Blakemore F. B. and Stannek W. (1997). Modelling and simulation of pasteurization and staling effects during tunnel pasteurization of bottled beer. Food and Bioproducts Processing 75(1), 23-33.

Ibrahim G.A., Ahmed H.M., Hussain S., Khalaf A. S. (2015). A Theoretical Study on the Overall Performance of a Falling Film Vertical Tube Absorber. Journal of Advanced Science and Engineering Research 5(2), 9-25.

Incropera F.P., Dewitt D.P., Bergman T.L., Lavine A.S. (2006). Principles of Heat and Mass Transfer (Seventh Edition). International Student Version. John Wiley and Sons, Inc.

James S.J., Evans J.A. (2006). Predicting the reduction in microbes on the surface of foods during surface pasteurisation—the 'BUGDEATH' project. Journal of Food Engineering 76(1), 1-6.

James, S. and James C. (2014). Chapter 32 - Minimal Processing of Ready Meals, In Emerging Technologies for Food Processing (Second Edition), edited by Da-Wen Sun,, Academic Press, San Diego. Pages 599-612.

Kannan A. , Gourisankar Sandaka P.Ch.(2008). Heat transfer analysis of canned food sterilization in a still retort. Journal of Food Engineering 88(2), 213–228.

Kitt A. Heat Transfer in Spray Pasteurisation. Research project (2015). University of Birmingham.

Kitt A., Wainwright A., Bakalis S., Fryer P.J., Lopez-Quiroga E.(2015). Heat transfer in spray pasteurisation; defining an energy minimum. 29th EFFoST International Conference Proceedings.

Kızıltaş S., Erdoğdu F., Koray Palazoğlu T. (2010). Simulation of heat transfer for solid–liquid food mixtures in cans and model validation under pasteurization conditions. Journal of Food Engineering 97(4), 449-456.

Lambourne, T., & Tucker, G.S. (2001). Time temperature Integrators for validation of thermal processes. R&D report (pp. 132). Campden & Chorleywood Food Research Association.

Lambourne, T., Adams, J.B., Lach, A., (2002). Application of a biochemical time–temperature integrator to estimate pasteurisation values in continuous food processes. Innovative Food Science and Emerging Technologies 3 (2), 165-174.

Lareo C., Branch C.A., Fryer P.J. (1997a). Particle velocity profiles for solid-liquid food flows in vertical pipes part I. Single particles. Powder Technology 93(1), 23-34.

Lareo C., Fryer P.J., Barigou M. (1997b). The Fluid Mechanics of Two-Phase Solid-Liquid Food Flows A Review. Food and Bioproducts Processing 75(2), 73-105.

Lareo C., Nedderman R.M., Fryer P.J. (1997c). Particle velocity profiles for solid-liquid food flows in vertical pipes part II. Multiple particles. Powder Technology 93(1), 35-45.

Leadley, C., Tucker, G, and Fryer, P. (2008). A comparative study of high pressure sterilisation and conventional thermal sterilisation: Quality effects in green beans.Innovative Food Sci and Emerg Technol, 9 : 70–79.

Lee, S-Y. (2004). Microbial safety of pickled fruits and vegetables and hurdle technology. Internet Journal of Food Safety. 4: 21-32.

Lewicki P.P. (1984) . Heat transfer in a tunnel pasteuriser. Part II: Heat transfer coefficients. Journal of Food Engineering 3(2), 91-115.

Lewicki P.P. (1985). Heat transfer in a tunnel pasteuriser. Part III. Application of the Schultz-Olson theory. Journal of Food Engineering 4(4), 265-289.

Lewicki P.P., Walczak W., Goss B. (1983). Heat transfer in a tunnel pasteuriser. Part I. Factors affecting the rate of heating of liquid in a bottle. Journal of Food Engineering 2(4), 309-322.

Lewis, M.J. (1990). Physical properties of food sand food processing systems. Woodhead Publishing.

Lewis, M.J. and Heppell, N.J. (2000). Continuous Thermal Processing of Foods: Pasteurization and UHT Sterilization. Food Engineering Series. Springer.

Mankad, S. Nixorf K. M., Fryer P. J. (1997). Measurements of particle-liquid heat transfer in systems of varied solids fraction. Journal of Food Engineering 31(1), 9-33.

Marra, F. and Romano, V. (2003) A mathematical model to study the influence of wireless temperature sensor during assessment of canned food sterilization. Journal of Food Engineering 59, 245-252.

Mehauden K. , Cox P.W., Bakalis S., Simmons M.J.H., Tucker G.S., Fryer P.J. (2007).   "A novel method to evaluate the applicability of time temperature. integrators to different temperature profiles"   Innovative Food Science & Emerging Technologies 8(4), 507-514.

Mehauden, K., Bakalis, S., Cox, P.W., Fryer, P.J., Simmons, M.J.H., (2008). Use of time–temperature integrators for determining process uniformity in agitated vessels. Innovative Food Science and Emerging Technologies 9(3), 385–395.

Mehauden, K.(2008). Evaluation of the thermal and mixing performance of an agitated vessel for processing of complex liquid foodstuffs. A thesis for the degree of DOCTOR OF PHILOSOPHY. The University of Birmingham. 236 p.

Meng Y., Ramaswamy H.S. (2005). Heat transfer coefficients associated with canned particulate/non-Newtonian fluid (CMC) system during end-over-end rotation.Food and Bioproducts Processing 83(3), 229-237.

Meng Y., Ramaswamy H.S. (2007a). Effect of system variables on heat transfer to canned particulate non Newtonian fluids during end-over-end rotation. Food and Bioproducts Processing 85(1), 34-41.

Meng Y., Ramaswamy H.S. (2007b). Dimensionless heat transfer correlations for high viscosity fluid-particle mixtures in cans during end-over-end rotation. Journal of Food Engineering 80(2), 528-535.

Miri T., Tsoukalas A. , Bakalis S., Pistikopoulos E.N., Rustem B., Fryer P.J. (2008). Global optimization of process conditions in batch thermal sterilization of food. Journal of Food Engineering 87(4), 485-494.

Mohamed I.O. (2007). Determination of an effective heat transfer coefficients for can headspace during thermal sterilization process. Journal of Food Engineering 79(4), 1166-1171.

Perry, R. H., & Green, D. W. (2008). Perry's Chemical Engineers' Handbook. New York, McGraw-Hill.

Plazl I., Lakner M., Koloini T. (2006). Modeling of temperature distributions in canned tomato based dip during industrial pasteurization. Journal of Food Engineering 75(3), 400-406.

Prost J.S., González M.T., Urbicaina, M.J. (2006). Determination and correlation of heat transfer coefficients in a falling film evaporator. Journal of Food Engineering 73(4), 320–326.

Purnell G. , James C. (2012). Chapter 8 - Advances in food surface pasteurisation by thermal methods, In Woodhead Publishing Series in Food Science, Technology and Nutrition. Microbial Decontamination in the Food Industry, Woodhead Publishing.

Randox (2006). Amylase ethylidene blocked-p-NPG7 manual. [AY1582].

Saikia, S., Mahnot, N.K., Mahanta, C.L. (2015). A comparative study on the effect of conventional thermal pasteurisation, microwave and ultrasound treatments on the

antioxidant activity of five fruit juices. Food Science and Technology International 22 (4), 288-301.

Silva F. V. M., Gibbs P. A. (2012). Thermal pasteurization requirements for the inactivation of Salmonella in foods. Food Research International 45(2), 695-699.

Simpson R., Almonacid S., Mitchell M. (2004). Mathematical model development, experimental validation and process optimization: retortable pouches packed with seafood in cone frustum shape. Journal of Food Engineering 63(2), 153-162.

Singh A., Ramaswamy H.S. (2016). Heat transfer coefficients during thermal processing of model particulate mixtures in non-Newtonian fluids undergoing reciprocation agitation as affected by process variables. LWT - Food Science and Technology 65, 185-196.

Singh A., Singh A.P., Ramaswamy H.S. (2015a). Computational techniques used in heat transfer studies on canned liquid particulate mixtures. Trends in Food Science & Technology 43(1), 83-103.

Singh A., Singh A.P., Ramaswamy H.S. (2015b). A refined methodology for evaluation of heat transfer coefficients in canned particulate fluids under rapid heating conditions. Food and Bioproducts Processing 94, 169-179.

Singh A.,Ramaswamy H.S. (2015c). Effect of product related parameters on heat-transfer rates to canned particulate non-Newtonian fluids (CMC) during reciprocation agitation thermal processing. Journal of Food Engineering 165, 1-12.

Singh A.P., Singh A., Ramaswamy H.S. (2016). Dimensionless correlations for heat transfer coefficients during reciprocating agitation thermal processing (RA-TP) of Newtonian liquid/particulate mixtures.Food and Bioproducts Processing 97, 76-87.

Singh A.P., Singh A., Ramaswamy H.S. (2015). Modification of a static steam retort for evaluating heat transfer under reciprocation agitation thermal processing. Journal of Food Engineering 153, 63-72.

Singh A.P., Ramaswamy H.S. (2016). Simultaneous optimization of heat transfer and reciprocation intensity for thermal processing of liquid particulate mixtures undergoing reciprocating agitation. Innovative Food Science & Emerging Technologies 33, 405-41.

Sinkunas S., Gylys J. and Kielka A. (2005). Analysis of laminar liquid film flowing down a vertical surface. Fourth International Conference on CFD in the Oil and Gas, Metallurgical & Process Industries SINTEF / NTNU Trondheim, Norway 6-8 June.

Tolasa, S., Cakli, S., Kisla, D., Dincer, T. (2012). Quality and shelf-life assessment of pasteurized trout soup during refrigerated storage. Journal of Aquatic Food Product Technology 21 (4),321-329.

Tucker G., Hanby E., Brown H. (2009). Development and application of a new time–temperature integrator for the measurement of P-values in mild pasteurisation processes. Food and Bioproducts Processing 87(1), 23-33.

Tucker, G. S., Lambourne, T., Adams, J. B., & Lach, A. (2002). Application of a Biochemical time–temperature integrator to estimate pasteurisation values in continuous food processes. Innovative Food Science & Emerging Technologies, 3(2), 165–174.

Tucker, G.S., Brown, H.M., Fryer, P.J., Cox, P.W., Poole, F.L.I., Lee, H.-S., Adams, M.W.W., (2007). A sterilisation time–temperature integrator based on amylase from the hyperthermophilic organism *Pyrococcus furiosus*. Innovative Food Science and Emerging Technologies 8 (1), 63–72.

Tutar M., Erdogdu F. (2012). Numerical simulation for heat transfer and velocity field characteristics of two-phase flow systems in axially rotating horizontal cans. Journal of Food Engineering 111(2), 366-385.

Van der Plancken, I., Grauwet, T., Oey, I., Van Loey, A., & Hendrickx, M. (2008). Impact evaluation of high pressure treatment on foods: Considerations on the

development of pressure–temperature–time integrators (pTTIs). Trends in Food Science and Technology, 19, 337−348.

Van Loey, A., Arthawan, A., Henrickx, M., Haentjens, T., Tobback, P., (1997). The development and use of an α-amylase -based time–temperature integrator to evaluate in-pack pasteurization processes. Lebensmittel-Wissenschaft und-Technologie 30, 94–100.

Van Loey, A.M., Hendrickx, M.E., De Cordt, S., Haentjens, T.H. and Tobback, P.P. (1996)Quantitative evaluation of thermal processes using time–temperature integrators. Trends in Food Science and Technology, 7: 16–26.

Vozár L., Srámková T. (1997). Two data reduction methods for evaluation of thermal diffusivity from step heating measurements. International   Journal of Heat and Mass Transfer 40(7), 1647-1655.

Welti-Chanes J., Vergara-Balderas F., Bermúdez-Aguirre D. (2005). Transport phenomena in food engineering basic concepts and advances. Journal of Food Engineering 67(1–2), 113-128.

Xie G., Sheard M.A. (1996). Comparison of two methods used to determine apparent heat transfer coefficient for pouches pasteurized in a combination oven.   LWT - Food Science and Technology 29(1–2), 100-105.

Yang Z., Fan X. , Bakalis S., Parker D.J., Fryer P.J. (2008). Impact of solids fraction and fluid viscosity on solids flow in rotating cans. Food Research International 41(6), 658-666.

Yao L-S., Molla Md. M. (2008). Forced convection of non-Newtonian fluids on a heated flat plate. International Journal of Heat and Mass Transfer 51(21–22), 5154-5159.

Yataghene M., Legrand J. (2013). A 3D-CFD model thermal analysis within a scraped surface heat exchanger. Computers & Fluids 71, 380-399.

Zhang L. ,Fryer P.J. (1995). A model for conduction heat transfer to particles in a hold tube using a moving mesh finite element method. Journal of Food Engineering 26 (2) 193-208.

Appendix I:

Table A.I. 1: Pasteurisation values corresponding to water bath temperatures of 60°C, 70°C and 80°C for a 660 ml jar containing a 3% agar solution.

Forced convection							
T(°C)	**Loc 1**	**Loc 2**	**Loc 3**	**Loc 4**	**Loc 5**	**Loc 6**	**Loc 7**	**Loc 8**
60	0.00 ± 0.00	0.00 ± 0.00	0.01 ± 0.00	0.00 ± 0.00	0.00 ± 0.00	0.20 ± 0.01	0.40 ± 0.01	0.45 ± 0.02
70	0.00 ± 0.00	0.00 ± 0.00	0.07 ± 0.01	0.01 ± 0.00	0.02 ± 0.00	1.54 ± 0.13	3.56 ± 0.42	4.50 ± 0.12
80	0.01 ± 0.00	0.00 ± 0.00	0.26 ± 0.23	0.03 ± 0.01	0.10 ± 0.04	13.24 ± 1.94	33.55 ± 5.97	43.13 ± 0.95
Natural convection							
T(°C)	**Loc 1**	**Loc 2**	**Loc 3**	**Loc 4**	**Loc 5**	**Loc 6**	**Loc 7**	**Loc 8**
60	0.00 ± 0.00	0.00 ± 0.00	0.01 ± 0.00	0.00 ± 0.00	0.01 ± 0.00	0.15 ± 0.02	0.28 ± 0.03	0.45 ± 0.03
70	0.00 ± 0.00	0.00 ± 0.00	0.02 ± 0.00	0.01 ± 0.00	0.02 ± 0.00	1.15 ± 0.08	2.36 ± 0.16	4.15 ± 0.31
80	0.01 ± 0.00	0.00 ± 0.00	0.12 ± 0.01	0.02 ± 0.00	0.09 ± 0.00	9.76 ± 0.40	23.44 ± 0.77	41.39 ± 1.18

Table A.I. 2: Pasteurisation values corresponding to water bath temperatures of 60°C, 70°C and 80°C for a 330 ml jar containing a 3% agar solution.

Forced convection								
T(°C)	Loc 1	Loc 2	Loc 3	Loc 4	Loc 5	Loc 6	Loc 7	Loc 8
60	0.02 ± 0.00	0.01 ± 0.00	0.03 ± 0.01	0.04 ± 0.01	0.09 ± 0.02	0.14 ± 0.02	0.31 ± 0.02	0.34 ± 0.00
70	0.09 ± 0.01	0.06 ± 0.01	0.17 ± 0.03	0.23 ± 0.06	0.71 ± 0.10	1.19 ± 0.30	3.00 ± 0.21	3.36 ± 0.05
80	0.52 ± 0.02	0.30 ± 0.03	0.93 ± 0.26	1.62 ± 0.46	7.82 ± 3.90	9.99 ± 2.14	25.77 ± 2.02	32.97 ± 0.99
Natural convection								
T(°C)	Loc 1	Loc 2	Loc 3	Loc 4	Loc 5	Loc 6	Loc 7	Loc 8
60	0.01 ± 0.00	0.01 ± 0.00	0.03 ± 0.02	0.02 ± 0.00	0.07 ± 0.01	0.11 ± 0.01	0.19 ± 0.03	0.34 ± 0.00
70	0.07 ± 0.01	0.04 ± 0.00	0.13 ± 0.00	0.16 ± 0.03	0.53 ± 0.03	0.90 ± 0.10	1.71 ± 0.22	3.25 ± 0.04
80	0.31 ± 0.06	0.19 ± 0.04	0.73 ± 0.10	0.98 ± 0.16	4.15 ± 0.65	7.35 ± 0.95	16.75 ± 0.79	30.90 ± 0.32

Table A.I. 3: Pasteurisation values corresponding to water bath temperatures of 60°C, 70°C and 80°C for a 660 ml jar containing water.

Forced convection								
T(°C)	Loc 1	Loc 2	Loc 3	Loc 4	Loc 5	Loc 6	Loc 7	Loc 8
60	0.14 ± 0.00	0.16 ± 0.00	0.22 ± 0.02	0.15 ± 0.00	0.15 ± 0.00	0.19 ± 0.02	0.29 ± 0.02	0.34 ± 0.00
70	1.30 ± 0.02	1.47 ± 0.02	1.91 ± 0.04	1.32 ± 0.02	1.32 ± 0.02	1.60 ± 0.09	2.72 ± 0.16	3.37 ± 0.05
80	12.25 ± 0.16	13.91 ± 0.15	18.12 ± 0.38	12.50 ± 0.17	12.31 ± 0.08	14.63 ± 0.76	26.39 ± 2.06	33.27 ± 0.82
Natural convection								
T(°C)	Loc 1	Loc 2	Loc 3	Loc 4	Loc 5	Loc 6	Loc 7	Loc 8
60	0.09 ± 0.00	0.11 ± 0.00	0.19 ± 0.00	0.10 ± 0.00	0.10 ± 0.00	0.12 ± 0.00	0.20 ± 0.01	0.33 ± 0.01
70	0.76 ± 0.02	1.00 ± 0.03	1.66 ± 0.06	0.92 ± 0.02	0.87 ± 0.03	0.59 ± 0.02	2.27 ± 0.39	3.14 ± 0.11
80	5.68 ± 0.35	7.41 ± 0.54	12.22 ± 1.62	6.65 ± 0.60	6.42 ± 0.51	8.33 ± 0.54	15.53 ± 1.31	23.40 ± 2.03

Table A.I. 4: Pasteurisation values corresponding to water bath temperatures of 60°C, 70°C and 80°C for a 330 ml jar containing water.

Forced convection								
T(°C)	Loc 1	Loc 2	Loc 3	Loc 4	Loc 5	Loc 6	Loc 7	Loc 8
60	0.19 ± 0.00	0.20 ± 0.01	0.22 ± 0.01	0.19 ± 0.01	0.19 ± 0.00	0.22 ± 0.01	0.30 ± 0.03	0.34 ± 0.01
70	1.88 ± 0.04	1.96 ± 0.07	2.11 ± 0.09	1.81 ± 0.07	1.85 ± 0.05	2.08 ± 0.09	3.10 ± 0.21	3.37 ± 0.09
80	18.21 ± 0.66	18.89 ± 0.73	20.79 ± 1.17	17.48 ± 0.69	17.62 ± 0.69	19.64 ± 0.68	29.93 ± 2.17	32.24 ± 1.47
Natural convection								
T(°C)	Loc 1	Loc 2	Loc 3	Loc 4	Loc 5	Loc 6	Loc 7	Loc 8
60	0.14 ± 0.01	0.15 ± 0.01	0.18 ± 0.02	0.14 ± 0.01	0.14 ± 0.00	0.15 ± 0.02	0.22 ± 0.03	0.32 ± 0.01
70	1.39 ± 0.02	1.52 ± 0.12	1.78 ± 0.15	1.40 ± 0.11	1.41 ± 0.16	1.57 ± 0.06	2.33 ± 0.06	3.20 ± 0.23
80	15.12 ± 2.12	16.13 ± 2.28	18.97 ± 2.09	15.17 ± 2.33	14.77 ± 1.77	17.24 ± 1.31	24.09 ± 4.01	33.69 ± 2.16

Table A.I. 5: Pasteurisation values corresponding to water bath temperatures of 60°C, 70°C and 80°C for a 330 ml jar containing a 10% sucrose solution.

Forced convection								
T(°C)	Loc 1	Loc 2	Loc 3	Loc 4	Loc 5	Loc 6	Loc 7	Loc 8
60	0.19 ± 0.01	0.20 ± 0.01	0.22 ± 0.02	0.19 ± 0.01	0.19 ± 0.00	0.21 ± 0.02	0.31 ± 0.01	0.34 ± 0.00
70	1.86 ± 0.08	1.94 ± 0.07	2.08 ± 0.11	1.78 ± 0.11	1.81 ± 0.06	1.99 ± 0.15	3.01 ± 0.04	3.41 ± 0.07
80	18.11 ± 0.21	18.54 ± 0.08	19.65 ± 0.14	17.43 ± 0.40	17.45 ± 0.38	18.56 ± 1.15	30.99 ± 1.35	32.87 ± 0.26
Natural convection								
T(°C)	Loc 1	Loc 2	Loc 3	Loc 4	Loc 5	Loc 6	Loc 7	Loc 8
60	0.14 ± 0.01	0.15 ± 0.01	0.18 ± 0.02	0.15 ± 0.01	0.14 ± 0.01	0.15 ± 0.00	0.22 ± 0.00	0.33 ± 0.00
70	1.27 ± 0.19	1.36 ± 0.18	1.57 ± 0.15	1.31 ± 0.19	1.31 ± 0.12	1.42 ± 0.07	2.03 ± 0.11	3.27 ± 0.12
80	13.18 ± 0.50	14.06 ± 0.39	16.27 ± 0.09	13.65 ± 0.98	13.65 ± 0.29	14.78 ± 0.93	20.57 ± 0.65	31.64 ± 1.13

Table A.I. 6: Pasteurisation values for two different percentages of headspace: 5% (w/v) and 10% (w/v) in a jar filled with water. The heating temperature was 70 °C in all the cases presented. T_{ref} = 80 ^{0}C, z value= 10 ^{0}C.

% Headspace	Loc 1	Loc 2	Loc 3	Loc 8
5	23.41 ± 0.47	28.42 ± 1.76	22.75 ± 2.91	34.20 ± 2.37
10	27.76 ± 0.87	31.78 ± 1.07	23.85 ± 3.62	34.20 ± 2.38

Table A.I. 7: Pasteurisation values calculated from the temperatures measured using thermocouples with those calculated employing the TTIs data for different heating scenarios: heating temperature of 60ºC during 60 min, heating temperature of 70ºC during 15 and finally water bath at 80ºC during 15 min for water and a 3%(w/v) agar. T_{ref} = 80 ºC, z value = 8.9 ºC

Water, heating temperature of 60ºC during 60 min						
Monitoring type	loc. 1	loc. 2	loc. 3	loc. 4	loc. 6	loc. 7	loc. 8
TTI	2.325	2.837	3.010	3.009	3.661	4.372	-
Thermocouple	1.2514	1.2588	1.2798	1.1559	1.3241	1.3885	1.5336
A 3%(w/v) agar, heating temperature of 60ºC during 60 min						
Monitoring type	loc. 1	loc. 2	loc. 3	loc. 4	loc. 6	loc. 7	loc. 8
TTI	3.264	2.098	1.410	1.629	3.345	4.231	-
Thermocouple	0.4858	0.2736	0.2785	0.4332	0.4190	0.9894	1.5860
Water , heating temperature of 60ºC during 60 min						
Monitoring type	loc. 1	loc. 2	loc. 3	loc. 4	loc. 6	loc. 7	loc. 8
TTI	3.992	4.964	5.243	5.441	4.372	4.900	-
Thermocouple	0.6804	0.7797	1.0202	0.7472	2.5608	3.0532	2.4710
A 3%(w/v) agar, heating temperature of 60ºC during 60 min						
Monitoring type	loc. 1	loc. 2	loc. 3	loc. 4	loc. 6	loc. 7	loc. 8
TTI	2.649	1.814	1.564	1.064	1.719	3.107	-
Thermocouple	0.0002	0.0026	0.0010	0.0017	0.6040	0.5817	3.2814
Water , heating temperature of 60ºC during 60 min						
Monitoring type	loc. 1	loc. 2	loc. 3	loc. 4	loc. 6	loc. 7	loc. 8
TTI	7.327	8.105	10.646	9.290	8.248	12.504	-
Thermocouple	4.2747	4.8935	6.3501	4.8878	5.6614	20.2344	15.9322
A 3%(w/v) agar, heating temperature of 60ºC during 60 min						
Monitoring type	loc. 1	loc. 2	loc. 3	loc. 4	loc. 6	loc. 7	loc. 8
TTI	2.273	2.426	2.980	2.070	3.550	15.804	-
Thermocouple	0.0002	0.0205	0.0042	0.0031	2.7539	2.8705	19.1147

Table A.I. 8: Pasteurisation values for both liquid and solid phases when the fluid filling presents different viscosity values: water, 4%(w/v) starc , 4%(w/v) pregelatinised starch, and 1%(w/v) guar gum .

Water									
% Solid fraction	loc 1	loc 2	loc 3	loc 4	loc 5	loc 6	loc 7	loc 8	loc 9
10	15.08 ± 0.28	17.15 ± 0.24	19.87 ± 0.37	17.89 ± 0.23	17.42 ± 0.39	19.55 ± 0.34	20.08 ± 0.63	16.83 ± 0.42	29.90 ± 0.13
50	13.42 ± 0.85	15.59 ± 1.58	18.43 ± 1.21	17.14 ± 0.60	15.34 ± 1.05	17.52 ± 1.55	18.20 ± 1.53	16.22 ± 0.42	28.97 ± 0.47
4%(w/v) starch									
% Solid fraction	loc 1	loc 2	loc 3	loc 4	loc 5	loc 6	loc 7	loc 8	loc 9
10	0.68 ± 0.08	0.37 ± 0.07	0.35 ± 0.11	5.77 ± 2.64	0.78 ± 0.15	0.48 ± 0.05	0.26 ± 0.08	0.62 ± 0.21	29.16 ± 0.57
50	0.71 ± 0.16	0.32 ± 0.11	0.31 ± 0.04	4.86 ± 6.81	0.75 ± 0.17	0.42 ± 0.10	0.30 ± 0.02	0.97 ± 0.41	28.75 ± 0.17
4%(w/v) pregelatinised starch									
% Solid fraction	loc 1	loc 2	loc 3	loc 4	loc 5	loc 6	loc 7	loc 8	loc 9
10	6.33 ± 0.13	6.91 ± 0.30	13.54 ± 1.12	18.37 ± 2.33	6.86 ± 0.26	8.08 ± 0.50	12.57 ± 0.37	8.52 ± 0.25	29.02 ± 0.22
50	4.31 ± 1.58	7.03 ± 1.34	11.22 ± 1.90	10.55 ± 3.40	4.83 ± 1.83	6.41 ± 1.91	10.63 ± 1.22	8.25 ± 2.75	28.61 ± 0.25
1% guar gum									
% Solid fraction	loc 1	loc 2	loc 3	loc 4	loc 5	loc 6	loc 7	loc 8	loc 9
10	1.90 ± 0.18	4.32 ± 0.38	7.54 ± 0.30	4.08 ± 0.45	1.74 ± 0.05	3.85 ± 0.21	8.53 ± 0.37	16.23 ± 4.79	28.90 ± 0.23
50	0.65 ± 0.03	0.41 ± 0.00	0.46 ± 0.10	0.71 ± 0.03	0.55 ± 0.02	0.39 ± 0.02	0.54 ± 0.14	0.78 ± 0.26	28.80 ± 0.53

Appendix II

Table A.II. 1: Processing values for three different flow rate values: 0.53, 0.78 and 1.08 l/min. The temperature of the spray nozzle was 60°C in all cases, with an initial temperature of the filling water of 20°C. The z-value considered in the calculations was z = 10°C and the value of the temperature reference used was T$_{ref}$ = 70°C.

Location	Flow rate (l/min)		
	0.53	**0.78**	**1.1**
Loc 1	0.71 ± 0.03	2.36 ± 0.21	2.09 ± 0.30
Loc 2	0.73 ± 0.05	2.30 ± 0.21	2.13 ± 0.30
Loc 3	0.79 ± 0.07	2.43 ± 0.23	2.15 ± 0.27
Loc 4	0.61 ± 0.05	2.09 ± 0.19	1.87 ± 0.21
Loc 5	0.64 ± 0.02	3.24 ± 0.30	2.13 ± 0.54
Loc 6	0.78 ± 0.02	2.80 ± 0.26	2.46 ± 0.24
Loc 7	1.53 ± 0.03	2.92 ± 0.27	2.83 ± 0.53
Loc 8	6.13 ± 0.61	7.28 ± 0.65	6.83 ± 0.25
Loc 9	3.71 ± 0.06	2.15 ± 0.20	3.63 ± 0.33

Table A.II. 2: Processing values calculated for three different spray nozzle temperatures: 50, 60, and 70°C in a jar filled with water. The starting temperature was 20°C in all cases, and the Z-value considered in the calculations was z = 10°C. The reference temperature considered was T$_{ref}$ = 70°C. The data shown was measured for a mass flow rate through the nozzle of 1.09 l/min.

Location	Spray nozzle temperatures (^{o}C)		
	50	60	70
Loc 1	0.24 ± 0.03	2.21 ± 0.29	13.12 ± 2.84
Loc 2	0.24 ± 0.02	2.24 ± 0.27	12.85 ± 2.74
Loc 3	0.27 ± 0.03	2.38 ± 0.28	13.57 ± 2.47
Loc 4	0.23 ± 0.04	1.95 ± 0.23	11.82 ± 2.06
Loc 5	0.24 ± 0.03	2.05 ± 0.20	13.36 ± 2.41
Loc 6	0.27 ± 0.04	2.29 ± 0.30	13.82 ± 2.92
Loc 7	0.38 ± 0.03	2.93 ± 0.06	19.63 ± 3.51
Loc 8	0.64 ± 0.03	6.43 ± 0.10	64.75 ± 3.89
Loc 9	0.35 ± 0.01	3.71 ± 0.34	17.93 ± 0.41

Table A.II. 3: Processing values for five different solution systems: water, 5%(w/v) pre-gelatinised starch, 5% corn starch , 1%(w/v) gaur gum and 3%(w/v) agar. The spray nozzle temperature was 70ºC in all cases, with a starting temperature for the filling of 20ºC. The Z-value considered in the calculations was z = 10ºC, T_{ref} = 70ºC. The data shown was recorded for a mass flow rate through the nozzle of 1.1 l/min.

Location	Solution system				
	water	pre-gelatinised starch	5% corn starch	1%(w/v) gaur gum	3%(w/v) agar
Loc 1	13.12 ± 2.84	9.24 ± 1.54	3.26 ± 0.25	7.10 ± 0.22	2.39 ± 0.09
Loc 2	12.85 ± 2.74	10.06 ± 1.46	2.45 ± 0.20	7.15 ± 0.22	1.77 ± 0.08
Loc 3	13.57 ± 2.47	11.10 ± 1.52	2.26 ± 0.11	9.14 ± 0.28	2.20 ± 0.11
Loc 4	11.82 ± 2.06	9.66 ± 1.33	3.58 ± 0.19	8.06 ± 0.24	2.79 ± 0.10
Loc 5	13.36 ± 2.41	12.18 ± 1.10	8.52 ± 0.30	15.26 ± 0.46	7.81 ± 0.63
Loc 6	13.82 ± 2.92	13.65 ± 1.48	12.04 ± 2.18	14.09 ± 0.43	11.41 ± 0.49
Loc 7	19.63 ± 3.51	18.77 ± 1.86	17.88 ± 2.33	20.26 ± 0.61	14.79 ± 1.32
Loc 8	64.75 ± 3.89	63.10 ± 3.59	60.77 ± 1.59	68.53 ± 2.13	66.79 ± 1.90
Loc 9	17.93 ± 0.41	18.94 ± 1.44	19.13 ± 1.08	19.38 ± 1.29	18.48 ± 0.67

Table A.II. 4: **Pasteurisation values for four different relative positions of nozzle and vessel. The heating temperature was 60 °C and flow rate 0.78 l/min in all cases. The starting temperature was 20°C, the z-value considered in the calculations was z = 10°C and T$_{ref}$ = 70°C.**

Location	Relative positions of nozzle and vessel at point			
	1	2	3	4
Loc 1	2.78 ± 0.26	2.36 ± 0.21	2.44 ± 0.22	2.17 ± 0.20
Loc 2	2.82 ± 0.26	2.30 ± 0.21	2.47 ± 0.23	2.26 ± 0.21
Loc 3	2.82 ± 0.26	2.43 ± 0.23	2.56 ± 0.24	2.40 ± 0.22
Loc 4	2.41 ± 0.23	2.09 ± 0.19	2.19 ± 0.20	1.99 ± 0.18
Loc 5	3.22 ± 0.30	3.24 ± 0.30	2.30 ± 0.21	2.23 ± 0.21
Loc 6	3.15 ± 0.30	2.80 ± 0.26	2.62 ± 0.25	2.51 ± 0.24
Loc 7	2.75 ± 0.26	2.92 ± 0.27	3.48 ± 0.32	3.93 ± 0.36
Loc 8	7.15 ± 0.64	7.28 ± 0.65	7.55 ± 0.68	8.29 ± 0.74
Loc 9	1.99 ± 0.18	2.15 ± 0.20	2.35 ± 0.21	2.25 ± 0.20

Note: point 1 (25 cm), point 2 (18.5 cm.), point 3 (12 cm.), and point 4 (25 cm)

Table A.II. 5: Pasteurisation values for three different heights of the nozzle: 35 , 26.5, and 18.6 cm. The z-value considered in the calculations was z = 10°C, and the reference temperature was T$_{ref}$ = 70 0C.

Location	Heights of the nozzle (cm)		
	18.5	**26.5**	**35**
Loc 1	2.32 ± 0.22	2.28 ± 0.21	13.12 ± 2.84
Loc 2	2.41 ± 0.22	2.30 ± 0.21	12.85 ± 2.74
Loc 3	2.50 ± 0.23	2.37 ± 0.22	13.57 ± 2.47
Loc 4	2.16 ± 0.20	1.85 ± 0.17	11.82 ± 2.06
Loc 5	2.47 ± 0.23	2.15 ± 0.20	13.36 ± 2.41
Loc 6	2.97 ± 0.28	2.20 ± 0.21	13.82 ± 2.92
Loc 7	3.04 ± 0.28	2.82 ± 0.26	19.63 ± 3.51
Loc 8	6.96 ± 0.62	7.29 ± 0.65	64.75 ± 3.89
Loc 9	2.14 ± 0.19	2.20 ± 0.20	17.93 ± 0.41

Table A.II. 6 Pasteurisation values for five different containers set up systems: 1, 2, 3, 4, and 9 jars. The z-value considered in the calculations was z = 10ºC and T_{ref} = 70ºC.

Location	Containers set up (jars)				
	1	**2**	**3**	**4**	**9**
Loc 1	2.17 ± 0.20	2.44 ± 0.22	2.36 ± 0.21	2.78 ± 0.26	2.78 ± 0.26
Loc 2	2.26 ± 0.21	2.47 ± 0.23	2.30 ± 0.21	2.82 ± 0.26	2.82 ± 0.26
Loc 3	2.40 ± 0.22	2.56 ± 0.24	2.43 ± 0.23	2.82 ± 0.26	2.82 ± 0.26
Loc 4	1.99 ± 0.18	2.19 ± 0.20	2.09 ± 0.19	2.41 ± 0.23	2.41 ± 0.23
Loc 5	2.23 ± 0.21	2.30 ± 0.21	3.24 ± 0.30	3.22 ± 0.30	3.22 ± 0.30
Loc 6	2.51 ± 0.24	2.62 ± 0.25	2.80 ± 0.26	3.15 ± 0.30	3.15 ± 0.30
Loc 7	3.93 ± 0.36	3.48 ± 0.32	2.92 ± 0.27	2.75 ± 0.26	2.75 ± 0.26
Loc 8	8.29 ± 0.74	7.55 ± 0.68	7.28 ± 0.65	7.15 ± 0.64	7.15 ± 0.64
Loc 9	2.25 ± 0.20	2.35 ± 0.21	2.15 ± 0.20	1.99 ± 0.18	1.99 ± 0.18

Table A.II. 7: Pasteurisation values for two different flow rate of conditions: minimal flow rate and maximum flow rate for each type of nozzle: single jet and muti jet. The jars contained water and heating nozzle temperatures of 70°C. The z-value considered in the calculations was z = 10°C and the reference temperature was T_{ref} = 70°C.

Single jet nozzle									
Flow rate (/min)	Loc 1	Loc 2	Loc 3	Loc 4	Loc 5	Loc 6	Loc 7	Loc 8	Loc 9
0.92	35.09 ± 0.00	34.38 ± 0.00	34.98 ± 0.00	31.15 ± 0.00	29.00 ± 0.00	39.97 ± 0.00	26.02 ± 0.00	66.27 ± 0.00	12.74 ± 11.08
1.91	54.00 ± 0.00	55.05 ± 0.00	54.37 ± 0.00	48.93 ± 0.00	44.03 ± 0.00	54.37 ± 0.00	51.51 ± 0.00	65.35 ± 0.00	12.74 ± 11.08
Muti jet									
Flow rate (/min)	Loc 1	Loc 2	Loc 3	Loc 4	Loc 5	Loc 6	Loc 7	Loc 8	Loc 8
0.98	34.74 ± 0.00	34.05 ± 0.00	34.66 ± 0.00	30.85 ± 0.00	28.74 ± 0.00	39.75 ± 0.00	27.56 ± 0.00	67.35 ± 0.00	12.74 ± 11.08
1.78	52.20 ± 0.00	53.21 ± 0.00	52.51 ± 0.00	47.28 ± 0.00	42.49 ± 0.00	52.45 ± 0.00	49.76 ± 0.00	64.62 ± 0.00	12.74 ± 11.08

Table A.II. 8: Pasteurisation values for two different flow rate of conditions: minimal flow rate and maximum flow rate for each type of nozzle: single jet and muti jet. The jars contained a 5%(w/v) starch and heating nozzle temperatures of 70ºC. The z-value considered in the calculations was z = 10ºC and the reference temperature was T_{ref} = 70ºC.

Single jet nozzle									
Flow rate (/min)	Loc 1	Loc 2	Loc 3	Loc 4	Loc 5	Loc 6	Loc 7	Loc 8	Loc 9
0.92	3.04 ± 0.00	1.85 ± 0.00	2.89 ± 0.00	1.98 ± 0.00	18.54 ± 0.00	25.49 ± 0.00	1.22 ± 0.00	67.15 ± 0.00	12.74 ± 11.08
1.91	10.85 ± 0.00	10.23 ± 0.00	10.47 ± 0.00	10.65 ± 0.00	23.89 ± 0.00	41.07 ± 0.00	0.85 ± 0.00	65.45 ± 0.00	12.74 ± 11.08
Muti jet									
Flow rate (/min)	Loc 1	Loc 2	Loc 3	Loc 4	Loc 5	Loc 6	Loc 7	Loc 8	Loc 8
0.98	14.13 ± 0.00	11.67 ± 0.00	11.57 ± 0.00	13.80 ± 0.00	25.61 ± 0.00	41.42 ± 0.00	24.52 ± 0.00	64.93 ± 0.00	12.74 ± 11.08
1.78	15.06 ± 0.00	13.80 ± 0.00	12.76 ± 0.00	15.27 ± 0.00	27.98 ± 0.00	48.07 ± 0.00	43.92 ± 0.00	67.17 ± 0.00	12.74 ± 11.08

Table A.II. 9: Pasteurisation values for a round jar containing water and a 5%(w/v) starch solution with 10 and 50 %(w/v) potato cubes in nine locations both in solution and potato using 120 degree spray nozzle. Temperature of the heating nozzle was 70°C, while the fluid filling the jar was initially at approx. 20°C. Nozzle flow rate 1.09 l/min. The z-value used in the calculations was z = 10°C and the reference temperature considered was T_{ref} = 70°C.

Water									
% Solid fraction	Loc 1, Solution	Loc 2, Solution	Loc 3, Solution	Loc 4, Solution	Loc 1, Potato	Loc 2, Potato	Loc 3, Potato	Loc 4, Potato	loc 8
10	5.00 ± 0.06	5.35 ± 0.59	5.73 ± 0.30	4.92 ± 0.59	3.66 ± 1.22	4.02 ± 1.43	4.10 ± 1.58	4.17 ± 1.53	68.53 ± 2.13
50	6.22 ± 0.10	6.79 ± 0.75	8.25 ± 0.21	7.01 ± 0.13	4.45 ± 1.85	5.03 ± 2.26	5.38 ± 2.81	5.15 ± 2.37	65.27 ± 2.09
5%(w/v) Starch									
% Solid fraction	Loc 1, Solution	Loc 2, Solution	Loc 3, Solution	Loc 4, Solution	Loc 1, Potato	Loc 2, Potato	Loc 3, Potato	Loc 4, Potato	loc 8
10	2.11 ± 0.28	1.86 ± 0.50	2.25 ± 0.44	2.12 ± 0.30	2.02 ± 0.08	1.56 ± 0.16	1.81 ± 0.27	1.83 ± 0.32	60.77 ± 1.59
50	2.06 ± 0.38	1.78 ± 0.57	2.10 ± 0.38	2.12 ± 0.31	2.11 ± 0.05	1.59 ± 0.28	1.74 ± 0.18	1.85 ± 0.05	63.10 ± 3.59

Table A.II. 10: Pasteurisation values for a hexagonal jar containing water and a 5%(w/v) starch solution with 10 and 50 %(w/v) potato cubes in nine locations both in solution and potato using 120 degree spray nozzle. Temperature of the heating nozzle was 70°C, while the fluid filling the jar was initially at approx. 20°C. Nozzle flow rate 1.09 l/min. The z-value used in the calculations was z = 10°C and the reference temperature considered was T_{ref} = 70°C.

Water									
% Solid fraction	Loc 1, Solution	Loc 2, Solution	Loc 3, Solution	Loc 4, Solution	Loc 1, Potato	Loc 2, Potato	Loc 3, Potato	Loc 4, Potato	loc 8
10	7.21 ± 2.45	7.91 ± 3.47	8.55 ± 3.41	7.47 ± 3.47	5.81 ± 3.03	6.26 ± 3.45	6.41 ± 3.48	5.93 ± 3.17	66.79 ± 1.90
50	7.21 ± 0.13	7.09 ± 0.09	7.65 ± 0.40	6.93 ± 0.57	4.78 ± 2.30	4.95 ± 2.29	5.07 ± 2.52	5.02 ± 2.28	70.64 ± 15.07
5%(w/v) starch									
% Solid fraction	Loc 1, Solution	Loc 2, Solution	Loc 3, Solution	Loc 4, Solution	Loc 1, Potato	Loc 2, Potato	Loc 3, Potato	Loc 4, Potato	loc 8
10	3.09 ± 0.18	2.36 ± 0.66	2.31 ± 0.57	2.45 ± 0.55	2.68 ± 0.30	2.22 ± 0.23	2.82 ± 0.90	2.95 ± 0.97	64.75 ± 3.89
50	2.62 ± 0.32	2.38 ± 0.05	2.86 ± 0.61	3.34 ± 0.00	3.06 ± 0.08	2.40 ± 0.39	2.68 ± 0.45	3.09 ± 0.28	64.75 ± 3.89

Table A.II. 11: Pasteurisation values for a jar containing water and a 5%(w/v) starch solution with 50 %(w/v) potato cubes in nine locations both in solution and potato using a single jet nozzle. Temperature of the heating nozzle was 70°C, while the fluid filling the jar was initially at approx. 20°C. Nozzle flow rate 0.92 l/min. The z-value used in the calculations was z = 10°C and the reference temperature considered was T_{ref} = 70°C.

Water									
Flow rate (/min)	Loc 1, Solution	Loc 2, Solution	Loc 3, Solution	Loc 4, Solution	Loc 1, Potato	Loc 2, Potato	Loc 3, Potato	Loc 4, Potato	loc 8
0.92	18.35 ± 10.09	22.33 ± 11.41	27.34 ± 13.30	21.15 ± 11.15	14.72 ± 7.25	19.01 ± 9.20	28.48 ± 14.66	22.75 ± 10.66	62.75 ± 7.70
1.91	33.89 ± 17.08	38.62 ± 17.12	33.43 ± 29.61	34.02 ± 15.07	23.67 ± 9.62	30.00 ± 12.08	41.03 ± 17.09	38.23 ± 14.95	67.19 ± 2.37
2.56	32.55 ± 5.69	40.43 ± 2.11	42.12 ± 1.14	36.83 ± 1.46	32.71 ± 7.06	33.63 ± 0.93	42.98 ± 4.34	39.97 ± 1.61	64.75 ± 3.89
10.57	49.49 ± 6.05	55.41 ± 1.47	53.74 ± 1.74	47.05 ± 2.24	36.06 ± 3.00	42.22 ± 2.65	55.42 ± 7.80	49.86 ± 5.06	68.82 ± 11.73
5%(w/v) starch									
Flow rate (/min)	Loc 1, Solution	Loc 2, Solution	Loc 3, Solution	Loc 4, Solution	Loc 1, Potato	Loc 2, Potato	Loc 3, Potato	Loc 4, Potato	loc 8
0.98	3.85 ± 1.25	4.44 ± 2.36	3.00 ± 1.16	3.70 ± 1.86	3.58 ± 0.83	3.39 ± 1.32	5.30 ± 1.20	4.10 ± 2.52	60.17 ± 1.74
1.78	2.00 ± 1.97	2.42 ± 2.43	0.00 ± 0.00	2.49 ± 2.43	1.81 ± 1.83	1.80 ± 1.82	2.70 ± 2.76	2.56 ± 2.55	64.55 ± 5.42